Stretto di Messina

Concessionaria per la progettazione, realizzazione e gestione del collegamento stabile tra la Sicilia
e il Continente Organismo di Diritto Pubblico
(Legge n° 1158 del 17 dicembre 1971, modificata dal D.Lgs. n°114 del 24 aprile 2003)

EurolinK

PONTE SULLO STRETTO DI MESSINA

PROGETTO DEFINITIVO

EUROLINK S.C.p.A.

IMPREGILO S.p.A. (MANDATARIA)
SOCIETÀ ITALIANA PER CONDOTTE D'ACQUA S.p.A. (MANDANTE)
COOPERATIVA MURATORI E CEMENTISTI - C.M.C. DI RAVENNA SOC. COOP. A.R.L. (MANDANTE)
SACYR S.A.U. (MANDANTE)
ISHIKAWAJIMA - HARIMA HEAVY INDUSTRIES CO. LTD (MANDANTE)
A.C.I. S.C.P.A. - CONSORZIO STABILE (MANDANTE)

IL PROGETTISTA Ing E.M.Veje COWI EurolinK Dott. Ing. E. Pagani Ordine Ingegneri Milano n° 15408	IL CONTRAENTE GENERALE Project Manager (Ing. P.P. Marcheselli)	STRETTO DI MESSINA Direttore Generale e RUP Validazione (Ing. G. Fiammenghi)	STRETTO DI MESSINA Amministratore Delegato (Dott. P. Ciucci)

Unità Funzionale	OPERA D'ATTRAVERSAMENTO	PS0076_F0
Tipo di sistema	SOVRASTRUTTURE	
Raggruppamento di opere/attività	Implicato	
Opera - tratto d'opera - parte d'opera	Generale	
Titolo del documento	General Design Principles for Suspended Deck	

CODICE: C G 1 0 0 0 | P | R G | D | P | S V | I 3 | 0 0 | 0 0 | 0 0 | 0 0 | 0 1 | F0

REV	DATA	DESCRIZIONE	REDATTO	VERIFICATO	APPROVATO
F0	20/06/2011	EMISSIONE FINALE	JESO,AMOL	HPO	HPO/LSJ

NOME DEL FILE: PS0076_F0

INDICE

1 Introduction

This report describes the design of the following structural elements for the suspended deck:

- Roadway girders: comprising steel sections stiffened by longitudinal trough stiffeners and transverse diaphragms. Individual box girders connected to supporting cross girders. The box girders are completed by aerodynamic fairings.
- Railway girder: comprising steel sections stiffened by longitudinal stiffeners and transverse diaphragms; in particular, longitudinal structural members are arranged under each track. The railway girder sections are connected to the supporting cross girders.
- Cross girders: arranged at 30 m centres, and supported by the hangers, they support the railway and roadway girders; formed as a closed box section of variable height.

In general the design is based on the design shown in the Tender Design.

1.1 Scope

This report describes the design principles for the structural steel elements of the suspended deck, from the terminal structures of Sicilia (stationing 88.49) to the terminal structure of Calabria (stationing 3,723.99). The suspended deck is 60 m wide and entirely made of steel. It is formed by three independent longitudinal box girders, two for the roadway and the central one for the railway. The girders are connected by closed cross girders at 30 metres spacing.

In general the Progetto Definitivo of the suspended deck is based on the Tender Design. The Progetto Definitivo specifies the most important design aspects and other technical topics considered of importance and/or special solutions to the design demands.

Design verifications are summarised in “Specialist Technical Design Report – Suspended Deck”. More detailed calculations are being presented in the design reports for each structural component.

1.2 Bridge Elevation, Plan and Cross Section of Suspended Deck

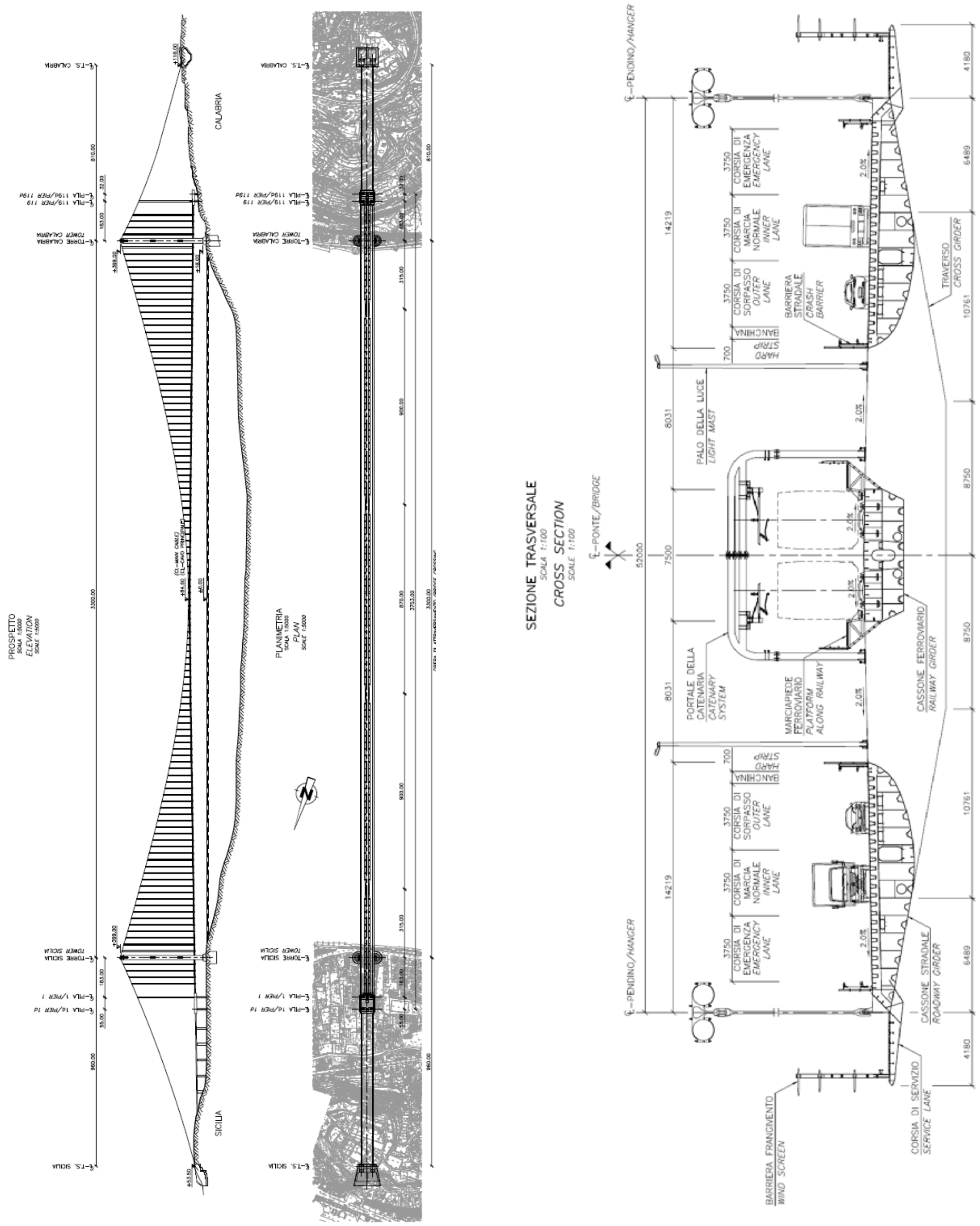

Figure 1-1 Bridge elevation, plan and cross section of suspended deck

1.3 References

1.3.1 Design Specifications

GCG.F.04.01 “Engineering – Definitive and Detailed Design: Basis of Design and Expected Performance Levels,” Stretto di Messina, 2004 October 27.

GCG.F.05.03 “Design Development – Requirements and Guidelines,” Stretto di Messina, 2004 October 22.

GCG.G.03.02 “Structural Steel Works and Protective Coatings,” Stretto di Messina, 2004 July 30.

CG.10.00-P-RG-D-P-GE-00-00-00-00-00-02 “Design Basis, Structural, Annex.”

1.3.2 Design Codes

“Norme tecniche per le costruzioni,” 2008 (NTC08).

EN 1991 Eurocode 1: Actions on Structures – Part 2: Traffic loads on bridges

EN 1993 Eurocode 3: Design of Steel Structures – Part 1-1: General rules and rules for buildings

EN 1993 Eurocode 3: Design of Steel Structures – Part 1-5: Plated structural elements

EN 1993 Eurocode 3: Design of Steel Structures – Part 1-8: Design of joints

EN 1993 Eurocode 3: Design of Steel Structures – Part 1-9: Fatigue

EN 1993 Eurocode 3: Design of Steel Structures – Part 1-10: Selection of steel for fracture toughness and through thickness properties

EN 1993 Eurocode 3: Design of Steel Structures – Part 2: Steel Bridges

Rete Ferroviaria Italia - Istruzione No. 44F “Verifiche a fatica dei ponti ferroviari”

Recommendations for Fatigue Design of Welded Joints and Components, International Institute of Welding (IIW), doc. XIII-2151-07/XV-1254-07, May 2007

Recommendations on Post Weld Fatigue Life Improvement of Steel and Aluminium Structures, International Institute of Welding (IIW), doc. XIII-2200r7-07, 06 July 2010

European Convention for Constructional Steelwork (ECCS), Eurocode, Design Manual, 1-9CL_Pics-v40, September 2010

1.3.3 Material Specifications

EN 10025-1:2004 Hot-rolled products of structural steels – Part 1: General delivery conditions.

EN 10025-2:2004 Hot-rolled products of structural steels – Part 2: Technical delivery conditions for non-alloy structural steels.

EN 10025-3:2004 Hot-rolled products of structural steels – Part 3: Technical delivery conditions for normalised / normalised weldable fine grain structural steels.

EN 10025-4:2004 Hot-rolled products of structural steels – Part 4: Technical delivery conditions for thermomechanical rolled weldable fine grain structural steels.

EN 10164:2004 Steel products with improved deformation properties perpendicular to the surface of the product – Technical delivery conditions.

EN ISO 898-1:2009 Mechanical properties of fasteners made of carbon steel and alloy steel – Part 1: Bolts, screws and studs.

EN ISO 3506-1:2009 Mechanical properties of corrosion-resistance stainless-steel fasteners – Part 1: Bolts, screws and studs

EN ISO 3506-2:2009 Mechanical properties of corrosion-resistance stainless-steel fasteners – Part 2: Nuts

EN 20898-2:1994 Mechanical properties of fasteners – Part 2: Nuts with special proof load values – coarse thread (ISO 898-2:1992).

UNI EN 14399:2005-3 High-strength structural bolting assemblies for preloading - Part 3: System HR - Hexagon bolt and nut assemblies

EN ISO 14555:1998 Welding-Arc stud welding of metallic materials. May 1995.

EN ISO 13918:1998 Welding-Studs for arc stud welding-January 1997.

1.3.4 Drawings

The reference suspended deck design drawings for this report are listed in Table 1-1.

Table 1-1 Reference suspended deck drawings

Drawing Title	Drawing Number
Overview, Elevation	CG.10.00-P-AX-D-P-SV-I3-00-00-00-00-01_0
Overview Plan, Sicilia	CG.10.00-P-PX-D-P-SV-I3-00-00-00-00-01_0
Overview Plan, Calabria	CG.10.00-P-PX-D-P-SV-I3-00-00-00-00-04_0
Main Span, Plan and Section	CG.10.00-P-PX-D-P-SV-I3-00-00-00-00-02_0
Tower Location, Plan	CG.10.00-P-PX-D-P-SV-I3-00-00-00-00-03_0
Tower Location, Sections	CG.10.00-P-WX-D-P-SV-I3-00-00-00-00-01_0
Side Span, Plan and Section	CG.10.00-P-LX-D-P-SV-I3-00-00-00-00-01_0
Bridge End Sicilia, Plan and Section	CG.10.00-P-LX-D-P-SV-I3-00-00-00-00-02_0
Bridge End Sicilia, Sections	CG.10.00-P-WX-D-P-SV-I3-00-00-00-00-02_0
Bridge End Calabria, Plan and Section	CG.10.00-P-LX-D-P-SV-I3-00-00-00-00-03_0
Bridge End Calabria, Sections	CG.10.00-P-WX-D-P-SV-I3-00-00-00-00-03_0
Roadway - Main and Side Span - Section	CG.10.00-P-WX-D-P-SV-I3-CS-00-00-00-01_0
Roadway - Main and Side Span - Diaphragms	CG.10.00-P-AX-D-P-SV-I3-CS-00-D0-00-01_0
Roadway - Main and Side Span - Details 1	CG.10.00-P-BX-D-P-SV-I3-CS-00-00-00-01_0
Roadway - Main and Side Span - Details 2	CG.10.00-P-BX-D-P-SV-I3-CS-00-00-00-02_0
Roadway - Tower Location - Section and Elevation	CG.10.00-P-AX-D-P-SV-I3-CS-00-00-00-01_0
Roadway - Tower Location - Diaphragms	CG.10.00-P-AX-D-P-SV-I3-CS-00-0D-00-02_0
Roadway - Tower Location - Details	CG.10.00-P-BX-D-P-SV-I3-CS-00-00-00-03_0
Roadway - Bridge End - Section	CG.10.00-P-LX-D-P-SV-I3-CS-00-00-00-01_0
Roadway - Bridge End - Diaphragms	CG.10.00-P-AX-D-P-SV-I3-CS-00-D0-00-03_0
Railway - Main Span - Section	CG.10.00-P-WX-D-P-SV-I3-CF-00-00-00-01_0
Railway - Main Span - Diaphragms	CG.10.00-P-AX-D-P-SV-I3-CF-00-D0-00-01_0
Railway - Main Span - Details 1	CG.10.00-P-BX-D-P-SV-I3-CF-00-00-00-01_0
Railway - Main Span - Details 2	CG.10.00-P-BX-D-P-SV-I3-CF-00-00-00-02_0

Railway - Tower Location - Section	CG.10.00-P-WX-D-P-SV-I3-CF-00-00-00-02_0
Railway - Tower Location - Diaphragms	CG.10.00-P-AX-D-P-SV-I3-CF-00-D0-00-02_0
Railway - Tower Location - Details	CG.10.00-P-BX-D-P-SV-I3-CF-00-00-00-03_0
Railway - Side Span - Section	CG.10.00-P-WX-D-P-SV-I3-CF-00-00-00-03_0
Railway - Side Span - Diaphragms	CG.10.00-P-AX-D-P-SV-I3-CF-00-D0-00-03_0
Railway - Bridge End - Section	CG.10.00-P-WX-D-P-SV-I3-CF-00-00-00-04_0
Railway - Bridge End - Diaphragms	CG.10.00-P-AX-D-P-SV-I3-CF-00-D0-00-04_0
Railway - Bridge End - Elevation	CG.10.00-P-AX-D-P-SV-I3-CF-00-00-00-01_0
Railway - Bridge End - Intersection	CG.10.00-P-AX-D-P-SV-I3-CF-00-00-00-02_0
Cross Girder - Main Span - Section 1	CG.10.00-P-WX-D-P-SV-I3-TP-00-00-00-01_0
Cross Girder - Main Span - Section 2	CG.10.00-P-WX-D-P-SV-I3-TP-00-00-00-02_0
Cross Girder - Main Span - Diaphragms 1	CG.10.00-P-AX-D-P-SV-I3-TP-00-D0-00-01_0
Cross Girder - Main Span - Diaphragms 2	CG.10.00-P-AX-D-P-SV-I3-TP-00-D0-00-06_0
Cross Girder - Main Span - Details 1	CG.10.00-P-BX-D-P-SV-I3-TP-00-00-00-01_0
Cross Girder - Main Span - Details 2	CG.10.00-P-BX-D-P-SV-I3-TP-00-00-00-02_0
Cross Girder - Tower Location - Section 1	CG.10.00-P-WX-D-P-SV-I3-TP-00-00-00-03_0
Cross Girder - Tower Location - Section 2	CG.10.00-P-WX-D-P-SV-I3-TP-00-00-00-07_0
Cross Girder - Tower Location - Sections 3	CG.10.00-P-WX-D-P-SV-I3-TP-00-00-00-04_0
Cross Girder - Tower Location - Diaphragms 1	CG.10.00-P-AX-D-P-SV-I3-TP-00-D0-00-02_0
Cross Girder - Tower Location - Diaphragms 2	CG.10.00-P-AX-D-P-SV-I3-TP-00-D0-00-03_0
Cross Girder - Tower Location - Diaphragms 3	CG.10.00-P-AX-D-P-SV-I3-TP-00-D0-00-07_0
Cross Girder - Tower Location - Diaphragms 4	CG.10.00-P-AX-D-P-SV-I3-TP-00-D0-00-08_0
Cross Girder - Side Span - Section 1	CG.10.00-P-WX-D-P-SV-I3-TP-00-00-00-05_0
Cross Girder - Side Span - Section 2	CG.10.00-P-WX-D-P-SV-I3-TP-00-00-00-08_0
Cross Girder - Side Span - Diaphragms 1	CG.10.00-P-AX-D-P-SV-I3-TP-00-D0-00-04_0
Cross Girder - Side Span - Diaphragms 2	CG.10.00-P-AX-D-P-SV-I3-TP-00-D0-00-09_0
Cross Girder - Bridge End - Section 1	CG.10.00-P-WX-D-P-SV-I3-TP-00-00-00-06_0
Cross Girder - Bridge End - Section 2	CG.10.00-P-WX-D-P-SV-I3-TP-00-00-00-09_0
Cross Girder - Bridge End - Diaphragms	CG.10.00-P-AX-D-P-SV-I3-TP-00-D0-00-05_0

Cross Girder - Hanger Anchorage 1	CG.10.00-P-AX-D-P-SV-I3-TP-00-00-00-03_0
Cross Girder - Hanger Anchorage 2	CG.10.00-P-AX-D-P-SV-I3-TP-00-00-00-04_0
Cross Girder - Hanger Anchorage 3	CG.10.00-P-AX-D-P-SV-I3-TP-00-00-00-05_0
Cross Girder - Hanger Anchorage 4	CG.10.00-P-AX-D-P-SV-I3-TP-00-00-00-06_0
Cross Over - Plan and sections	CG.10.00-P-WX-D-P-SV-I3-00-00-00-00-04_0
Cross Over – Details 1	CG.10.00-P-BX-D-P-SV-I3-00-00-00-00-01_0
Cross Over – Details 2	CG.10.00-P-BX-D-P-SV-I3-00-00-00-00-02_0
Cross Over – Consoles	CG.10.00-P-AX-D-P-SV-I3-00-00-00-00-06_0
Portal for Road Signs - Consoles	CG.10.00-P-AX-D-P-SV-I3-00-00-00-00-07_0
Base Plates	CG.10.00-P-AX-D-P-SV-I3-00-00-00-00-05_0
Accesses 1	CG.10.00-P-AX-D-P-SV-I3-00-00-00-00-02_0
Accesses 2	CG.10.00-P-AX-D-P-SV-I3-00-00-00-00-03_0
Accesses 3	CG.10.00-P-AX-D-P-SV-I3-00-00-00-00-04_0
Dehumidification - General Layout	CG.10.00-P-PX-D-P-SV-I3-00-00-00-00-05_0
Dehumidification - Cross Girder Layout 1	CG.10.00-P-AX-D-P-SV-I3-00-00-00-00-08_0
Dehumidification - Cross Girder Layout 2	CG.10.00-P-AX-D-P-SV-I3-00-00-00-00-09_0
Dehumidification - Cross Girder Layout 3	CG.10.00-P-AX-D-P-SV-I3-00-00-00-00-10_0
Cable Trays and Transits - Cross Girder Layout	CG.10.00-P-AX-D-P-SV-I3-00-00-00-00-11_0
Cable Trays and Transits - Roadway Girder Layout	CG.10.00-P-AX-D-P-SV-I3-00-00-00-00-12_0
Cable Trays and Transits - Details	CG.10.00-P-BX-D-P-SV-I3-00-00-00-00-03_0

1.3.5 Reports for Suspended Deck

The suspended deck design reports listed in Table 1-2 provide all the information regarding the suspended deck design principles and verifications.

Table 1-2 Reference suspended deck design reports

Report Title	Report Number
Specialist Technical Design Report, Suspended Deck	CG.10.00-P-RX-D-P-SV-I3-IM-00-00-00-01_0
General Design Principles for Suspended Deck	CG.10.00-P-RG-D-P-SV-I3-IM-00-00-00-01_0
Design Report - Roadway, Railway and Cross Girders	CG.10.00-P-CL-D-P-SV-I3-00-00-00-00-01_0
Design Report - Support Structures	CG.10.00-P-CL-D-P-SV-I3-00-00-00-00-02_0
Design Report - Local FE-models of Suspended Deck	CG.10.00-P-CL-D-P-SV-I3-00-00-00-00-03_0
Design Report - Fatigue Assessment of Suspended Deck	CG.10.00-P-CL-D-P-SV-I3-00-00-00-00-04_0
Design Report - Special Design Investigations	CG.10.00-P-CL-D-P-SV-I3-00-00-00-00-05_0

1.4 Nomenclature

The section provides descriptions of terms commonly used throughout the report to refer to various suspended deck components:

Roadway girder - orthotropic steel box for roadway traffic connected by the cross girders.

Railway girder - orthotropic steel box for railway traffic connected by the cross girders.

Cross girder – the transverse beams connecting the railway girder and roadway girders every 30m.

Longitudinal Stiffeners – the longitudinal plate elements used to stiffen the vertical suspended deck plate, bottom plates and webs as well as the deck-, bottom plates and webs of the cross girders.

Transverse Diaphragms – diaphragms implemented at both the roadway, railway and cross girders.

Hanger Anchorage – the connection of the hanger cables to the cross girders.

Railway Fastening System – the connection of the railway tracks to the railway girder.

T-beam – Longitudinal T-beams underneath the four rails carrying the local train loads.

Drop-in span – the 60 m road girder span at the towers.

1.5 Design Changes

For some part of the suspended deck structures it has been found advantageous to introduce the following changes to the tender design:

1.5.1 Roadway Girders

1. Compared with the cross section in the tender design the primary modification is the 2.0 % outward inclination of the top plate which previously had an inward slope. As a consequence of this change the gully for drainage of the pavement is moved to the outer edge of the deck plate, the position of the crash barriers are adjusted slightly due to that the longitudinal water channel is placed at the outer edge of the deck plate.

2. Besides the primarily modification on the cross section, the direction of the road traffic has been inverted, which has an impact of the deck plate thickness for lane configuration.

3. Due to optimisation of the overall cross section, simplification of the hanger anchorage and connection details to the service lane the overall width of the roadway girder has been reduced. The outer edge plate of the roadway girder has become more inclined to ease the connection to the hanger anchorages, and the radius forming the connection between roadway deck plate and edge plate has been modified to give better room for the longitudinal water channel. The theoretical horizontal width of the roadway girder now becomes 14.227 m.

4. The two L-stiffeners underneath the edge plate has been changed to flat stiffeners to comply with manufacturing optimisation. The first deck trough under the crash barrier at the emergency lane is exchanged by two flat stiffeners and the trough underneath inspection corridor is also exchanged to two flat stiffeners to comply with demands for high fatigue detail categories. To fulfil the fatigue demands, the tooth plate supporting the troughs at the diaphragms is increased from 10 mm to 15 mm in the slow and fast lane together with a modified shape of the cut outs.

5. The verifications are made under the assumption that the pavement thickness of 12 mm might change to 40 mm, whereas the thickness of 12 mm is used for stress concentration verification of the orthotropic deck and the thickness of 40 mm will be used for the global dead load.

6. Preparations carried out for 3 more cross-overs for later implementation

7. Safety factors for fatigue strength have been increased giving thicker plates. The roadway deck plate in the two traffic lanes is increased from 16 mm to 17 mm, and the troughs underneath are in general increased from 7 mm to 9 mm.

8. To fulfil the fatigue demands at the trough joints, the troughs underneath the deck plate are increased locally at a width of 7.3m. The thickness is increased from 9 mm to 10 mm and 14 mm at the cross girder joints from 9 mm to 11 mm and 13 mm at the erection joints.

9. To fulfil the fatigue demands at the joints in the bottom plate, the thickness is in general increased locally from 8 mm to 13 mm at the cross girder joints and at the erection joints (every 60m).

10. Tab plates for the bottom trough stiffeners are removed and replaced by a direct attachment of the troughs to the diaphragm. Cope holes are maintained at the flange of the trough stiffener.

11. The base plates for roadway crash barrier have been changed from welded to bolted solution to comply with demands for high fatigue detail categories.

12. To comply with the fatigue demands, the fixation of the gullies is changed from welded to bolted solution with two joint sealants.

13. The number of drainage pipes inside the roadway girder has been reduced from 3 to 1 pipe and the holes in the roadway diaphragms for cables have been relocated.

14. Manhole inside the roadway girder has been changed in size to 1300x800 mm due to shear forces in the diaphragm.

15. Termination of stiffeners and diaphragms have in general been improved by adding endplates with a radius of min 150 mm. Thereby the fatigue detail category can be improved fulfilling the fatigue demands.

16. To comply with the fatigue demands, weld improvement has furthermore been introduced in general by ground smoothening of all the 6 bottom flange/diaphragm joints between the cross girders.

The above mentioned modifications have changed the overall geometry of the cross section as shown in Figure 1-2.

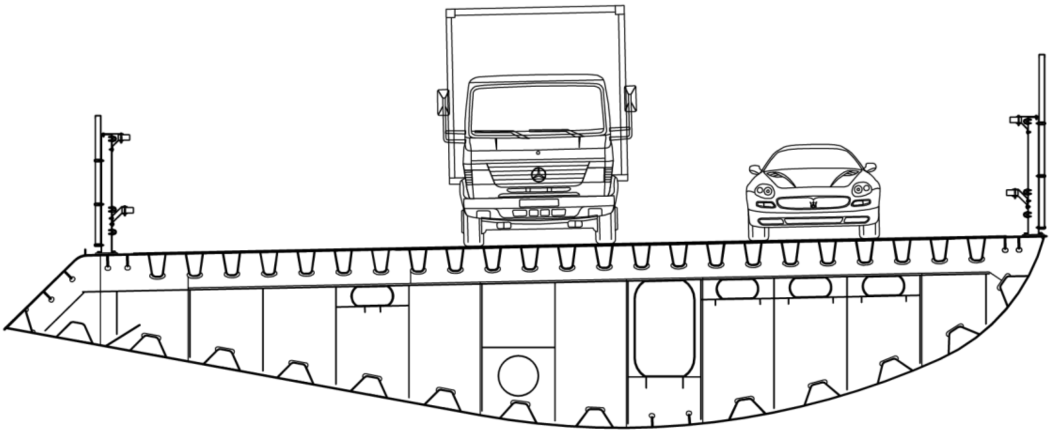

Figure 1-2 Modified cross section for roadway girder (service lane not shown)

1.5.2 Railway Girder

1. Since tender design, changes have been made to the overall shape of the steel box girder. The angle of the inclined web is changed from 44 deg to 63 deg while the vertical web plate remains unchanged. The thickness of the bottom plate is lowered from 12 mm to 10 mm to keep cross section properties almost unchanged.

2. Angle profiles stiffening the deck plate, inclined bottom plate and web plates in the tender design, are replaced with flat stiffeners to comply with manufacturing optimisation.

3. The troughs underneath the deck plate are furthermore exchanged by flat stiffeners to comply with demands for high fatigue detail categories. The extra steel within the flat stiffeners is almost balanced out by reducing the deck plate thickness from 16 mm to 15 mm.

4. T-beams, flat and trough stiffeners are continuous throughout the diaphragms to eliminate fatigue problems by interruption. The diaphragm at support of T-stiffeners is reinforced locally from 10 mm to 15 mm.

5. Safety factors for fatigue strength have been increased giving demands for thicker plates.

6. The rail fastening system has been modified since the tender design to a full welded solution with additional stiffening per 1250 mm. The L-profiles of the railway track superstructure will furthermore allow for dewatering per 10 m.

7. The distance between the intermediate stiffeners supporting the railway superstructure is changed from 1875 mm down to 1250 mm. This implies that the number of stiffeners is doubled.
8. To comply with the fatigue demands the bottom plateis increased locally from 10 mm to 15 mm at the erection joints (every 60 m). The bottom plate is furthermore reinforced locally in all spans at the 4 centre diaphragms at the inclined webs. For the spans in vicinity of the towers, a partial increment of the bottom plate is further required throughout the cross girder.
9. Railway crash barriers have been implemented into the platform along the railway and their base plates have been modified from welded to bolted solution to comply with demands for high fatigue detail categories. The same argument applies for fixation of the gullies which is changed from welded to bolted solution with two joint sealants.
10. Termination of stiffeners and diaphragms have in general been improved by adding endplates with a radius of min 150 mm. Thereby the fatigue detail category can be improved fulfilling the fatigue demands.
11. Changes have been made to the diaphragm where the stiffener and weld layout have been modified. Holes in the railway diaphragms for cables have been relocated and the high voltage cables have been removed from the railway girder. The number of drainage pipes inside the railway girder has furthermore been reduced from 4 to 2 pipes.
12. To comply with the fatigue demands, weld improvement has furthermore been introduced in general by ground smoothening of the 2 centre diaphragm joints. These two diaphragms plus two additional are fully welded by K-welds

The above mentioned modifications have changed the overall geometry of the cross section as shown in Figure 1-3.

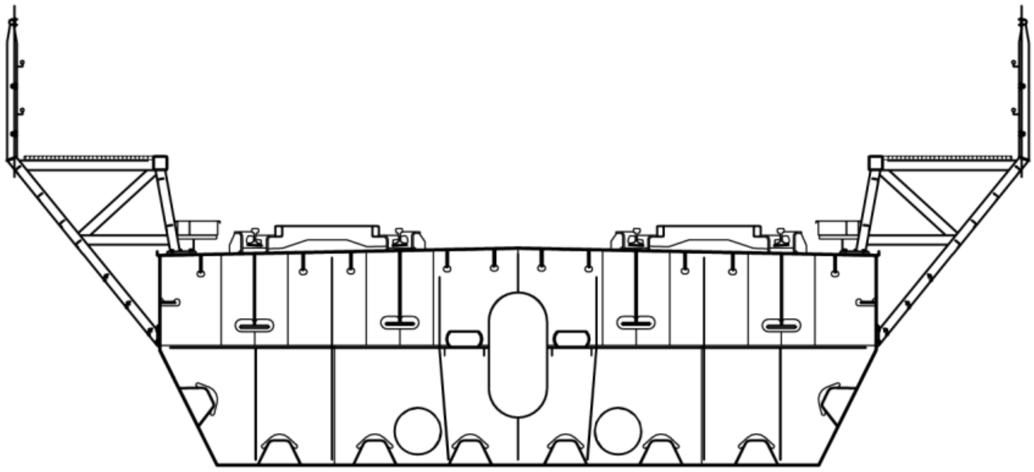

Figure 1-3 Modified cross section for railway girder inclusive walkway along railway

1.5.3 Cross Girders

1. Since the tender design, the direction of the road traffic has been inverted. This change led to a continuous 2.0 % outward slope of the top plate throughout the entire length of all cross girders, see Figure 1-4 (type T1-T3 shown).

2. The tender design solution presented the diaphragms next to the railway girder with the spacing of 2.5 m. This configuration had been reinforced by an extra transverse stiffener thereby halves the buckling length of the plate as shown in Figure 1-4.

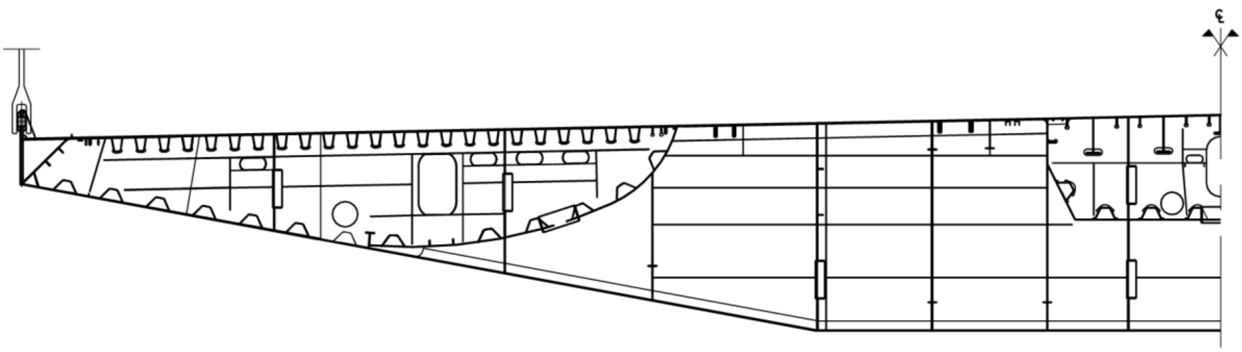

Figure 1-4 Continuous outwards slope of cross girder

3. T-stiffeners at the webs and bottom plate have been replaced with flat stiffeners to comply better with manufacturing optimisation, see Figure 1-5. T- and flat stiffeners are preferred as

stiffeners in the cross girders as they are easier to implement in the complicated geometry than ordinary trough profiles.

4. The centre 4.4 m of the bottom plate has been increased in thickness by 8 mm, while the two neighbouring plates (2 x 4.05 m) have been increased by 3 mm. The top plate in the vicinity of the railway girder is also increased in thickness by 3-4 mm. All changes have been done to comply with the fatigue demands.

5. The geometry of the hanger anchorage has in general been altered to optimise the design by having a load distribution from the main anchor plate directly into the cross girder web.

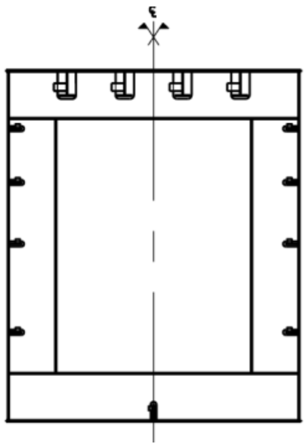

Figure 1-5 Flat stiffeners on cross girder webs and bottom plate

6. To comply with the fatigue demands, weld improvement has furthermore been introduced by ground smoothening all the diaphragms positioned at the horizontal bottom plate. Both the bottom- and top plate and 500 mm of the belonging webs are treated.

7. Termination of stiffeners and diaphragms have in general been improved by adding end plates with a radius of min 150 mm. Thereby the detail fatigue category can be improved fulfilling the fatigue demands.

8. Changes have also been made to the cross girder T7 at the terminal structure. The high demand of torsional capacity due to the adjoining spans led to widen the cross section from 1700 mm to 2700 mm. The width has also been determined to accommodate the expansion joint movement.

1.5.4 Intersections between Roadway, Railway and Cross Girders

1. The arrangements of stiffeners in the cross girder is such that all the stiffeners of roadway and railway decks pass through the interior of the cross girder. This is done to give more favourable interconnection to the road and railway girder sections and to improve the fatigue strength. In addition this arrangement ensures a high driving comfort when passing the cross girder due to the uniform deck stiffness. In the remaining part of the cross girder, longitudinal T-stiffeners are applied to the deck plate in longitudinal direction of the cross girder itself.

2. The web and bottom troughs at the roadway girder are interrupted at the cross girder web, but extra short trough sections are introduced at both sides of the web being welded to the web by double sided full penetrations welds. Thereby cut outs are avoided in the web towards the hanger anchorage and the demand for a high fatigue detail category has been kept.

3. To fulfil the fatigue demands, the tooth plate supporting the troughs at the web of the roadway girder is increased from 16 mm to 25 mm in the slow and fast lane together with a modified shape of the cut outs.

4. The bottom plate, inclined webs and belonging troughs are passing trough the web of the cross girder, while the vertical web plates are interrupted.

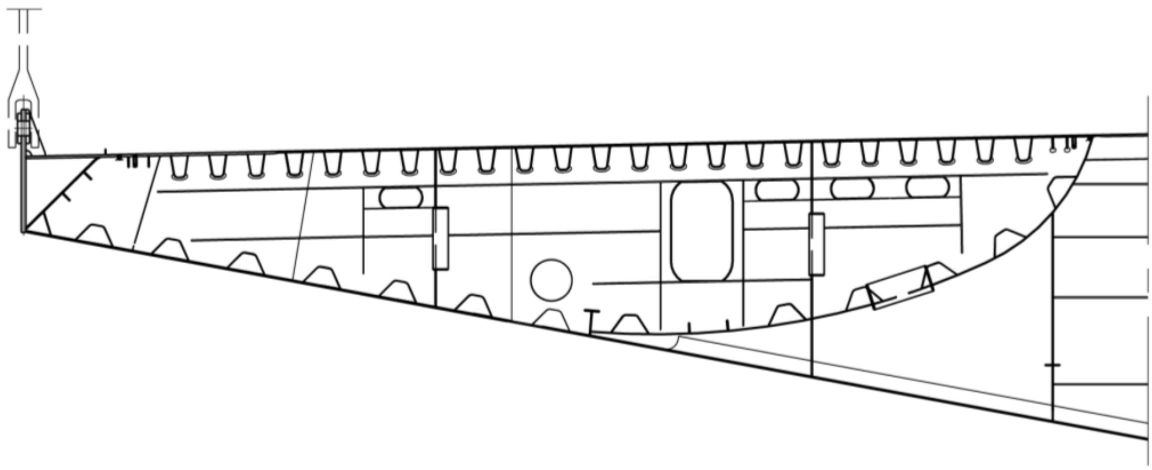

Figure 1-6 Roadway troughs – cross girder webs intersection detail

The intersections of the cross girder to roadway and railway girders can be seen in Figure 1-6 and

Figure 1-7.

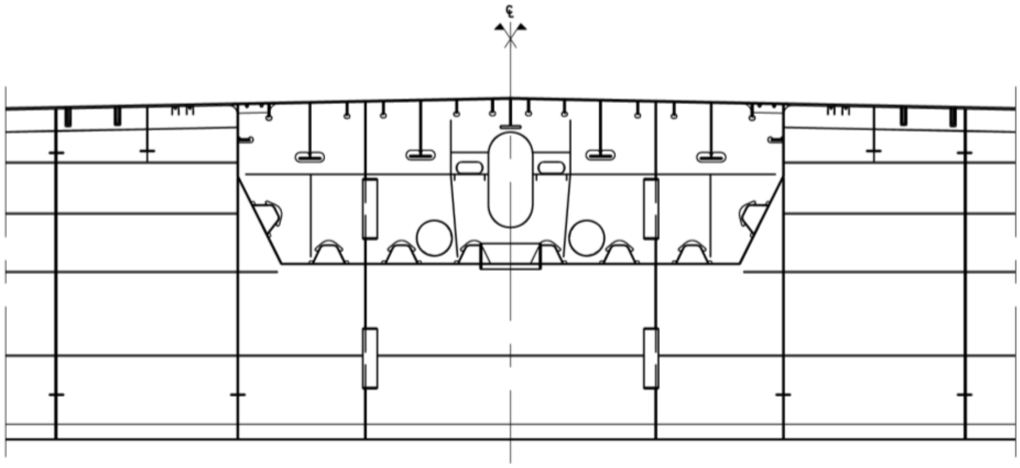

Figure 1-7 Railway troughs – cross girder web intersection detail

2 Limit States

This section describes the limit states and corresponding performance requirements governing the proportioning of the suspended deck components, in accordance with the project design basis GCG.F.04.01 and NTC08. The deck component performances are verified at serviceability limit states (SLS1 and SLS2) and the ultimate limit states (ULS).

2.1 Serviceability Limit States (SLS)

NTC08 Section 2.2.2 defines the following serviceability limit states (SLS) that are to be evaluated in a structural design:

- Local damage that can reduce the durability of the structure
- Displacement or deformations that could limit the use of the structure, its efficiency and its appearance
- Displacement or deformations that could compromise the efficiency and appearance of non-structural elements, plants and machinery
- Vibrations that could compromise the use of the structure

- Damage caused by fatigue that could compromise durability
- Corrosion and/or excessive deterioration in materials due to atmospheric exposure

The project design basis GCG.F.04.01 Section 3.1 specifies the performance requirements for the structure under two levels of serviceability, or normal usage loads. The SLS performance requirements are listed in Table 2-1.

Table 2-1 SLS performance requirements

Limit State	Performance Requirement
SLS1	Road and rail runability is guaranteed. No structural damage. Structure remains elastic and all deformations are reversible.
SLS2	As for SLS1 except that only rail runability is guaranteed.

Limit state SLS2 is used to verify suspended deck components for temporary construction conditions and for the verification of particular components in the completed bridge.

The specific SLS that are verified for the suspended deck components are:

- Stresses on effective cross-sections are all less than the material yield strength
- Deformation of deck and track also in relation to the issue of comfort and safety of travelling vehicles

2.2 Ultimate Limit States

NTC08 Section 2.2.1 defines the following Ultimate Limit States (ULS) that are to be evaluated in a structural design:

- Loss of equilibrium of the structure or part of it.
- Excessive displacement or deformation.
- Arrival at the maximum resistance capacity of parts of the structure, joints or foundations.

- Arrival at the maximum resistance capacity of the structure as a whole.
- Arrival at ground collapse mechanisms.
- Failure of frames and joints due to fatigue.
- Failure of frames and joints due to other time-related effects.
- Instability of parts of the structure or structure as a whole.

The project design basis GCG.F.04.01 Section 3.1 specifies the performance requirements for the structure under ultimate or rare loads. The performance requirements are listed in Table 2-2.

Table 2-2 ULS performance requirements

Limit State	Performance Requirement
ULS	Temporary loss of serviceability is allowed. The main structural system maintains its full integrity. Structural damage to secondary components is repairable by means of extraordinary maintenance works.

The specific ULS that are evaluated for the suspended deck components are:

- Stresses on effective cross-sections are in general less than the material yield strength. Yielding of local areas of limited sizes is however allowed.
- Welded connections provide sufficient capacity
- Through thickness stresses on plates are less than the allowable stresses for the steel type specified

For the suspended deck hanger replacement is considered with in the normal ULS load combinations. Also the accidental load case with hanger rupture is considered at the ULS load combinations to make sure the bridge deck may maintain its full integrity in case of loss of a hanger.

2.3 Fatigue Limit States

NTC08 Sections 2.2.1 and 2.2.2 due not distinguish fatigue limit states (FLS) from serviceability and ultimate limits states with similar consequences and performance requirements. However, in NTC08 Section 4.2.2.1 FLS are distinguished because the loads and load combinations used for verification are different, as are the means by which the elements are verified. NTC08 Sections 2.2.1 and 2.2.2 define the following fatigue related SLS and ULS that are to be evaluated in a structural design:

- Damage caused by fatigue that could compromise durability (SLS).
- Failure of frames and joints due to fatigue (ULS).

The specific FLS that are evaluated for the suspended deck components are:

- Elastic buckling at serviceability limit state, known as plate breathing.
- Steel stresses under fatigue loading are less than the stress limit for the design details used and the expected number of cycles.

2.4 Structural Integrity Limit States

There are no requirements for the suspended deck under Structural Integrity Limit States (SILS).

3 Materials

The mechanical properties of the suspended deck construction materials are described in this section.

3.1 Structural Steel

Suspended deck structural components are primary foreseen to be fabricated from grade S355ML, S420ML and grade S460 ML structural steels, produced in accordance with EN 10025-4. The steels are assumed to have the mechanical properties listed in Table 3-1, in accordance with NTC08 Section 11.3.4.1. The steel fabricator has confirmed that the mechanical properties will not vary with material thickness for thicknesses less than 100 mm, as is typical for rolled steel products.

Table 3-1 Structural steel mechanical properties for thicknesses less than 100 mm

Grade	Yield Strength, f_{yk} (MPa)	Tensile Strength, f_{tk} (MPa)
S355ML	355	470
S420ML	420	520
S460ML	460	540

All structural steel is also assumed to have the following properties, in accordance with NTC08 Section 11.3.4.1:

- Elastic modulus: E=210,000 MPa
- Poisson's ratio: $\nu = 0.3$
- Shear modulus: G=77,000 MPa
- Coefficient of thermal expansion: $\alpha = 12 \times 10^{-6}$ / °C
- Density: $\rho = 7850$ kg/m^3

The material partial factors (safety coefficients) used to verify structural steel elements are in accordance with NTC08 Sections 4.2.4.1.1, 4.2.4.1.4 and are listed in Table 3-2.

Table 3-2 Material partial factors for structural steel (ULS)

Verification	Partial Factor
Resistance of Class 1, 2, 3 and 4 sections	$\gamma_{M0} = 1.05$
Resistance to instability of members in road and rail bridges	$\gamma_{M1} = 1.10$
Resistance to fracture of sections under tension (weakened by holes)	$\gamma_{M2} = 1.25$
Fatigue resistance of roadway deck plate (safe life with low failure consequences)	$\gamma_{mf} = 1.15$
Fatigue resistance of roadway girder (safe life with high failure consequences)	$\gamma_{mf} = 1.35$
Fatigue resistance of all components in railway and cross girders (safe life with high failure consequences)	$\gamma_{mf} = 1.35$

Material partial factors for structural steel for accidental load situation within the ULS $\gamma_M = 1.00$

3.2 High Strength Bolts

High strength structural bolts of Grade 8.8 or Grade 10.9, produced in accordance with EN ISO 898, are used for all bolted connections. High strength bolts are assumed to have the mechanical properties listed in Table 3-3, in accordance with NTC08 Section 11.3.4.6.1. Where appropriate stainless steel bolts in grade A4-70 or A4-80 will be utilised for fastening of ancillary structure at the outside of the suspended deck.

Table 3-3 Structural bolt mechanical properties

Grade	Yield Strength, f_{yb} (MPa)	Tensile Strength, f_{tb} (MPa)
8.8	640	800
10.9	900	1000
A4-70	450	700
A4-80	600	800

The material partial factors (safety coefficients) used to verify bolted connections and splices are in accordance with NTC08 Section 4.2.8.1.1 and are listed in Table 3-4.

Table 3-4 Material partial factors for bolted connections (ULS)

Verification	Partial Factor
Resistance to bolt shear	$\gamma_{M2} = 1.25$
Resistance to bolt tension	
Resistance to bearing on plates	
ULS slip resistance	$\gamma_{M3} = 1.25$
SLS slip resistance	$\gamma_{M3} = 1.15$
Bolt preload force	$\gamma_{M7} = 1.10$

Material partial factors for bolted connections for accidental load situation within ULS $\gamma_M = 1.00$

3.3 Welding Consumables

Welding consumables shall comply with the requirements of EN 1993-1-8 Section 4.2.

The material partial factor in ULS, γ_{M2} = 1.25, used to verify welded connections and splices is in accordance with NTC08 Section 4.2.8.1.1. Material partial factors for welds for accidental load situation within ULS $\gamma_M = 1.00$

4 Articulation

4.1 Overall Static System

The static system for the suspended deck has in general been adopted from the Tender Design:

- The roadway girders are continuous between terminal structures except at two expansion joints placed +/- 30 m from each of the towers.
- The railway girder is continuous from one terminal structure to the other. At the terminal structures, bearings are arranged at two locations ensuring both the vertical and horizontal alignment requirements of the railway girder is fulfilled.
- A special structure is installed between the two cross girders in the tower area and consist of two interconnected triangles and a buffer connection to the towers legs. The structure ensures that no transverse bending will be transferred from the main span and through the device to the side span. The X-structure is supported in vertical direction with a pin connection to the railway girder. The X-structure is designed by the group handling Articulations.
- The road and railway girders are interconnected by closed cross girders.

4.2 Interconnection of the Suspended Deck Elements

The closed steel cross girders have great torsion rigidity. The interconnection to the longitudinal girders is designed using closed diaphragms, which makes transferring of moments in all 3 directions possible. This applies for the analyses carried out as well as the joint design reflected on the drawings. In this way live loads on the girders are distributed as much as possible to all the deck structures, which minimises adverse deflections.

5 Basis for Design and Load Combinations

5.1 Classification of Suspended Deck

According to the Design Basis (GCG.F.04.01) section 2, the suspended deck is classified as follows:

Table 5-1 Classification of the structural components of the suspended deck

Macro-level	Meso-level		Primary Components (C1)	Secondary Components (C2)
	Structures	**Sub-structures**		
Main structural system	Standard deck	Cross girders	X	
		Railway girder		X
		Roadway girder		X
	Special deck zones	End structures and expansion joints		X
		Near towers and restraint systems		X

Primary Components (C1): critical, non-repairable or which require the Bridge to be placed out of service for a protracted period in order for them to be repaired;
Secondary Components (C2): repairable, possibly with restrictions on the operation of the Bridge.

From Table 5-2 it is seen, that the cross girders are classified as primary components, while the remaining part of the suspended deck is classified as secondary components.

5.2 Allowable Damage Levels of Suspended Deck

Table 5-2 shows the allowable damage for the suspended deck components as function of the associated limit state, refer Design Basis section 4.1.

Table 5-2 Structural decomposition and allowable damage levels of the suspended deck

Macro-level	**Meso-level**		**SLS ULS SILS**			
	Structures	**Sub-structures**				
Main structural system	Standard deck	Cross girder	ND	MD	SD	SD
		Railway girder	ND	MD	SD	SD
		Roadway girder	ND	MD	SD	SD
	Special deck zones	End Structures and expansion joints	DD	MD	SD	SD
		Near towers and restraint systems	DD	MD	SD	SD

ND: No damage, DD: Degradation damage, MD: Minimal damage and SD: Significant damage.

Table 5-2 shows that for the suspended deck in general, no damage is allowed in the SLS load combinations, while degradation damage is allowed for mechanical components attached to the suspended deck in the SLS load combinations. For the SLS (SLS1 & SLS2) load combinations is moreover required, that the suspended deck components shall remain in an elastic state and deformations are reversible as also stated in section 2.1.

For the ULS load combinations, minimal damage is allowed for all the suspended deck components. For the ULS load combinations is moreover required, that the main structural system shall maintain its full integrity, which here means the cross girders. Structural damage to secondary components as railway girder and roadway girder shall be repairable by means of extraordinary maintenance works.

For the SILS load combinations it is seen, that significant damage is allowed for all the suspended deck components. The SILS load combinations are therefore not considered for the suspended deck components.

5.3 Load and Load Combinations

The variable man-generated actions to be considered in the design of the suspended deck structural components is noted QL according to Design Basis (GCG.F.04.01) section 5.2. QL loads shall be used for design of local structural system at micro- and meso-levels. The suspended deck structural components are verified using the QL load combinations listed in the Design Basis, Section 6.8. The QL load combinations for SLS and ULS are presented in Table 5-3 and Table 5-4.

Table 5-3 Combinations corresponding to Serviceability Limit States (SLS) Characteristic considering the QL load

	PP	PN	QL							VV	VT	VR	VS
			Road			Rail							
			LM1	LM2	Brake	LM71, SW/0, SW/2, HLSM(3)	Un-loaded	Brake & Acc	Nosing				
1	1.00	1.00	1.00	-	-	0.80	-	0/0.40	0/0.80	0.60	0.60	0.60	-
2	1.00	1.00	1.00	-	-	0.40/0.80	-	0.80	0/0.40	0.60	0.60	0.60	-
3	1.00	1.00	-	1.00	-	0.80	-	0/0.40	0/0.80	0.60	0.60	0.60	-
4	1.00	1.00	-	1.00	-	0.40/0.80	-	0.80	0/0.40	0.60	0.60	0.60	-
5	1.00	1.00	0.75(TS) 0.40(UDL)	-	1.00	0.80	-	0/0.40	0/0.80	0.60	0.60	0.60	-
6	1.00	1.00	0.75(TS) 0.40(UDL)	-	1.00	0.40/0.80	-	0.80	0/0.40	0.60	0.60	0.60	-
7	1.00	1.00	-	0.75	1.00	0.80	-	0/0.40	0/0.80	0.60	0.60	0.60	-
8	1.00	1.00	-	0.75	1.00	0.40/0.80	-	0.80	0/0.40	0.60	0.60	0.60	-
9	1.00	1.00	0.75(TS) 0.40(UDL)	-	-	1.00	-	0/0.50	0/1.00	0.60	0.60	0.60	-
10	1.00	1.00	0.75(TS) 0.40(UDL)	-	-	-	1.00	-	1.00	0.60	0.60	0.60	-
11	1.00	1.00	0.75(TS) 0.40(UDL)	-	-	0.50/1.00	-	1.00	0/0.50	0.60	0.60	0.60	-
12(2)	1.00	1.00	0.75(TS) 0.40(UDL)	-	-	0.60	-	0.60	0.60	0.60	0.60	0.60	-
13	1.00	1.00	0.75(TS) 0.40(UDL)	-	-	-	-	-	-	1.00	0.60	0.60	-
14	1.00	1.00	0.75(TS) 0.40(UDL)	-	-	0.80	-	0/0.40	0/0.80	0.60	1.00	0.60	-
15	1.00	1.00	0.75(TS) 0.40(UDL)	-	-	0.40/0.80	-	0.80	0/0.40	0.60	1.00	0.60	-
16	1.00	1.00	0.75(TS) 0.40(UDL)	-	-	0.80	-	0/0.40	0/0.80	0.60	0.60	1.00	-
17	1.00	1.00	0.75(TS) 0.40(UDL)	-	-	0.40/0.80	-	0.80	0/0.40	0.60	0.60	1.00	-
18	1.00	1.00	0.2	-	-	0.30(1)	-	-	-	-	0.60	-	1.00

[1]Only one track need to be loaded and load model SW/2 can be neglected.
[2] Load case is only to be applied for investigating cracking of concrete.
[3] Apply load groups as indicated in table 23A-1

Table 5-4 ULS road and rail combination for QL load

	PP	PN	QL							VV	VT	VR	VS	A
			Road			Rail								
			LM1	LM2	Brake	LM71, SW/0, SW/2, HLSM[2]	Un-loaded	Brake & Acc	Nosing					
1	1/1.35	1/1.5	1.35	-	-	1.16	-	0/0.58	0/1.16	0.60	0.60	0.60	-	-
2	1/1.35	1/1.5	1.35		-	0.58/1.16	-	1.16	0/0.58	0.60	0.60	0.60	-	-
3	1/1.35	1/1.5	-	1.35	-	1.16	-	0/0.58	0/1.16	0.60	0.60	0.60	-	-
4	1/1.35	1/1.5	-	1.35	-	0.58/1.16	-	1.16	0/0.58	0.60	0.60	0.60	-	-
5	1/1.35	1/1.5	1.01(TS) 0.54(UDL)	-	1.35	1.16	-	0/0.58	0/1.16	0.60	0.60	0.60	-	-
6	1/1.35	1/1.5	1.01(TS) 0.54(UDL)	-	1.35	0.58/1.16	-	1.16	0/0.58	0.60	0.60	0.60	-	-
7	1/1.35	1/1.5	-	1.01	1.35	1.16	-	0/0.58	0/1.16	0.60	0.60	0.60	-	-
8	1/1.35	1/1.5	-	1.01	1.35	0.58/1.16	-	1.16	0/0.58	0.60	0.60	0.60	-	-
9	1/1.35	1/1.5	1.01(TS) 0.54(UDL)	-	-	1.45	-	0/0.73	0/1.45	0.60	0.60	0.60	-	-
10	1/1.35	1/1.5	1.01(TS) 0.54(UDL)	-	-	-	1.45	-	1.45	0.60	0.60	0.60	-	-
11	1/1.35	1/1.5	1.01(TS) 0.54(UDL)	-	-	0.73/1.45	-	1.45	0/0.73	0.60	0.60	0.60	-	-
12	1/1.35	1/1.5	1.01(TS) 0.54(UDL)	-	-	0.87	-	0.87	0.87	0.60	0.60	0.60	-	-
13	1/1.35	1/1.5	1.01(TS) 0.54(UDL)	-	-	-	-	-	-	1.00	0.60	0.60	-	-
14	1/1.35	1/1.5	1.01(TS) 0.54(UDL)	-	-	1.16	-	0/0.58	0/1.16	0.60	1.00	0.60	-	-
15	1/1.35	1/1.5	1.01(TS) 0.54(UDL)	-	-	0.58/1.16	-	1.16	0/0.58	0.60	1.00	0.60	-	-
16	1/1.35	1/1.5	1.01(TS) 0.54(UDL)	-	-	1.16	-	0/0.58	0/1.16	0.60	0.60	1.00	-	-
17	1/1.35	1/1.5	1.01(TS) 0.54(UDL)	-	-	0.58/1.16	-	1.16	0/0.58	0.60	0.60	1.00	-	-
18	1	1	0.20	-	-	0.30[1]	-	-	-	-	0.50	-	1	-
19	1	1	0.20	-	-	0.30[1]	-	-	-	-	0.50	-	-	1

[1] Only one track need to be loaded and load model SW/2 can be neglected.
[2] Apply load groups as indicated in table 23A-1
Load combination no. 12 is only to be used for investigation of cracking in concrete

6 Global Structural FE-Analyses

The Messina Strait bridge is modelled and analysed in the COWI developed analysis program IBDAS (Integrated Bridge Design and Analysis System). This section describes the approach to particular aspects of the structural analysis that affect the suspended deck design. The bridge model and structural analysis, in general, are described in the report "CG.10.00-P-RG-D-P-CG-S5-00-00-00-00-01 Global IBDAS Model, Description."

6.1 IBDAS Global Beam Model and Semi-Local Shell Model

In the IBDAS global FE-model, the suspended deck structure is generally modelled with beam elements. This model is used for the overall verification of the suspended structure elements. Furthermore a semi-local IBDAS shell FE-model has been developed and implemented into the global beam FE-model. Hereby it is possible to investigate the stress flow within the suspended deck structure in more details with the benefit of getting boundary conditions automatically from the global beam model. During the design process, the semi-local IBDAS shell model have been utilised for comparisons with the verification spreadsheet ADVERS and the local FE-models.

All calculations performed with the structural self weight (PP) including self weight of non-structural elements (PN) based on theory of elasticity and second order analysis (geometric non-linear analysis). Additional bending moments due to global 2. order effects from the design actions of PP and PN are hence directly included in the results from the IBDAS global analysis model.

7 Verification - Longitudinal Steel

7.1 ADVERS

7.1.1 Introduction

In order to structure and generalise calculations of the longitudinal steel of road-, railway- and cross girders of the Messina Strait Bridge an **Ad**vanced Steel **Ver**ification **S**preadsheet (ADVERS) has been developed based on the Eurocodes. The verification of the longitudinal steel girders are based on computerised analyses (IBDAS), member sizing, section verification, stress and buckling checks. The design is made in accordance with the project specific Design Basis and with background in the Eurocodes (EC).

The overall verification of the suspended deck is done based on the derived section forces obtained from the Global IBDAS FE-model.

7.1.1.1 Codes

The verification of the longitudinal steel is based on the Design Basis and the therein referenced codes. The main codes for the verifications of the steel are:

- EC3 1993-1-1:2005 "General rules and rules for buildings".
- EC3 1993-1-5:2006 "Plated structural elements".
- EC3 1993-2:2006 "Steel Bridges".

7.1.2 Verification Basis

The verification spreadsheet is developed according to the guidelines stated in the Eurocodes for steel structures. The purpose made spreadsheet is designed to be used on a closed steel box with any type of outer geometry and location of longitudinal stiffeners. The spreadsheet calculates gross and effective section properties for a given set of parameters including the section geometry, plate thicknesses, stiffener types and spacing, diaphragm spacing and length of the moment diagram. The calculations are based on sectional forces from the global IBDAS FE-beam model.

The spreadsheet enables simultaneously verification of a random number of sections throughout the bridge length if only the plate thicknesses or steel quality changes and the outer geometry are fixed.

7.1.2.1 Loads

The spreadsheet is structured in such a way that the verification is dependent on IBDAS beam model output with sectional forces about "IBDAS main axis" in the global coordinate system. Maximum and minimum values for the 6 beam member sectional forces (Ns, My, Mz, Vy, Vz, Mt) are used in the calculations according to IBDAS left hand coordinate system, see Figure 7-1.

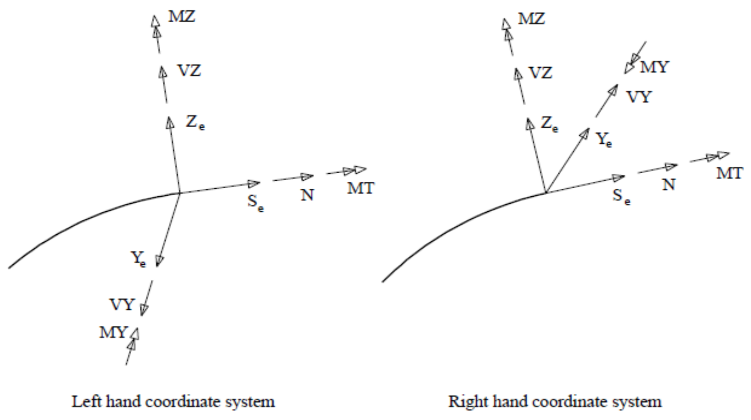

Figure 7-1 Definition of section forces

7.1.3 Section Properties

Based on the user defined geometry in the spreadsheet the gross and effective section properties are calculated according to a global reference coordinate system. In case the defined section is asymmetric around both axes, the principal axis will be rotated according to the global reference system as used in IBDAS. Hence the calculation of section properties and stresses are corrected according to this effect in the spreadsheet.

The sectional properties are calculated by first considering each individual plate and stiffener separately and then using the parallel axis theorem (Huygens-Steiner) relating these to the centre of gravity of the cross section. This method also enables local verifications of stiffened panels and plates in the spreadsheet.

The following properties are calculated in ADVERS:

- A, I_Y, I_Z and I_{yz} are calculated for gross and effective sections according to the reference coordinate system
- The angle between main and principal axis is calculated for all section properties
- I_1 and I_2 are calculated for gross and effective sections according to the principal axis
- Shear areas A_y, A_z according to principal axis and torsional area A_0 are calculated

7.1.4 Effective Cross Section Properties

For cross sections in class 4 which are unable to obtain the full yield stress under loading the effective section properties are calculated using the "reduced width method" as described in EN 1993-1-5:2006 taking into account the effect of shear lag and plate buckling. This method is preferred over the "reduced stress method", since it will have a greater structural economy due to the allowance for beneficial shedding of load from overstressed panels. Since the considered cross section has longitudinal stiffeners the derivation of the effective section is made considering both local buckling (column buckling) of plate sub-panels, stiffened panels and overall buckling of stiffened plates.

The effective width (e.g. effective area) of a plate/panel is calculated separately for axial loads and bending since these will vary with each load case, as prescribed in EN 1993-1-5:2006 section 4.3.

The following cases are considered according to the IBDAS left hand rule:

Table 7-1 Illustration of different load situations used as basis for properties calculation

Gross Section Properties	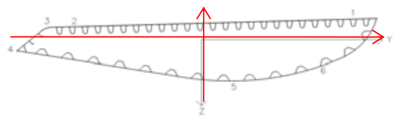
Effective Section Properties *Entire section in compression N<0*	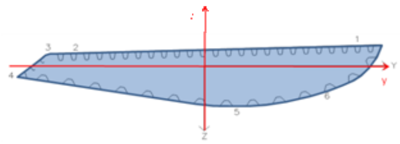
Effective Section Properties *Sagging moment $M_y>0$*	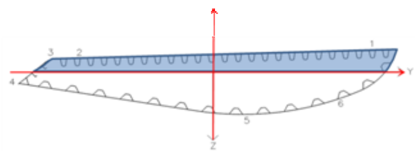
Effective Section Properties *Hogging moment $M_y<0$*	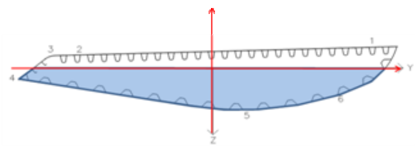
Effective Section Properties *Vertical moment $M_z>0$*	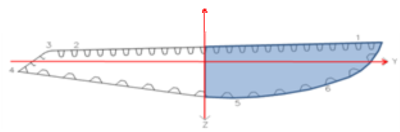
Effective Section Properties *Vertical moment $M_z<0$*	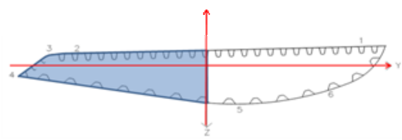

7.1.4.1 Local Buckling

A local verification of each single compression element (sub-panel and stiffened members) of the cross section is performed. The column type buckling behaviour is calculated according to EN

1993-1-1:2005 section 6.3 using the effective properties (A_{eff}, I_{eff}, W_{eff}) as prescribed in section 4.2 and 4.3 of EN 1993-1-5:2006 and plate reduction factors ρ according to EN 1993-1-5:2006 section 4.4, so: $A_{c.eff}=A_c \cdot \rho$

The distribution of the effective area within the element is determined according to Table 4.1 and 4.2 in section 4.4 of EN 1993-1-5:2006.

For each individual sub-panel and stiffened member a critical axial stress is calculated based on the reduced area, and compared to the actual stress calculated for the cross section at its given location, thus verifying any local instability problems. Due to local traffic loading also local bending will occur at some panels. The critical stress is then calculated according to EN 1993-1-1:2005 section 6.3.3 for combined axial force and bending:

$$\frac{N_{Ed}}{\dfrac{\chi_y N_{Rk}}{\gamma_{M1}}} + k_{yy}\frac{M_{y,Ed} + \Delta M_{y,Ed}}{\chi_{LT}\dfrac{M_{y,Rk}}{\gamma_{M1}}} \leq 1$$

Tables B1 and B3 of EN 1993-1-1:2005 are used to calculate the equivalent uniform moment factor, C_m, determined for concentrated load and the interaction factor, k_{yy}, using an iterative approach.

7.1.4.2 Shear Lag

The cross sectional area to be neglected in the sectional properties calculation due to shear lag is calculated based on EN 1993-1-5:2006 section 3. The values needed for L_e defining the length between zero bending moment is taken from the global IBDAS verification model and used to calculate the shear lag factors β accounting for width-to-span ratio and stiffening. For the Serviceability Limit State (SLS) the effective width $b_{eff}=b_0\beta$ for shear lag under elastic conditions are calculated according to 1993-1-5:2006 section 3.2, see illustration below for top flange.

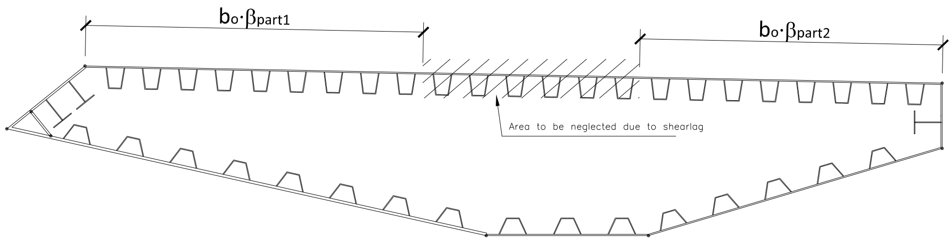

Figure 7-2 Illustration of area to be neglected due to shear lag

The effective area accounting for both plate buckling and shear lag effects is the effective plate area within b_{eff}.

For the Ultimate Limit State (ULS) EN 1993-1-5:2006 section 3.3, Note 3 is applied using $A_{eff}=A_{c,eff}\beta^{\kappa}$ on the entire plate area allowing for plastic redistribution.

7.1.4.3 Plate Buckling

For stiffened plates the interaction between plate and column buckling according to EN 1993-1-5 sec. 4.5 is investigated for each plate within the cross section using the plate reduction factor ρ_c formula (4.13) of section 4.5.4. A critical stress $\sigma_{Ed,\ Cr}$ for the plate is calculated by considering the plate and stiffeners as an equivalent orthotropic plate according to EN 1993-1-5:2006 Annex A1. For plates with less than three longitudinal stiffeners in the compression zone the method in Annex A1 can be simplified using Annex A2. In ADVERS it is chosen always to use the method as described in Annex A1 of EN 1993-1-5:2006. The calculated critical stress is compared with the axial stress σ_1 in the plate and the utilisation ratio is determined.

Since an open stiffener has very little post-buckling capacity, which is assumed calculating the plate buckling resistance as mentioned above, each individual stiffener is investigated for torsional buckling. Since torsional buckling can lead to a rapid collapse, this is in general prevented for all stiffeners when considering the effective width method for a class 4 section.

The torsional buckling verification is done according to EN 1993-1-5:2006 section 9.2.2 for longitudinal stiffeners using formula (9.3) of section 9.2.1:

$$\frac{I_T}{I_P} \geq 5.3\frac{f_y}{E}$$

This formula is valid for bulb and flat stiffeners, but considered too conservative when considering stiffeners with warping resistance, such as T- and L-stiffeners. In such a case the torsional resistance is calculated in ADVERS using:

$$\lambda = \sqrt{\frac{f_y}{\frac{1}{I_P}\left[GI_T + \frac{\pi^2 E C_w}{L^2}\right]}} \leq 0.4$$

where L is the distance between transverse restraints of the stiffener

I_P is the polar moment of area of the stiffener alone about the attachment point to the plate

I_T is the St Vernant torsional constant for stiffener alone

C_W is the warping constant of the stiffener about the attachment line to the plate

In determining the limit of 0.4 it is considered that the behaviour of these stiffeners are partly plate-like and partly column-like.

7.1.4.4 Properties

The following flow chart illustrates the procedure that has been used calculating the effective section properties:

Shear lag effect

- Determine reduction factor β and κ for tension/compression flanges
- EN 1993-1-5:2006 section 3

↓

Plate buckling of elements in compression zone

- Determine reduction in area due to local buckling of plates
- EN 1993-1-5:2006 section 4

↓

Subpanel buckling of individual plates

- Determine ρ_{loc} for each plate element/stiffener part
- $A_{eff,loc}=\sum\rho_{loc,i}*b_i*t_i$
- EN 1993-1-5:2006 section 4.4 and 4.5

↓

Plate buckling of stiffened plates

- Determine reduction for buckling of stiffened panel bounded by longitudinal webs and transverse diaphragms
- EN 1993-1-5:2006 Section 4.5.1

↓

Plate-like buckling

- Determine the reduction factor considering the plate as an orthotropic plate with stiffeners smeared over the plate
- ρ calculated acc. section 4.4 with $\sigma_{cr,p}$ using Annex A.1

Column-like buckling

- Determine the reduction factor of the stiffener treated as a column
- χ_c calculated acc. section 4.5.3 with consideration given to the critical stiffener as specified in Annex A.1

↓

Interaction between plate and column buckling

- Determine the total reduction factor for buckling of the stiffened panel
- ρ_c calculated according to EN 1993-1-5:2006 section 4.5.4
- Overall effective area $A_{c,eff}$ is calculated acc. section 4.5.1

↓

Determine total effective area

- $A_{c,eff}$= overall effective area of panels considering plate buckling
- A_{gross}= gross area of the panel
- β and β^{κ}= reduction factor for shear lag in SLS/ULS
- For elements in compression A_{eff}= $A_{c,eff}\beta^{\kappa}$ (ULS)
- For elements in tension A_{eff}= $A_{gross}\beta^{\kappa}$ (ULS)

Using the above effective areas, effective section properties are then calculated based on the diagram shown in Figure 7-3 for the case of sagging moment. All elements at the compression side of the neutral axis are treated as compression elements reduced for the effect of shear lag and plate buckling. Furthermore, the neutral axis and subsequently the effective section properties are determined based on pure bending of the section as allowed by EN 1993-1-5:2006 section 4.3(4). The effective area calculated for each plate element is used to determine an equivalent thickness of the plate, and then calculating the effective section properties of each individual plate element.

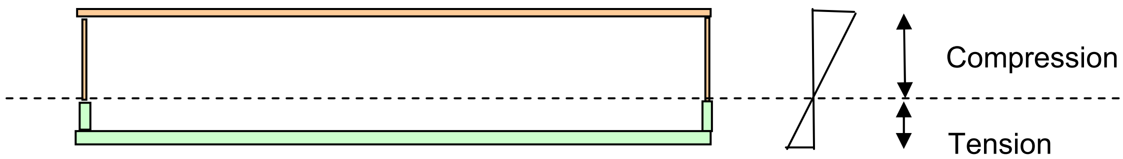

Figure 7-3 Illustration of the assumption used for calculating effective properties for a bridge girder cross section (plates only)

Regarding the effect of stiffeners in the section properties this is calculated according to their individual location in the section. Hence if a stiffener is located outside the effective width b_{eff} calculated for shear lag these are disregarded completely for both the compression and tension elements. The stiffeners within b_{eff} in the compression zone have the calculated reduced local section properties due to buckling effects. So the contribution of the local inertia of the stiffeners to the global inertia of the section is accounted for. A similar approach is used for the calculation of the section properties about the vertical axis.

7.1.5 Stresses

Stresses in considered stress points throughout the cross section are calculated based on both gross and effective sectional properties. The extreme stresses min/max σ_1 and τ including torsion are calculated. Any location within plates can be chosen for stress verification manually in the spreadsheet along with selected stiffeners etc.

Since Navier's equation is only valid for a symmetric cross section the axial stresses are calculated according to the effect around the principal axis:

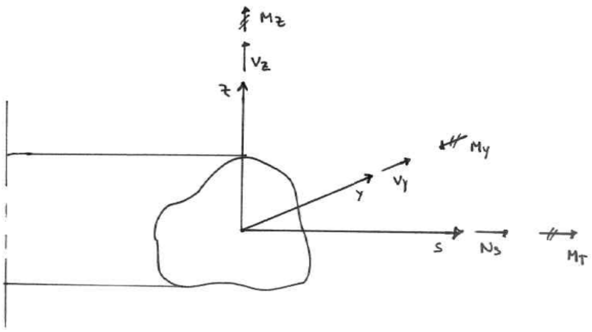

Figure 7-4 Axis and sectional force orientation used in IBDAS and for stress calculation

$$\sigma = \frac{N}{A} + M_y \frac{I_{yz}Y - I_z Z}{I_y I_z - I_{yz}{}^2} + M_z \frac{I_{yz}Z - I_y Y}{I_y I_z - I_{yz}{}^2}$$

where I_y and I_z is according to the principal axis.

The shear stress is conservatively calculated in all stress points using the formula given below

$$\tau = \left|\tau_{Vy}\right| + \left|\tau_{Vz}\right| + \left|\tau_{MT}\right|$$

7.1.6 Overall ULS Verification

In addition to local/global buckling stability check and stress calculation the following ULS verification of the cross section as a member is performed in the spreadsheet, and explained in the following sections:

- 7.1.6.1: Member in tension/compression
- 7.1.6.2: Member in bending
- 7.1.6.2: Global vertical bending, lateral bending and axial force

- 7.1.6.2: Global vertical bending, lateral bending, axial force (buckling resistance of member)
- 7.1.6.3: Shear and torsion
- 7.1.6.3: Combined shear, bending and axial force
- 7.1.6.4: Shear buckling resistance check for plates

7.1.6.1 Members in Tension/Compression

The design resistance of the cross section in tension is considered according to EN 1993-1-1:2005 section 6.2.3

$$N_{pl,Rd} = \frac{Af_y}{\gamma_{M0}}$$

The design resistance of the cross section in uniform compression is considered according to EN 1993-1-1:2005 section 6.3.1 considering the buckling resistance using effective section properties

$$N_{pl,Rd} = \frac{\chi A_{eff} f_y}{\gamma_{M1}}$$

where the buckling mode reduction factor is calculated using the imperfection factor α=0.34.

7.1.6.2 Bending and Axial Force

Due to the combined effect of bi-axial bending and axial force in the cross section - the capacity is checked according to the demands in EN 1993-1-1:2005, section 6.3.3 formulas (6.61) and (6.62), see below. The interaction factors are calculated according to Table B.1 of annex B. Due to the geometry of the section as a closed box lateral torsional buckling are unlikely to occur thus having χ_{LT}=1.0 as default.

Since the cross section is considered to be in compression there will be a shift e_N in centroid of the effective section relative to the centre of gravity of the gross cross section in both axis directions resulting in additional moments. This shift e_N is also accounted for in the calculations, thus having:

$$\frac{N_{Ed}}{\frac{\chi_y N_{Rk}}{\gamma_{M1}}} + k_{yy} \frac{M_{y,Ed} + N_{Ed} e_{Ny}}{\frac{\chi_{LT} M_{y,Rk}}{\gamma_{M1}}} + k_{yz} \frac{M_{z,Ed} + N_{Ed} e_{Nz}}{\frac{M_{z,Rk}}{\gamma_{M1}}} \leq 1$$

$$\frac{N_{Ed}}{\frac{\chi_z N_{Rk}}{\gamma_{M1}}} + k_{zy}\frac{M_{y,Ed} + N_{Ed}e_{Ny}}{\frac{\chi_{LT} M_{y,Rk}}{\gamma_{M1}}} + k_{zz}\frac{M_{z,Ed} + N_{Ed}e_{Nz}}{\frac{M_{z,Rk}}{\gamma_{M1}}} \leq 1$$

The formulas stated above apply considering the bridge girder as a member. However the capacity of the cross section for combined axial force and bending moment is also calculated according to EN 1993-1-1:2005 sec. 6.2.9. According to EN 1993-1-5:2006 section 4.3 and 4.6 if shear lag is accounted for then the method in EN 1993-1-1:2005 section 6.2.9 should be used for the verification of combined axial force and bending moment at each cross section. This verification applies at each bridge cross section and has been used as a combined check along with the above mentioned verification. The maximal utilisations of the two have been considered.

Section 6.2.9 of EN 1993-1-1:2005 prescribes that the maximum longitudinal stress shall satisfy the following, using effective properties if class 4 section:

$$\sigma_{x,Ed} \leq \frac{f_y}{\gamma_{M0}}$$

From this equation the critical moment can be calculated using that the max stress will be in the outer most stress point (SP) e.g. known y,z-coordinates in the cross section according to the principal axis. Thus any given point in the cross section can be investigated directly for this effect. So:

$$\frac{N_{Ed}}{\frac{\chi_z N_{Rk}}{\gamma_{M1}}} + \frac{M_{y,Ed} + N_{Ed}e_{Ny}}{\frac{f_y I_{y,eff}}{\gamma_{M1} z}} + \frac{M_{z,Ed} + N_{Ed}e_{Nz}}{\frac{f_y I_{z,eff}}{\gamma_{M1} y}} \leq 1$$

The calculation is thus depended on the load situation (different effective section properties) and the location considered.

7.1.6.3 Bending, Axial Force and Shear

Due to the presence of torsion producing additional shear stresses in the cross section, the combined effect is considered. The design resistance against shear and torsion is determined according to EN 1993-1-1:2005 section 6.2.3 and 6.3.1.

Without torsion: $V_{pl,Rd} = \dfrac{A_v(f_y/\sqrt{3})}{\gamma_{M0}}$; A_v is the shear area in the axis direction

With torsion: $$V_{pl,T,Rd} = \left[1 - \frac{\tau_{t,Ed}}{\dfrac{(f_y/\sqrt{3})}{\gamma_{M0}}}\right] V_{pl,Rd}$$

In principle the above verification is dealt with in ADVERS by using the calculated shear stress as described in section 7.1.5 taking the maximum value at any given location in the cross section and compare it with the shear capacity at that location:

$$Capacity: \quad \tau_{pl,Rd} = \frac{(f_y/\sqrt{3})}{\gamma_{M0}} \qquad \Rightarrow \qquad UR_i = \frac{\tau_i}{\tau_{pl,Rd}}$$

The resistance considering the combined effect of bending, axial force and shear is calculated according to EN 1993-1-1:2005 section 6.2.10. In case *UR_i>0.5* the yielding capacity is reduced for the shear area as described in section 6.2.10(3) of EN 1993-1-1:2005.

For plates the interaction between shear force, bending moment and axial force has also been investigated in ADVERS according to section 7.1 of EN 1993-1-5:2006. So in case the ration between shear resistance and shear force exceeds 50% the design resistance to bending moment and axial force is reduced to allow for the shear force using:

$$\frac{M_{Ed}}{M_{pl,Rd}} + \left(1 - \frac{M_{f,Rd}}{M_{pl,Rd}}\right)\left(2\frac{V_{Ed}}{V_{bw,Rd}} - 1\right)^2 \leq 1.0$$

$V_{bw,Rd}$ is determined according to section 5.2 of EN 1993-1-5:2006.

Same method as described above is used for verifying the flanges in the girders using $M_{f,Rd}$=0.

7.1.6.4 Shear Buckling Resistance

In ADVERS the rules regarding shear resistance of plates in shear buckling at the ULS is considered. It is investigated if a stiffened web needs to be checked for resistance to shear buckling by implementing the demand according to EN 1993-1-5:2006 section 5.1:

$\frac{h_w}{t} \leq \frac{31}{\eta}\varepsilon\sqrt{k_\tau}$ and for unstiffened webs $\frac{h_w}{t} \leq \frac{72}{\eta}\varepsilon$

However if this demand is not satisfied the design resistance is verified according to EN 1993-1-5:2006 section 5.2

$$V_{b,Rd} = V_{bw,Rd} + V_{bf,Rd} \leq \frac{\eta f_{yw} h_w t}{\sqrt{3}\gamma_{M1}}$$

In ADVERS the contribution from the flange $V_{bf,Rd}$ has conservatively been neglected. The contributions from the webs are calculated according to according to EN 1993-1-5:2006 section 5.3 non-rigid end posts are assumed in the calculations.

7.1.7 Web breathing

In order to avoid excessive breathing that might result in fatigue in plates web breathing is considered in ADVERS according to EN 1993-2 section 7.4. The calculation is disregarded if the following criteria's are met, *L* being the span length of minimum 20m:

$$b/t \leq 30 + 4.0 \cdot L \leq 300 \qquad for\ roadway\ bridges$$
$$b/t \leq 55 + 3.3 \cdot L \leq 300 \qquad for\ railway\ bridges$$

The above given statement is investigated for sub panels and plates without stiffeners.

In case the above stated criteria is not met the following criteria is investigated considering stresses for the frequent load combination (SLS):

$$\sqrt{\left(\frac{\sigma_{x,ED,ser}}{k_\sigma \cdot \sigma_E}\right)^2 + \left(\frac{1.1 \cdot \tau_{x,ED,ser}}{k_\sigma \cdot \sigma_E}\right)^2} \leq 1.1 \ ; \qquad \sigma_E = 19000 \cdot \left(\frac{t}{b}\right)^2$$

The elastic buckling coefficients, *k,* are determined using clause 4 and 5 of EN 1993-1-5 respectively.

7.1.8 Input and Output

Using the principles discussed above, stresses and local stability checks are calculated, thus verifying the overall longitudinal steel over the entire length of the bridge in ADVERS. The ULS envelopes of the section forces created in IBDAS are used for selected analysis sections (specific s-coordinates).

As user input the exact cross section geometry is defined along with the type and location of stiffeners. The input geometry is fixed for all calculations, but different cross sections can be defined by letting the thicknesses vary. From the global IBDAS model sectional forces have been applied according to selected s-coordinates (analysis sections) and for each of these locations a section type has been defined as input.

Since it is possible to have both hogging and sagging moments in most areas of the bridge, as well as both local hogging and sagging in the roadway troughs, minimum and maximum stresses at several critical points are considered. As an input to ADVERS it is defined in which points stresses needs to be considered and at which locations stiffeners are verified for local and global stability, an example is given in Figure 7-5.

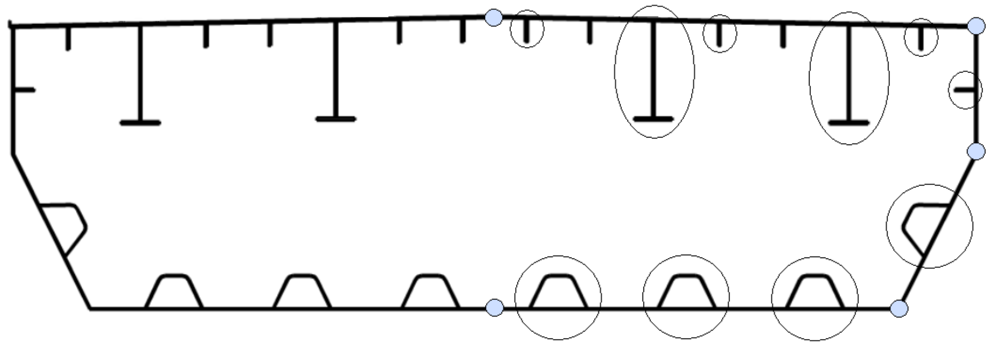

Stress Points (SP)

Selected Stiffeners

Figure 7-5 Illustration of stress points and selected stiffeners for verification

The selection as illustrated in Figure 7-5 is illustrated in ADVERS as shown in Figure 7-6.

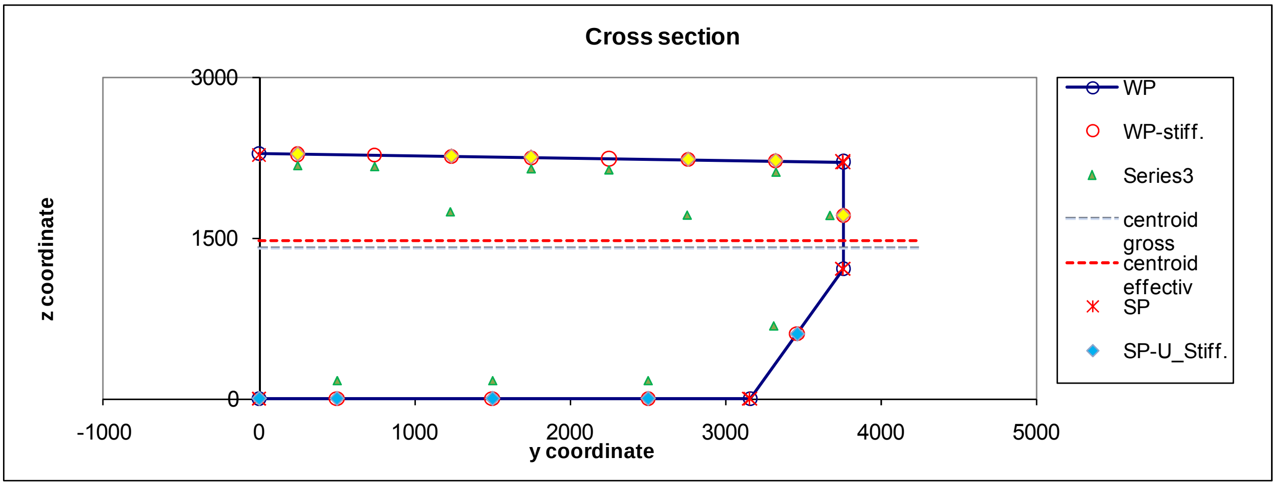

Figure 7-6 Plot of stress point location and selected stiffeners for full verification in ADVERS

The figure shows a sketch of one half of a symmetric cross section taken from ADVERS. The geometry is defined by work points marked with circles. The stress points marked with red crosses are the extreme positions in the perimeter geometry which has been verified. The centroid is marked with dotted lines both for the gross and effective cross section (full compression). The location of the centroid of the stiffeners is marked with green triangles and the selected stiffeners for full verification are marked with blue and yellow squares for trough-stiffeners and T-beams, respectively.

For each of the selected locations a full verification has been done according to the described methods in Section 7.1. The results of these verifications are a set of tables and figures plotting the utilisation ratios for each analysis section. An illustration for selected figures can be seen in Figure 7-7.

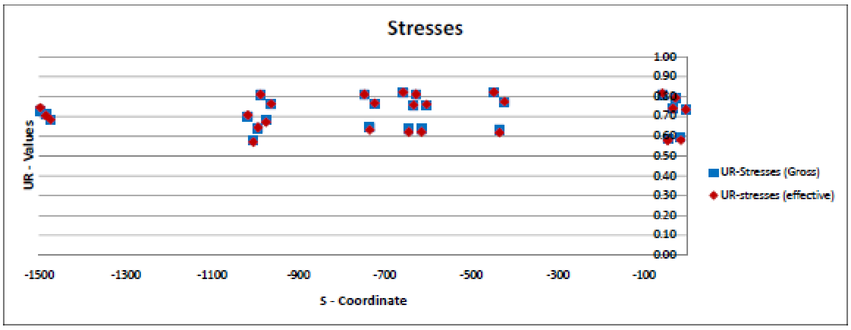

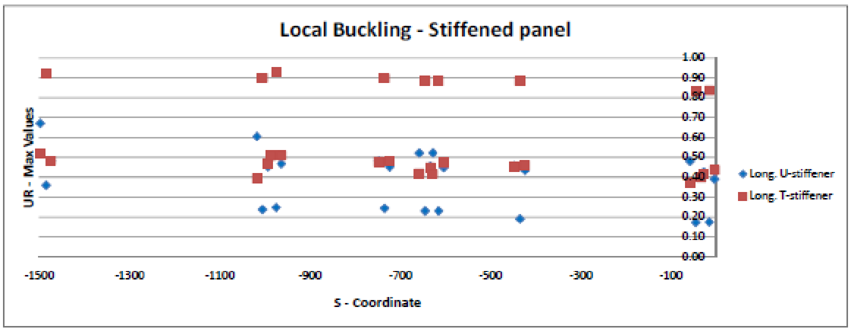

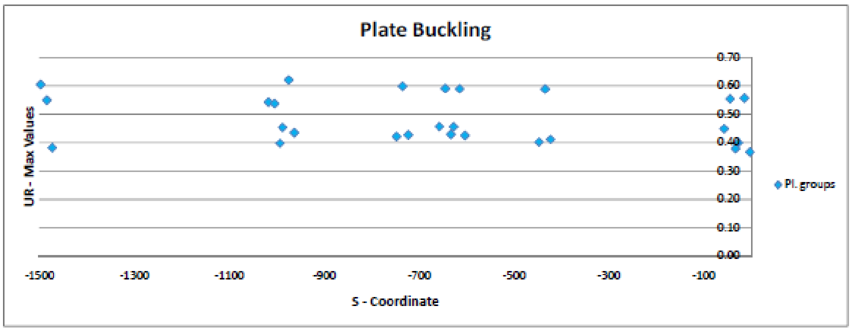

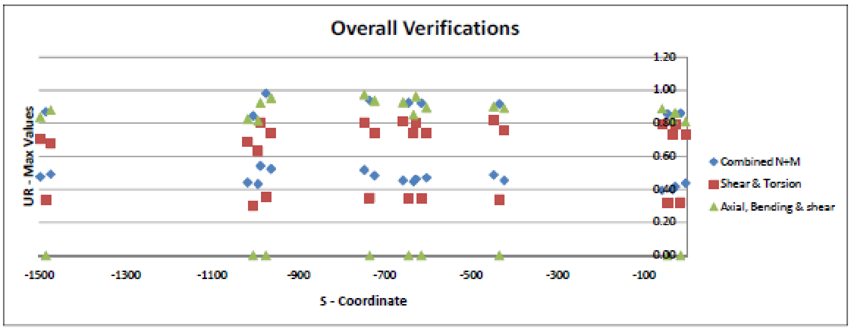

Figure 7-7 Illustration of ADVERS output results (figures only)

7.1.9 Overall ULS Verification with Transverse Stresses

Since the "effective width" method as used in ADVERS is not directly applicable in a case where there is uniform transverse stresses accompanying the longitudinal stresses the "reduced stress method" is used in that situation. This type of stress analysis is based on gross section properties and subsequent plate buckling checks according to EN1993-1-5:2006 section 10.

At the interconnection between the cross girder and the roadway- and railway girders the top plate is subjected to compression stresses in two directions. At the interconnections a spreadsheet and a calculation program for elastic buckling of plates is used to investigate the stability of the different plate fields. Compressive stresses have been calculated in a local FE-model at the location outside the plates of consideration.

The plate fields considered are modelled in an elastic buckling program, see Figure 7-8. For the roadway girder the top plate is divided into three plate fields separated by the cross girder diaphragms. The plate towards the railway girder is denoted "Plate 1". For the railway girder only one plate is considered.

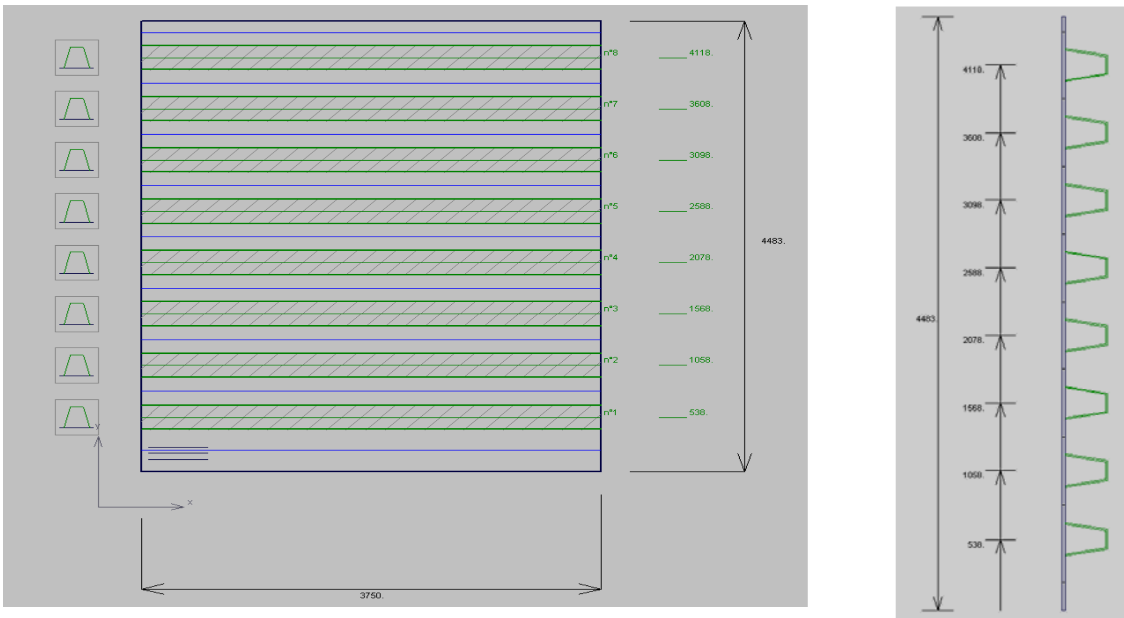

Figure 7-8 Illustration of a plate field of the roadway girder including dimensions

The critical buckling modes have also been calculated, and the governing for the illustrated plate is given in Figure 7-9.

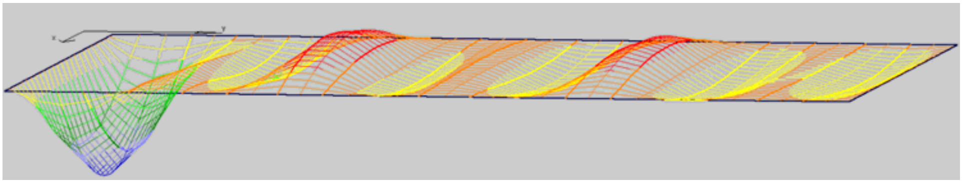

Figure 7-9 Illustration of critical buckling mode for determining critical stresses

From the elastic buckling program critical stresses are calculated considering the plate as an orthotropic plate. The critical stresses that have been calculated are corresponding to the stress limits used in the "reduced stress method" of EN 1993-1-5:2006 section 10. This method has been used to determine the utilisation ratios of the considered plates.

8 Verification Spread Sheets - Transverse Steel

8.1 Diaphragms

The longitudinal steel of the Roadway-, Railway- and Cross Girders are overall verified using ADVERS, but this spreadsheet does not consider the transverse diaphragms. Two different methods are considered verifying the diaphragms - firstly local FE-models are made in ROBOT of a bridge section, see Chapter 9. These models will give the different stress flows in the diaphragm, and investigate the behaviour around utility openings. Secondly a spreadsheet and a calculation program for elastic buckling of plates have been used to investigate the stability of the different sub-panels of the diaphragms.

The diaphragm is divided into sub-panels by distributed vertical stiffeners. It is verified that these stiffeners have sufficient capacity to support the diaphragm panels sufficiently. The capacities of these stiffeners are verified according to EN 1993-1-1:2005 section 6.3. Each sub-panel of the diaphragm is subjected to the stress distribution from both global and local traffic loading at its specific location, as illustrated on Figure 8-1. From this stress distribution it is possible to calculate a critical stress factor ϕ indicating the increase in stresses allowed before reaching the elastic critical load. The method used also accounts for stabilising effects such as rotational restraints at edges if any.

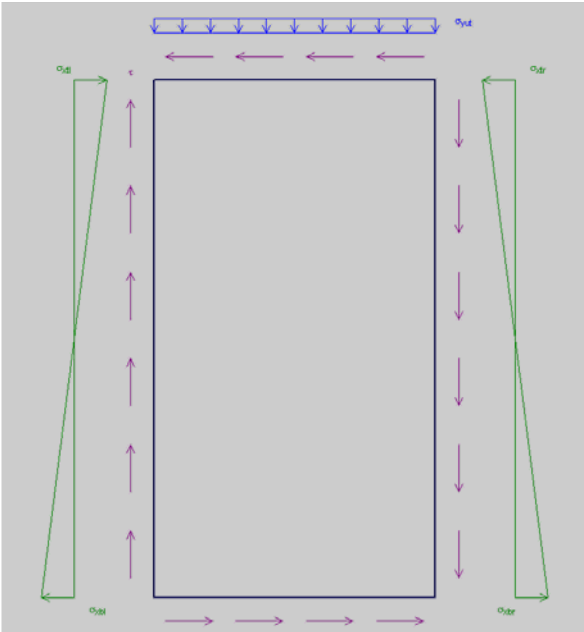

Figure 8-1 Stress distribution on diaphragm panel for buckling investigation

Since it is known that the bending stresses (eg. tension stress) may have a slightly stabilising effect on the panel a variation of load situations have been investigated to determine the most critical load situation for the panels.

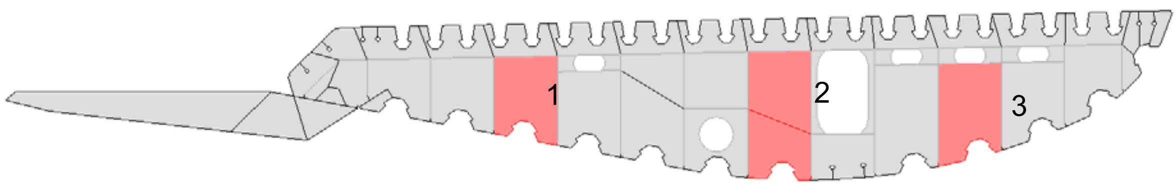

Figure 8-2 Critical panels chosen for stability verification, roadway girder diaphragm

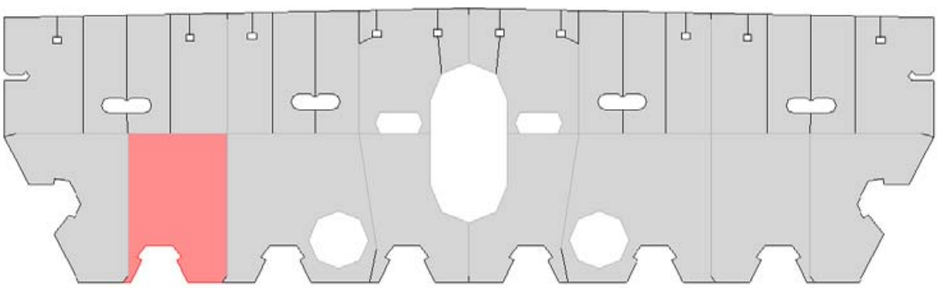

Figure 8-3 Critical panel chosen for verification, railway girder diaphragm

Subjecting the different panels, see Figure 8-2 and Figure 8-3, to calculated stress distribution from the local FE-models of the bridge the critical stress factor ϕ_{cr} has been calculated. The calculated critical factor is equal to α_{cr} used in the reduced stress method of EN 1993-1-5:2006, section 10. The calculated critical factor has thus been used directly in the reduced stress method on order to verify the panels considering both column-buckling and plate-buckling behaviour. The governing panels due to bending and shear respectively in combination with the maximum height of the panel have been chosen for verification.

9 Verification using Local FE-Models

9.1 Introduction

The local FE-models are performed in the computer program Robot Millennium 2010 an integrated graphic program used for modelling, analysing and designing various types of structures. In total four different models have been made:

- Bridge deck local FE-model dealing with the cross girder and the longitudinal roadway and railway girders determining the stress regime in the plate elements with special regards to stress in the cross girder outer plates, diaphragms and at the intersection between girders
- Roadway local FE-model describing the stress flow in the diaphragm of roadway girder with regards to the stress concentration at the troughs, cope holes, diaphragm stiffeners and openings
- Railway local FE-model describing the stress flow in the diaphragm of railway girder with regards to the stress concentration at the troughs, diaphragm stiffeners and openings

- Hanger anchorage local FE-model analysing the stress regime in the plates related to the hanger anchorages

The general purpose of the local models is to verify the proposed element solutions and to document that the stress flow is acceptable with respect to ULS load combination.

Furthermore contours plots of the FE-Local models have been compared with results from the semi-local IBDAS model. The latter has been developed within the global analysis model in the sense that for most parts of the bridge the global IBDAS model is used but for selected parts a more detailed modelling with shell elements and diaphragms is used. This ensures correct boundary conditions for the detailed model. The location and geometry of the semi-local IBDAS model is shown in Figure 9-1.

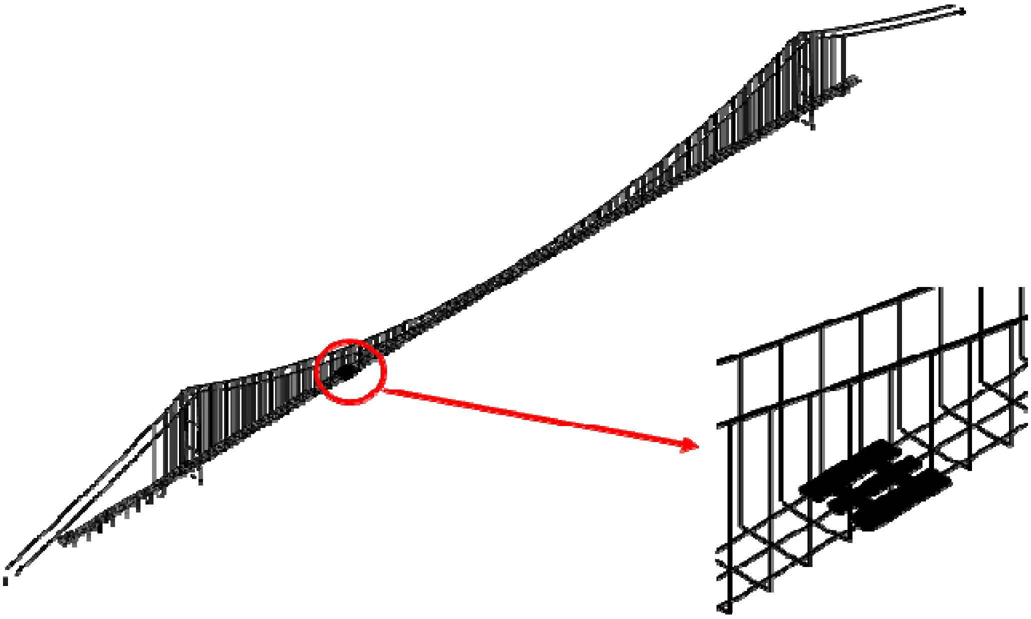

Figure 9-1 Location of the semi-local IBDAS model within the global analysis model

The shell model consists of 3 individual longitudinal girders connected by two cross girders. A rendered view of the model is shown in Figure 9-2.

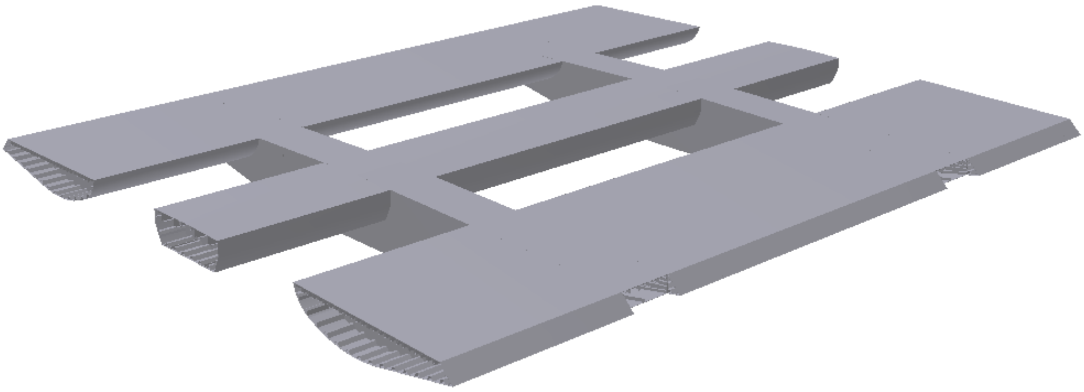

Figure 9-2 Rendered image of the suspended deck semi local IBDAS-model

All the longitudinal steel skin of the girders including stiffeners is modelled with their exact geometry and plate thicknesses. A detailed description of the model can be found in the report “Semi-local IBDAS Model, Suspended Deck”.

Further comparison with stress values given by the verification of the cross sections done by ADVERS has been performed.

The above mentioned stress comparisons as well as other relevant contour plots of stresses of relevant details modelled by the FE-local models can be found in “Design Report - Semi Local FE-model for Suspended Deck”.

9.2 Boundary Conditions and Calibration

The global boundary conditions are applied to beam elements whose section forces have been determined by Gauss Points in accordance with the global IBDAS bridge model. Beam elements create a connection between the applied IBDAS sectional forces and the centre of gravity of the girder through rigid links in each end of the shell model. The rigid links from the beam element to the shell elements combined with the relatively long span assumed for the model ensures a correct distribution of the applied IBDAS section forces when verifying the diaphragms and the elements in the intersection cross-longitudinal girders. A general description of the modelling layout applied can be found in Figure 9-3 where as an example the bridge deck FE-Local model is shown.

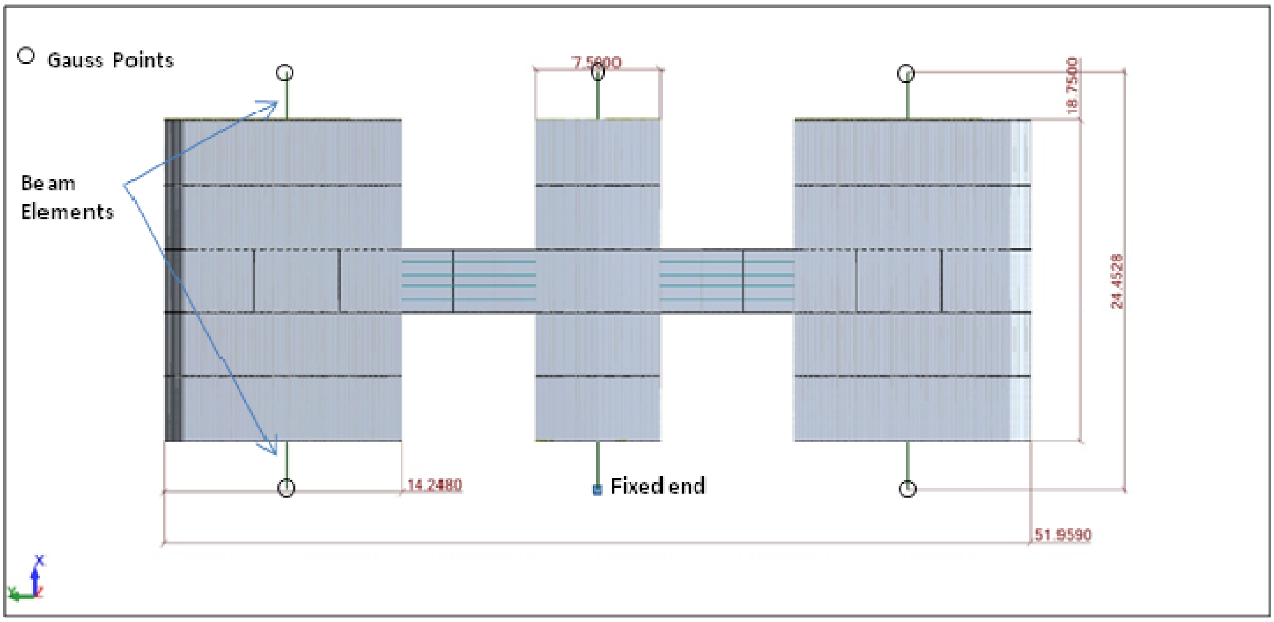

Figure 9-3 Boundary conditions and overall geometry

At Gauss Points section forces from IBDAS have been applied to the beam elements whereas the fixed end ensures restrain for all six degree of freedom. The beam elements are located in the centre of gravity of the longitudinal shell girders and the section properties correspond to the gross sectional properties of the elements they are connected to. The beam elements are connected to the shell elements through rigid links to each edge node of the shell mesh as shown in Figure 9-5.

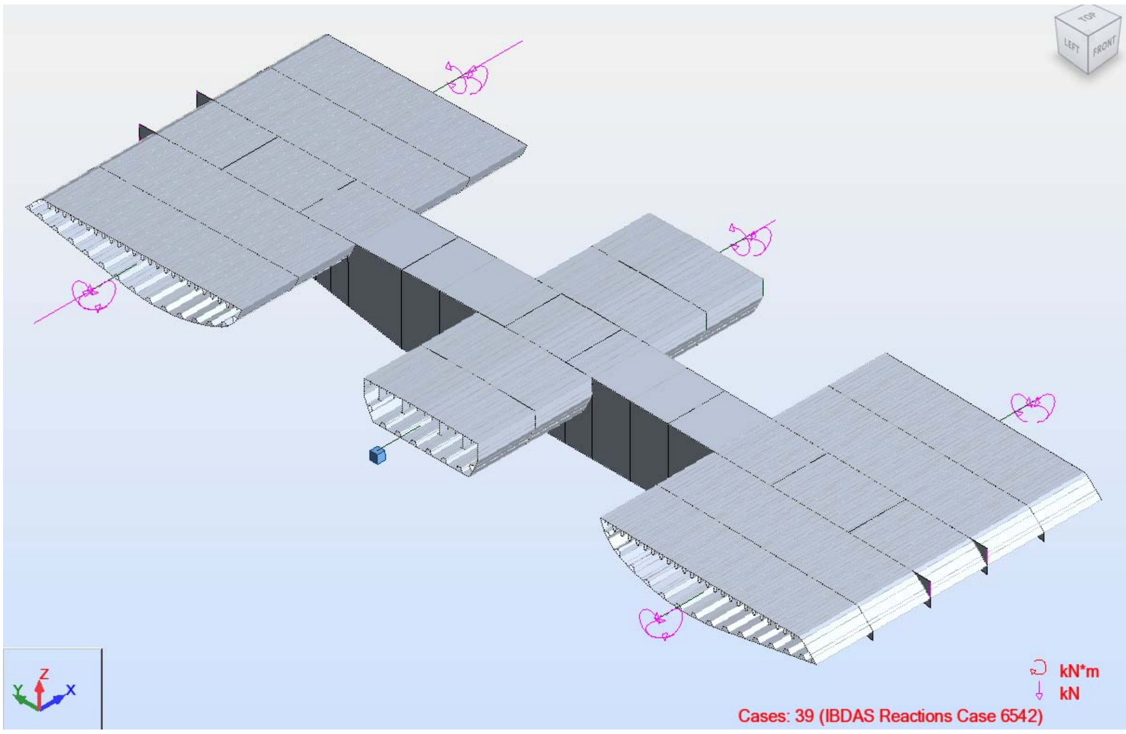

Figure 9-4 IBDAS sectional forces as Robot external forces and global coordinate system

The boundary conditions applied to the Robot model involves three axial forces and three bending moments for each node. These reflect the sectional forces present in the global IBDAS model at the same location and have been converted to external forces in the Robot local model to respect the difference of the hand rule, left for IBDAS and right for Robot. An example of the applied boundary condition is shown in Figure 9-4.

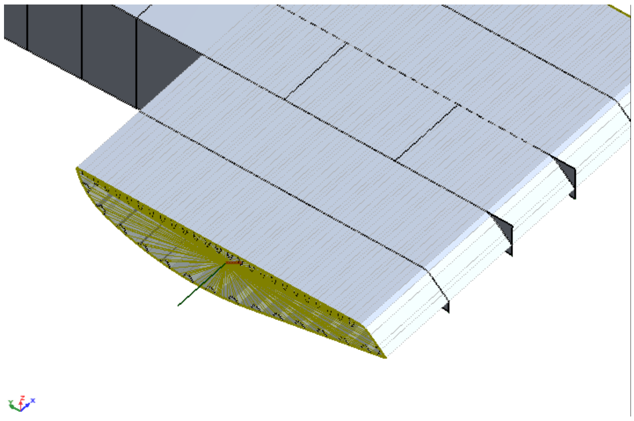

Figure 9-5 Rigid links from shell-elements to beam-elements

The models are calibrated by comparing the forces of the fixed end to the IBDAS section forces at the same location for the load combination that considers only dead loads (PP+PN) namely the reference condition case. The acting external loads are structural self weight (PP) and superimposed dead loads (PN) and the section forces are implemented considering the sign convention between the software. The investigation of the stress flow involves specific load combinations capable of maximising the effects (criteria) under consideration. IBDAS is able to perform automatic determination of bridge live load effects based on influence line calculation and the resulting loading layout has then been implemented in the ROBOT models.

9.2.1 Global and Local Coordinate System

In Robot positive orientation of forces and displacements are in accordance with the positive orientation of coordinate system axes. Positive orientations of angles, rotations or moments in the local or global coordinate system are determined on the basis of the right hand rule. This convention defines signs of external forces, nodal forces, displacements and rotations. Sign conventions are used in structure definition, during structure calculation and results display.

Loads are applied according to the global coordinate system. The global coordinate system used for reporting e.g. displacements and reactions, can be seen in Figure 9-4 and is defined as follows:

- The **X**-axis (1st axis) extends along the structure model with same orientation of IBDAS S-axis
- The **Y**-axis (2nd axis) is orthogonal to the **X**-axis and the **Z**-axis forming a right hand coordinate system with opposite orientation to IBDAS Y-axis

- The **Z**-axis (3rd axis) is vertical and extends positive upward with same orientation as IBDAS Z-axis

Every panel has a local coordinate system in which the stresses are calculated. In Figure 9-6 an example of a local system is shown which as the global system corresponds to the right hand rule.

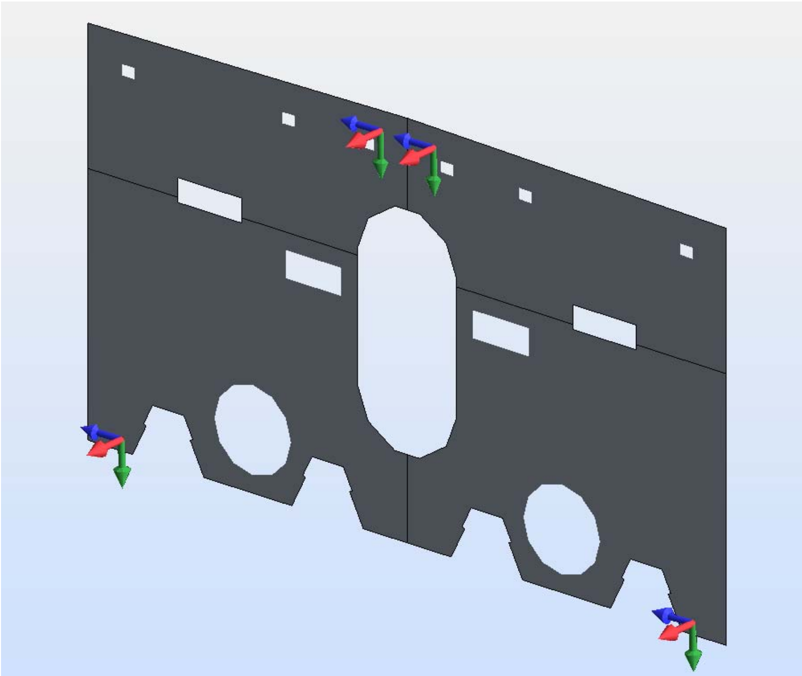

Figure 9-6 Panel local coordinate system

The local **X**-axis and **Y**-axis are always located in the panel plane while the local **Z**-axis always is orientated perpendicular to the panel.

9.2.2 Basic Assumption

The following material properties are used in the different ROBOT models:

Structural steel: Density: 77.0 kN/m^3

Young's modulus: 210000 MPa

Steel grade longitudinal elements:

f_{yk}: 460 MPa (Bridge deck FE-Local model)

f_{yk}: 420 MPa (Roadway FE-Local model)

f_{yk}: 355 MPa (Railway FE-Local model)

f_{yk}: 460 MPa (Hanger anchorage FE-Local model)

Steel grade transverse elements:

f_{yk}: 460 MPa (Bridge deck FE-Local model)

f_{yk}: 420 MPa (Roadway FE-Local model)

f_{yk}: 355 MPa (Railway FE-Local model)

f_{yk}: 460 MPa (Hanger anchorage FE-Local model)

Section properties used for the beam elements in the local FE-models are shown in Table 9-1.

Table 9-1 Section properties for beam elements used in the local FE-models

Section	y-distance to C.G. [m]	z-distance to C.G. [m]	Area [m^2]	Iy [m^4]	Iz [m^4]	J [m^4]
CS1	8.484	2.866	0.565	0.405	9.214	0.967
CS2	8.485	2.834	0.581	0.431	9.498	1.042
CF1	0	1.401	0.365	0.316	2.037	0.642

The position of origo for centre of gravity is shown in Figure 9-7.

Figure 9-7 Position of origo for centre of gravity

9.3 Bridge deck local FE-model

A local FE-model of the cross girder and adjoining roadway and railway girders has been carried out to determine the stress regime and stress concentrations of various plates with special regards to the cross girder elements and the intersection between longitudinal girders and cross girder. Moreover the model is used to assess the stress of the deck plates at the intersection with the cross girder subjects to stresses in two directions; this made possible the verification of the stability of the different plate fields. Additionally the stress plots will be compared with the one determined by the semi local IBDAS model and with the stress results from ADVERS.

9.3.1 Geometry

The overall dimensions of the model cover the full width of the bridge deck and extends by five modules each 3.75 m long and two beam elements a side for an overall plan dimension of approximately 24.5 m x 52 m (from IBDAS s-coordinate -432 and -417) as shown in Figure 9-8. It includes both the roadway and the railway girder enabling the determination of stress concentrations of the latter elements at the intersection with the cross girder as well as a detailed assessment of the stress regime in the outer plates and diaphragms of the cross girder.

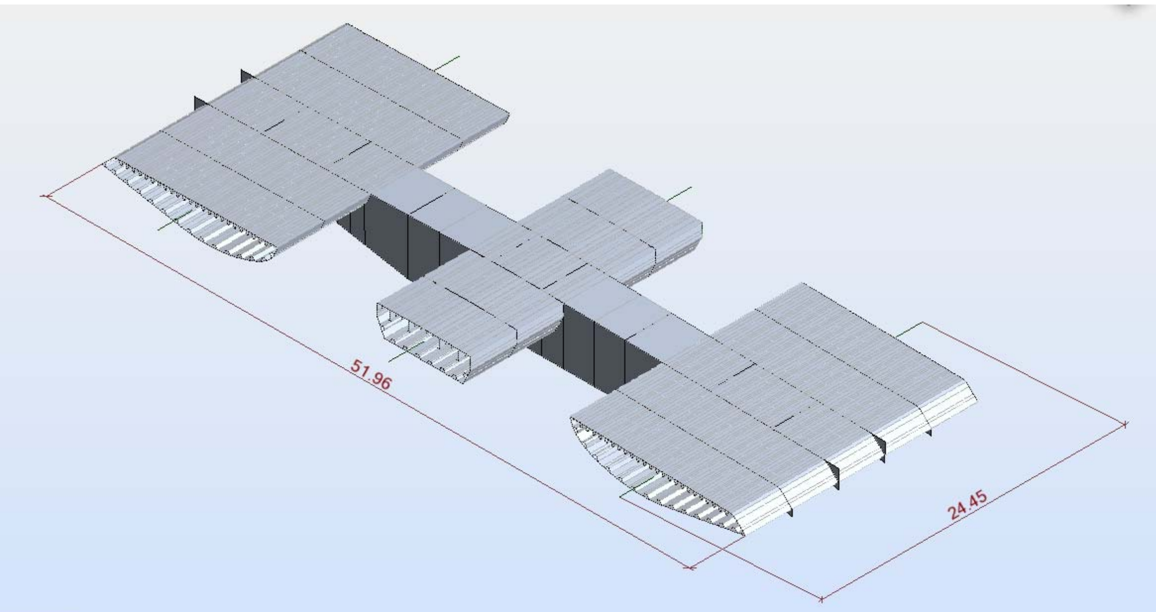

Figure 9-8 Overall geometry

The location of the model has been determined by selecting a section with the highest utilisation ratio among the cross girders in the main span. In order to make a conservative design the modelled cross girder is in correspondence of the cross over location which leads to an increment of the self weight. Further analysis can be done to the typically loaded cross girder that anyhow will lead to lower utilization ratio and thereby stress concentration of lower intensity. The model comprises the element CS1 for the roadway girders and CF1 for the railway girders therefore the steel grade used throughout the model is S460 in accordance with the steel grades used in the design. At the present stage the hatches in the cross girders webs are neglected. Those cross girders will anyhow be part of further investigation in the next phase of the design. For a description of the hatches and various accesses provided for the suspended deck, refer to the document "Performance Specification – General access facilities".

The model consists of shell elements (FE-panels) with thicknesses consistent in values and names to the ones stated in the design drawings mentioned in Table 9-2.

Table 9-2 Drawing used as geometrical basis of the model

CG1000	P	WX	D	P	SV	I3	CS	00	00	00	01
CG1000	P	AX	D	P	SV	I3	CS	00	D0	00	01
CG1000	P	WX	D	P	SV	I3	CF	00	00	00	01
CG1000	P	AX	D	P	SV	I3	CF	00	D0	00	01
CG1000	P	WX	D	P	SV	I3	TP	00	00	00	01
CG1000	P	WX	D	P	SV	I3	TP	00	00	00	02
CG1000	P	AX	D	P	SV	I3	TP	00	D0	00	01

A plot of the model with highlighted thickness differences for top and bottom plates is shown in Figure 9-9 and Figure 9-10. The thicknesses of the diaphragms and stiffeners are illustrated in Figure 9-11 and Figure 9-12 (for clarity only half bridge is shown for the diaphragms and only a module 3.75 m long is shown for the stiffeners).

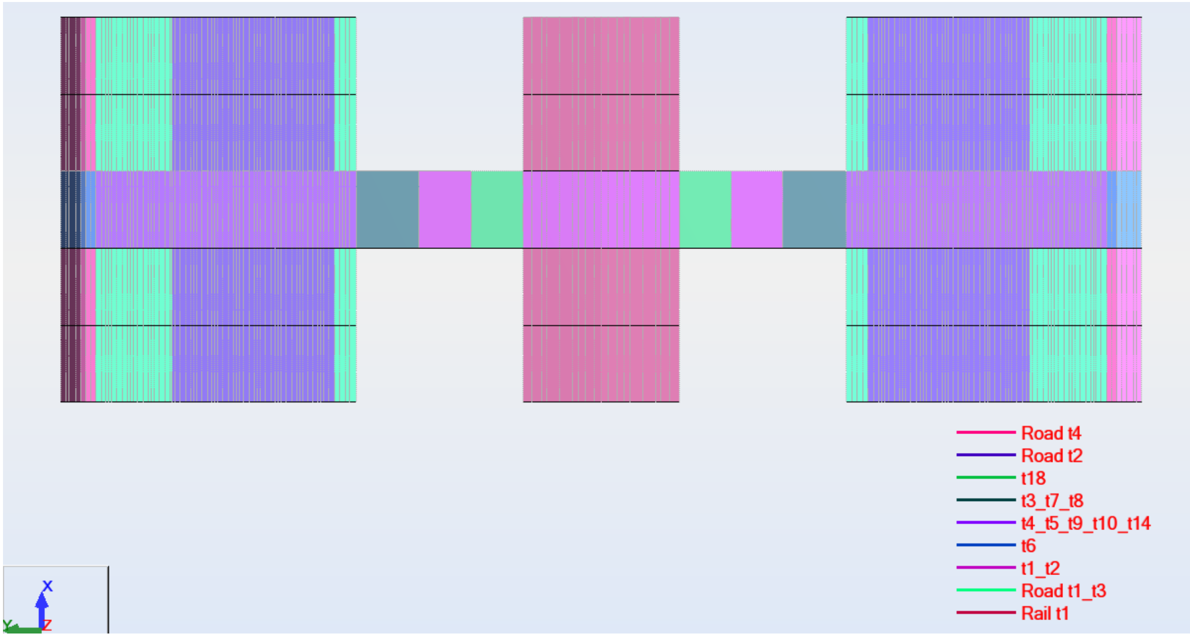

Figure 9-9 Thicknesses highlighted by means of colours – top plates

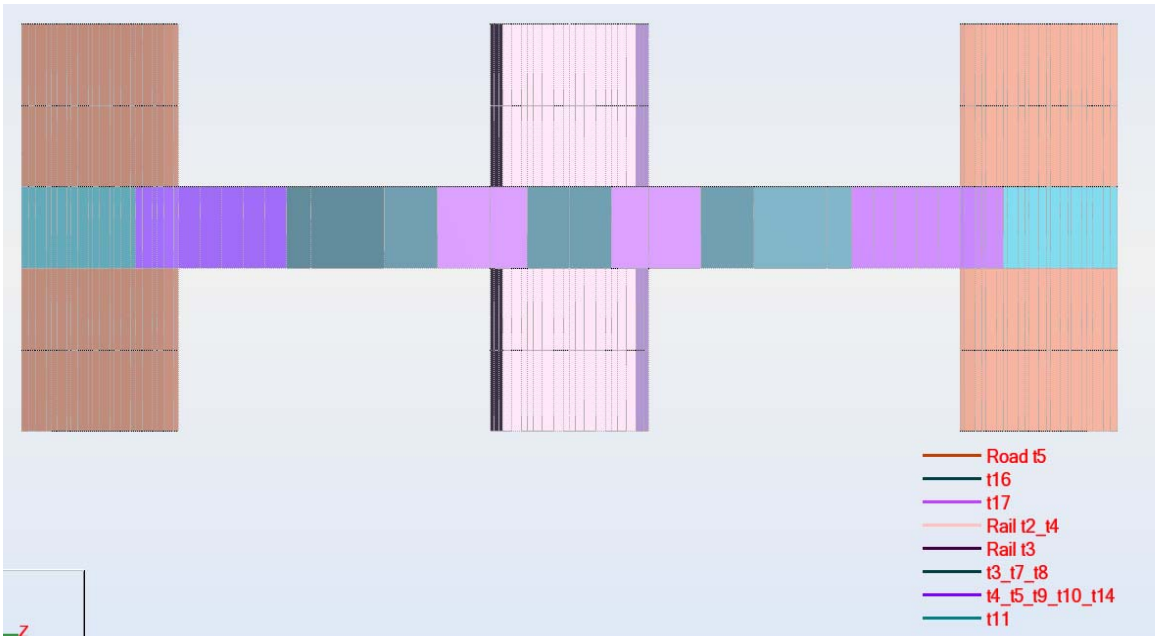

Figure 9-10 Thicknesses highlighted by means of colours – bottom plates

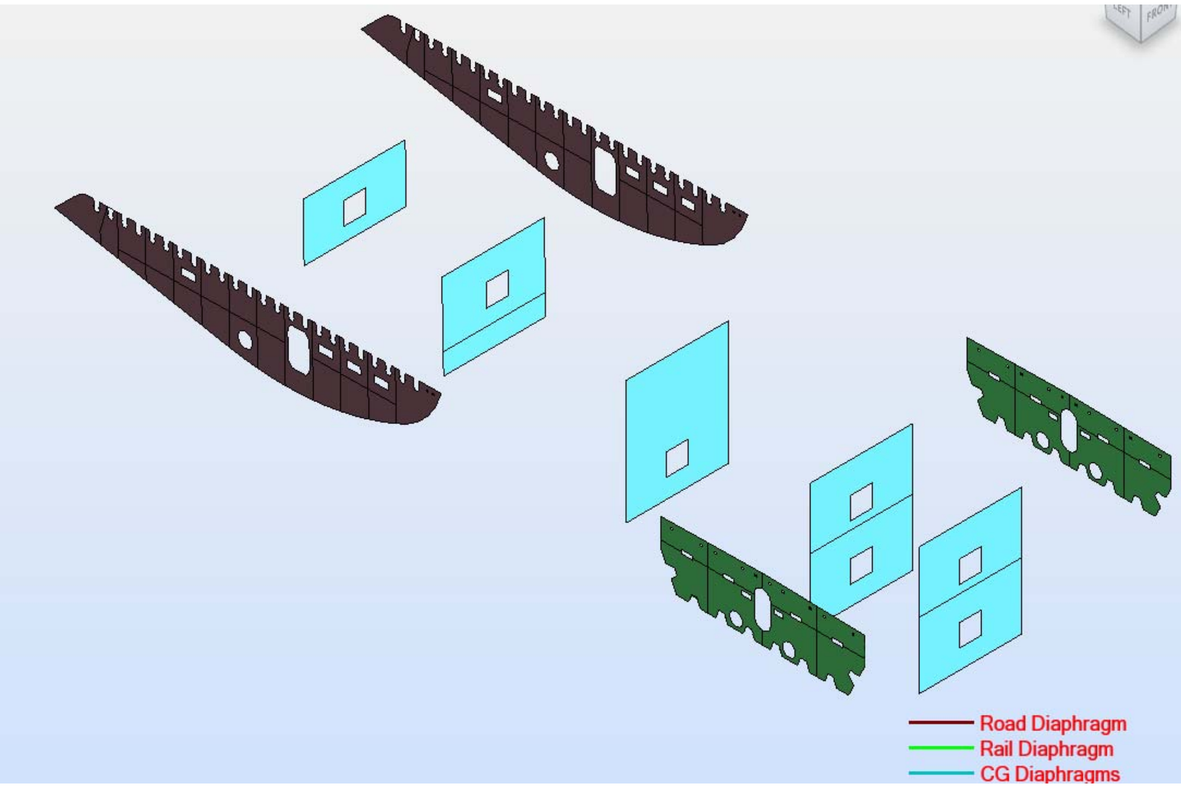

Figure 9-11 Thicknesses highlighted by means of colours – diaphragms

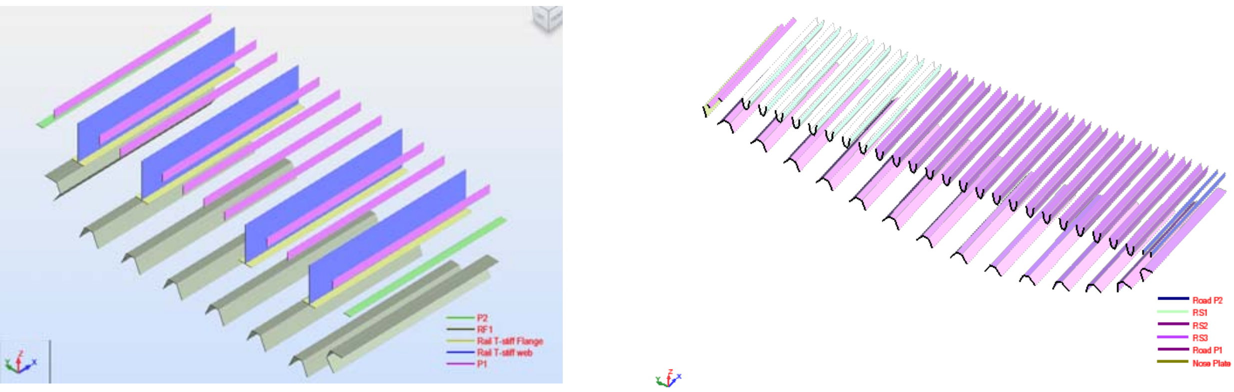

Figure 9-12 Thicknesses highlighted by means of colours – stiffeners

For the diaphragms an equivalent thickness has been assumed as the model does not include the stiffeners around the utility holes. Stiffening of the manholes has been instead achieved by means of beam elements which can guarantee the necessary stiffness in order to avoid critical stress concentration that otherwise would occur. Furthermore the model is composed by shell elements

(FE-panels) for the whole longitudinal girders whereas the stiffeners as well as the transverse stiffeners in the cross girders are modelled by beam elements linked to the plates, see Figure 9-13; this assumption have the goal of reducing significantly the complexity and the calculation time without affecting the accuracy of the analysis.

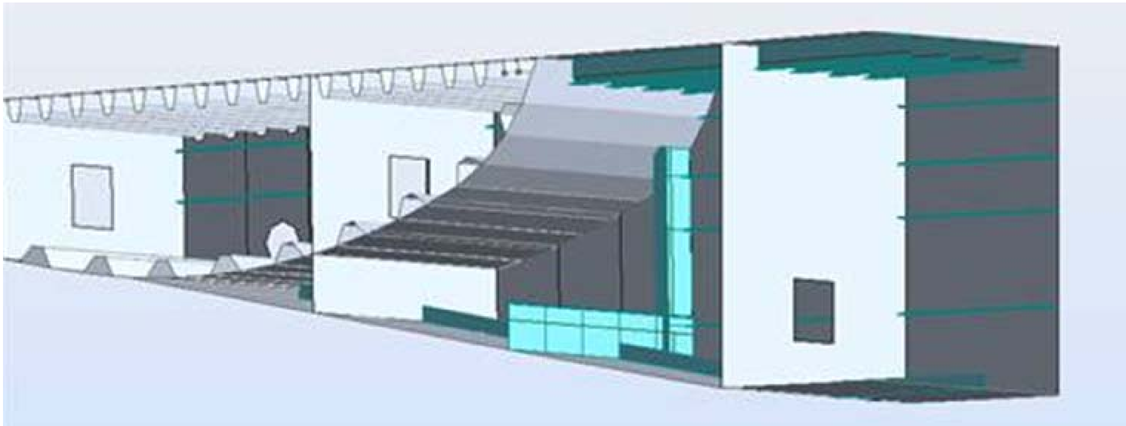

Figure 9-13 Detail of cross girder: transverse stiffeners, longitudinal stiffeners and diaphragms

Due to the fairly constant geometry in longitudinal direction, the generation of the longitudinal elements has been done by extrusion based on a given cross section with a mesh dimension of 75 cm in length (the modules of 3.75 m long has been split in 5 parts) and about 40 to 100 cm in width. The generated mesh comprises of 26517 nodes and can be seen in Figure 9-14.

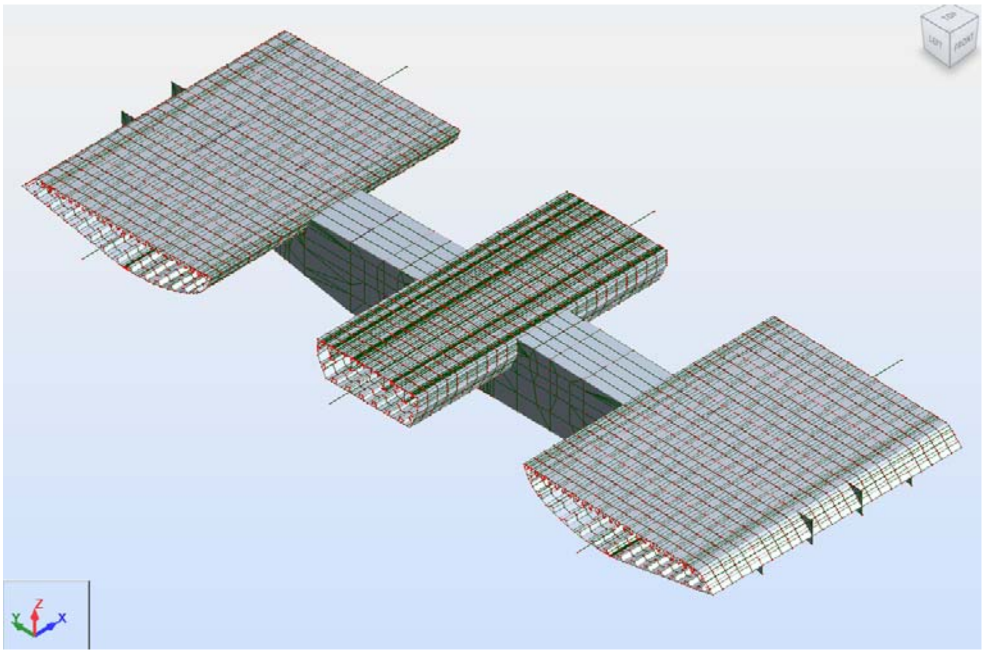

Figure 9-14 Overall mesh layout

Other mesh details can be seen in Figure 9-15 and Figure 9-16 concerning respectively with the cross girder and the longitudinal girder diaphragms.

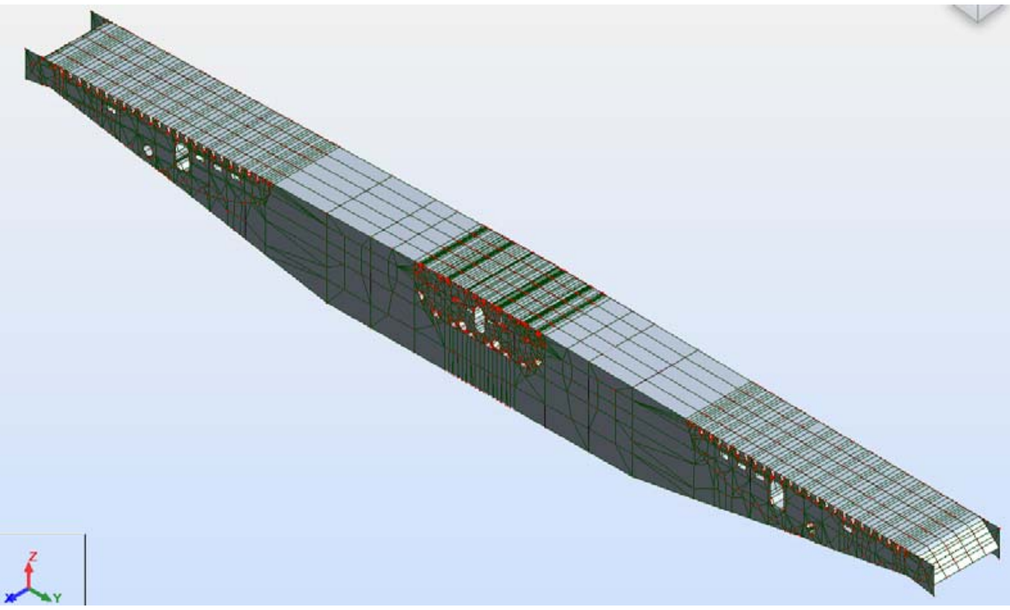

Figure 9-15 Cross girder mesh

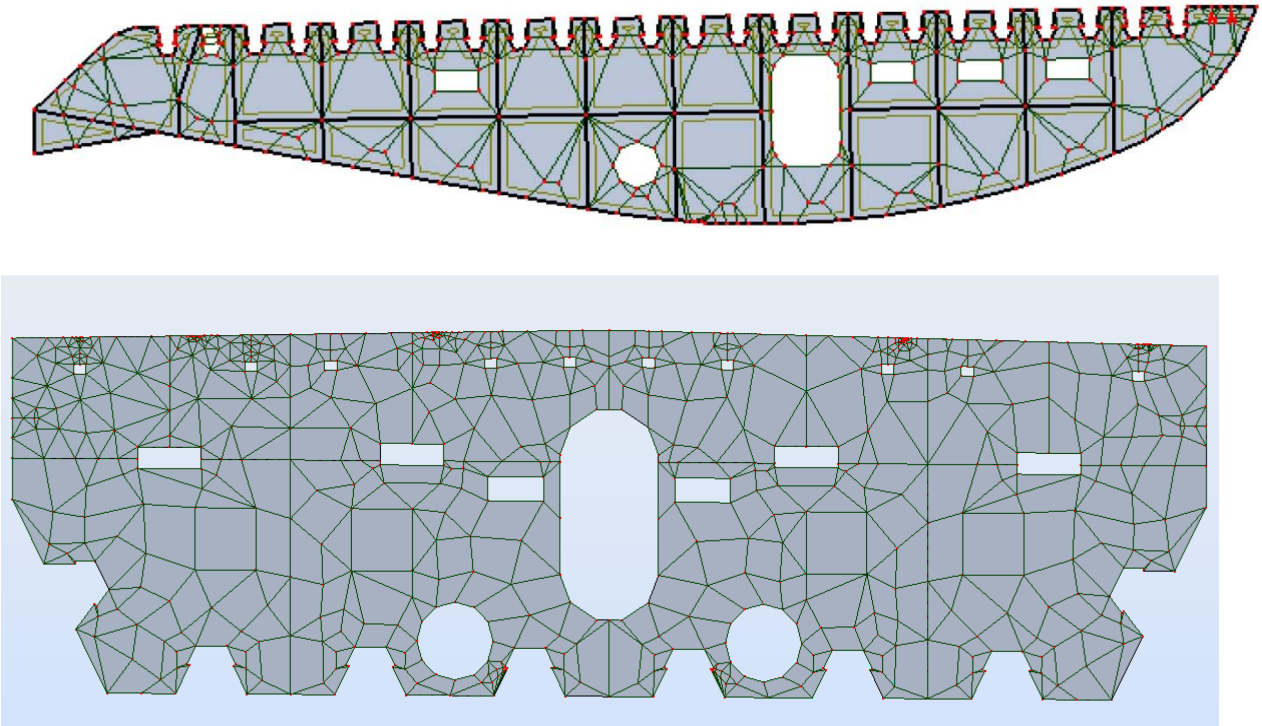

Figure 9-16 Roadway and railway diaphragms mesh

9.3.2 Loads and Load Combinations

The loads that have been applied are both superimposed dead loads and live loads. Generally the loads are specifically applied to their bearing elements e.g. cables and drainage pipes supported by the diaphragms parapets, light masts and wind screens to edges of the deck plate etc. A description of the dead loads is given in Table 9-3.

Table 9-3 Dead loads and application

Load Case	Load type	Application of the load
1: PP ALL	Self-weight	Automatically calculated by ROBOT
7: 40 mm pavement	Uniformly distributed load	Roadway deck
8: PN service lanes	Linear on panel edges and Point loads	Outer edges of roadway and railway diaphragms

9: PN rail	Uniformly distributed load	Railway Deck plates /Railway Girder diaphragms
10:PN road	Linear on panel edges	Roadway deck plates /Roadway girder diaphragms
15:Drainage system	Linear on panel edges	Girder diaphragms

Live loads have been applied as patch loads considering the real print of the loads into the deck plate

Table 9-4 Live loads and application

Load Case	**Load type**	**Value [kN/m^2]**
31:Road LM1 - TS 6542	Planar on contour 0,4 m x 0,4 m	312.5 – 625 – 937.5
32:Road LM1 - UDL 6542	Planar on contour. Strip load	2.5 – 9
33:L71 - Axles 6542	Planar on contour 0,2 m x 0,4 m per rail	1821.9
34:LM 71 - UDL 6542	Planar on contour. Strip load 0,2 m wide per rail	233.2
35:LM71 - Braking/acceleration 6542/6532	Planar on contour. Strip load 0,2 m wide per rail	14.6
36:Nosing Force 6542/6532	Planar on contour 0,2 m x 0,4 m per track	2750
45:SW2 - 6532	Planar on contour. Strip load 0,2 m wide per rail	397.5
48:Wind 6532	Linear on panel edges	varies

As an example a group of live loads used for a load combination is shown in Figure 9-17; for clarity braking and acceleration forces are not shown.

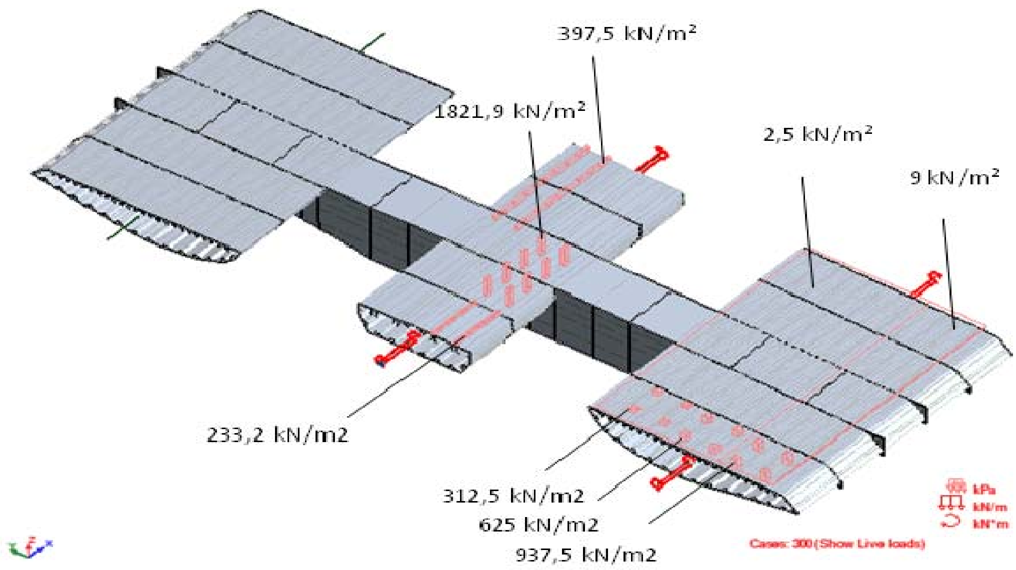

Figure 9-17 Live loads layout

Three load combinations reflecting different criteria have been chosen and the derived stress regimes of the relevant plate elements have been determined. A description of the load combinations and the relative criteria investigated is given in Table 9-5. Each load combination has been analysed implementing the right live loading layout in accordance with the load configuration found by IBDAS capable of maximising the sectional force under investigation.

Table 9-5 Load combinations and relative criteria

Load Combination	Section	Criteria	Description
6542	Hanger	Max Ns	Max tension in the hanger
6532	Cross girder	Max My	Maximum bending moment of roadway girder at intersection with cross girder
6524	Railway girder	Max Mt	Maximum torsional moment of railway girder at intersection with cross girder

For each load combination a description of the loads implemented and the relative partial coefficients are given in Table 9-6 to Table 9-7 where both load and load factors are in accordance with the Design Basis.

Table 9-6 Load combination 6542 – Loads implemented and partial factors

Load Case	Load Type	Description	Load factor
PP	Automatically calculated by ROBOT	Self-weight	1.35
PN	Linear load on panel edges and - Uniformly distributed load	Superimposed dead load	1.5
Boundary conditions	Section forces from global IBDAS model	Sectional forces applied at the end of each beam element	1.0
QL: Road load LM1	Patch loads - Uniformly distributed load	Load according to load model LM1. Position complies with global IBDAS model	1.35
QL: Rail load LM71	Patch loads	Load according to load model LM71. Position complies with global IBDAS model	1.16
QL: Braking Rail force	Patch loads	Braking Load. Position complies with global IBDAS model	1.16
QL: Nosing Rail force	Patch loads	Nosing force. Position complies with global IBDAS model	0.58
VV: Wind	Linear load on panel edges	Load from rails according to load model SW/2 applied on the whole length of track 2	0.6
Calibration load	Automatically calculated by ROBOT	Additional weight applied to all the structure with a fraction of the density – calculated from Reference condition case	1.45

Table 9-7 Load combination 6532 – Loads implemented and partial factors

Load Case	Load Type	Description	Load factor
PP	Automatically calculated by ROBOT	Self-weight	1.35
PN	Linear load on panel edges and - Uniformly distributed load	Superimposed dead load	1.5
Boundary conditions	Section forces from global IBDAS model	Sectional forces applied at the end of each beam element	1.0
QL: Road	Patch loads - Uniformly	Load according to load model LM1. Position complies	1.01 (TS)

load LM1	distributed load	with global IBDAS model	0.54 (UDL)
QL: Rail load SW/2	Patch loads	Load according to load model SW/2. Position complies with global IBDAS model	1.45
QL: Rail load LM71	Patch loads	Load according to load model LM71. Position complies with global IBDAS model	1.45
QL: Braking Rail force	Patch loads	Braking Load. Position complies with global IBDAS model	1.45
QL: Nosing Rail force	Patch loads	Nosing force. Position complies with global IBDAS model	0.73
VV: Wind	Linear load on panel edges	Load from rails according to load model SW/2 applied on the whole length of track 2	0.6
Calibration load	Automatically calculated by ROBOT	Additional weight applied to all the structure with a fraction of the density – calculated from Reference condition case	1.45

Table 9-8 Load combination 6524 – Loads implemented and partial factors

Load Case	**Load Type**	**Description**	**Load factor**
PP	Automatically calculated by ROBOT	Self-weight	1.35
PN	Linear load on panel edges and - Uniformly distributed load	Superimposed dead load	1.5
Boundary conditions	Section forces from global IBDAS model	Sectional forces applied at the end of each beam element	1.0
QL: Road load LM1	Patch loads - Uniformly distributed load	Load according to load model LM1. Position complies with global IBDAS model	1.35
QL: Rail load SW/2	Patch loads	Load according to load model SW/2. Position complies with global IBDAS model	1.16
QL: Rail load LM71	Patch loads	Load according to load model LM71. Position complies with global IBDAS model	1.16
QL: Braking Rail force	Patch loads	Braking Load. Position complies with global IBDAS model	0.58
QL: Nosing Rail force	Patch loads	Nosing force. Position complies with global IBDAS model	1.16
VV: Wind	Linear load on panel edges	Load from rails according to load model SW/2 applied on the whole length of track 2	0.6
Calibration load	Automatically calculated by ROBOT	Additional weight applied to all the structure with a fraction of the density – calculated from the calibration of dead load only	1.45

In "Local FE-models of Suspended Deck" plots of the load combinations and a full documentation of the von Mises stresses including a comparison with the results from the semi-local IBDAS model are given.

9.4 Local FE-model of Roadway and Railway Girder Diaphragms

9.4.1 Roadway Girder

The local roadway FE-model consists of shell elements with thicknesses consistent to the ones stated for roadway section CS2 in the design drawings mentioned in Table 9-9.

Table 9-9 Drawing used as geometrical basis of the model

CG1000	P	WX	D	P	SV	I3	CS	00	00	00	01
CG1000	P	AX	D	P	SV	I3	CS	00	D0	00	01
CG1000	P	AX	D	P	SS	R4	00	00	00	00	01

The overall geometry of the local FE-model for the roadway is presented in Figure 9-18 with the primary shell elements for the roadway girder, supported beam element and the rigid connection. Secondary the cantilevered support beams for the service lane are modelled as shell elements which are connected to the primary structure.

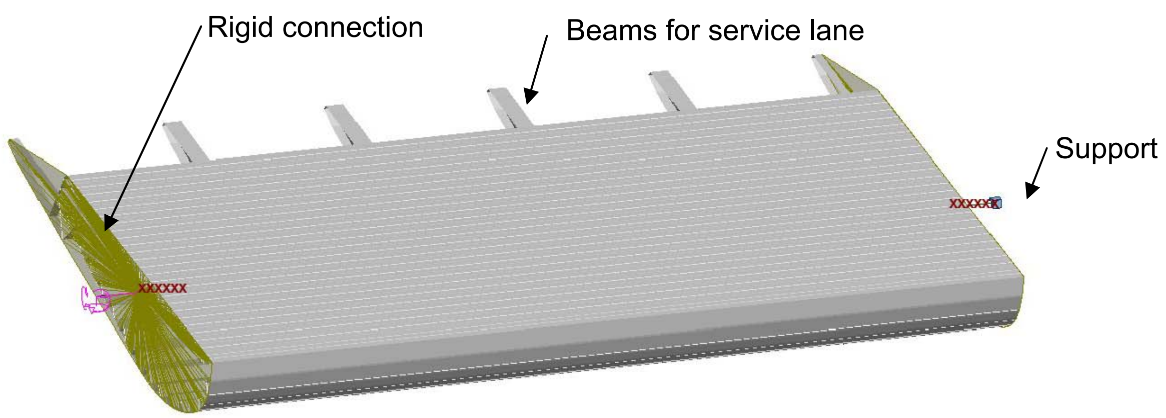

Figure 9-18 Plot of the overall geometry of the FE-model with the supported beam element and rigid connection

The plate thicknesses for the outer longitudinal steel are presented in Figure 9-19. The longitudinal stiffeners are shown in Figure 9-20. Figure 9-21 shows the cantilevered support beam for the service lane. In Figure 9-22 the diaphragm is presented. The change in thickness of the plates is marked with colours in all plots.

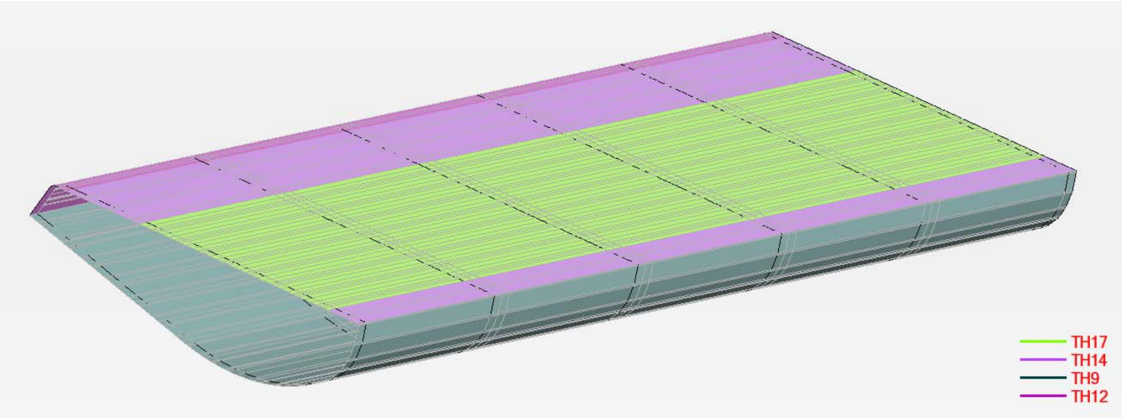

Figure 9-19 Plot of the outer longitudinal steel with the different plate thicknesses marked with colours

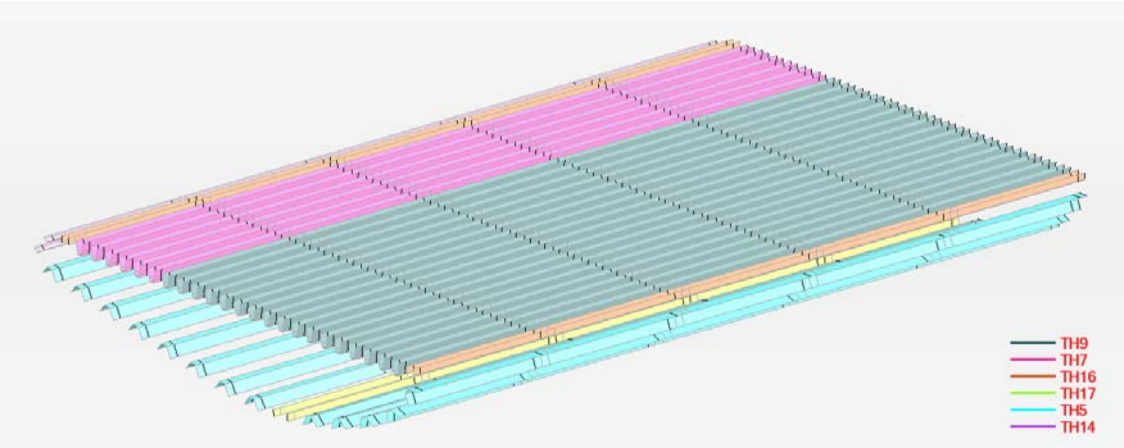

Figure 9-20 Plot of the stiffeners with the different plate thicknesses marked with colours

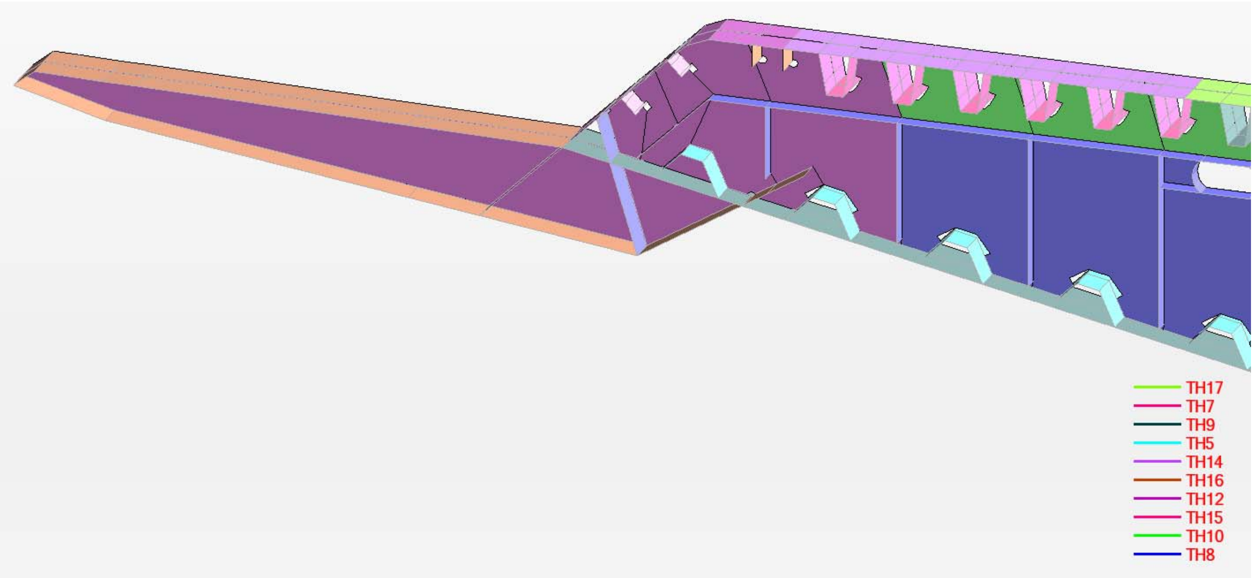

Figure 9-21 Plot of the cantilevered beam for the service lane with the different plate thicknesses marked with colours

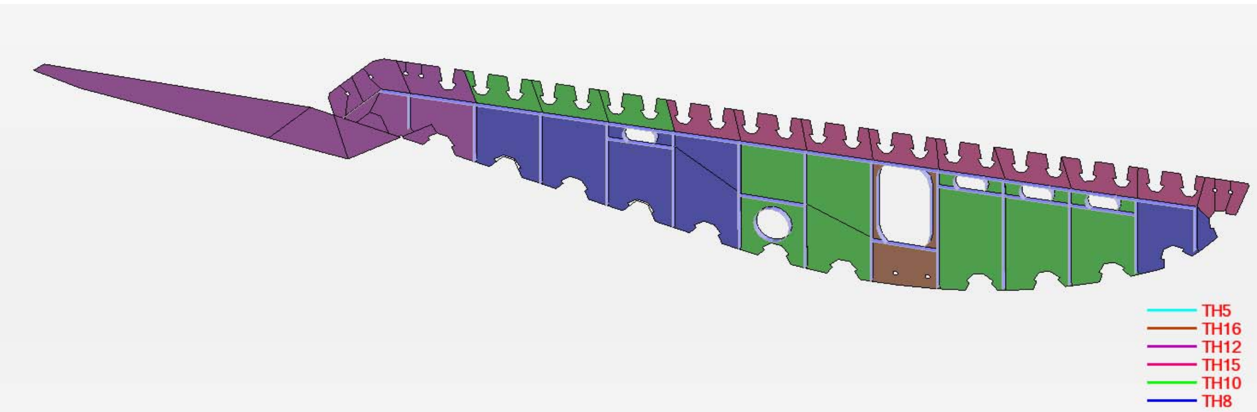

Figure 9-22 Plot of the diaphragm with the different plate thicknesses marked with colours

Due to the fairly constant geometry in the longitudinal direction, the generation of the longitudinal shell elements have been done by extrusion based on a given cross section with a relative dense mesh at each diaphragm. The generated mesh is automatic generated and comprises of 25392 nodes and is shown in Figure 9-23 and Figure 9-24 for the outer plates and diaphragm.

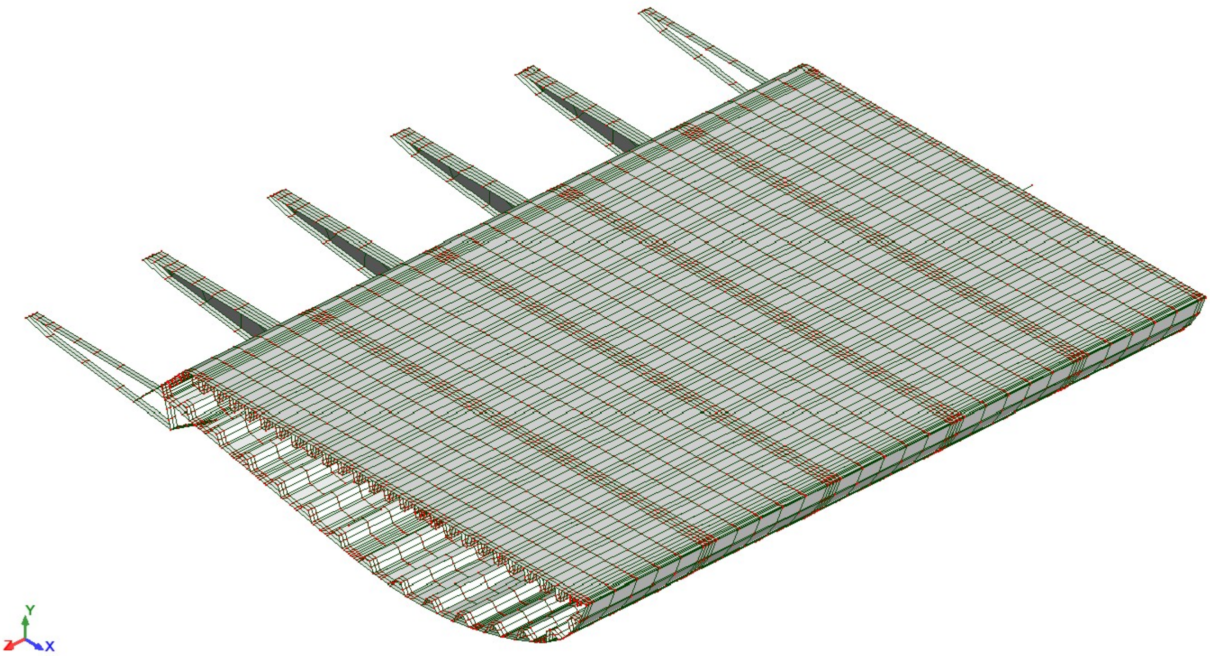

Figure 9-23 Plot of the mesh for the outer longitudinal steel.

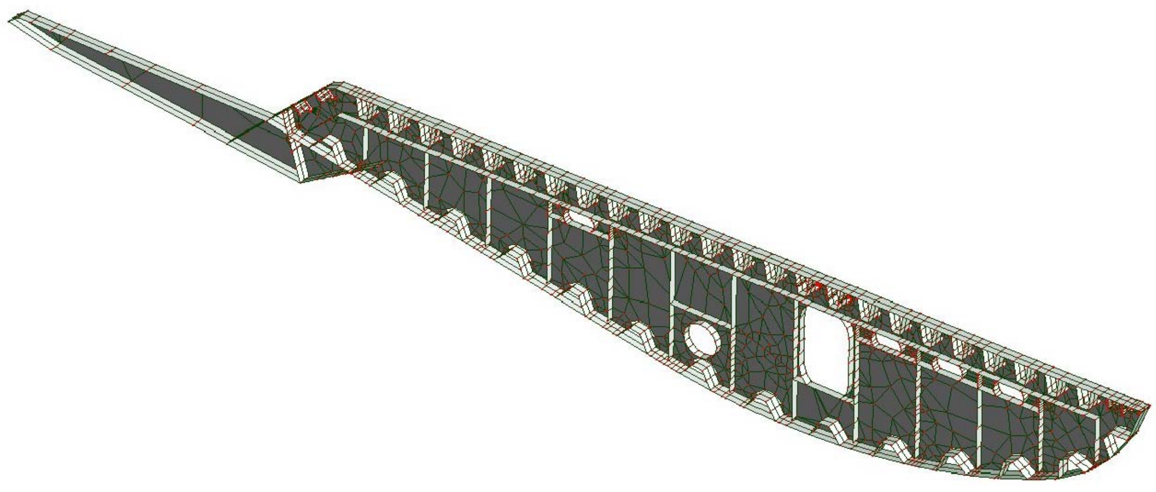

Figure 9-24 Plot of the mesh for diaphragm

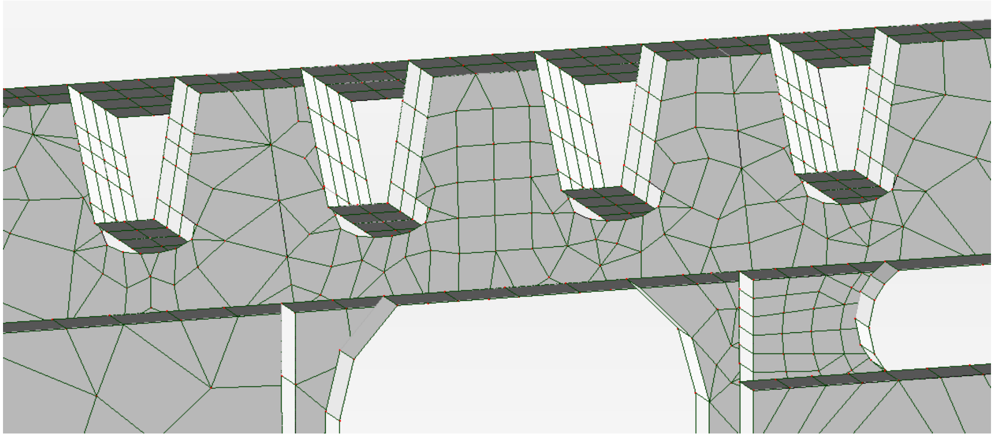

Figure 9-25 Plot of the mesh at openings and the troughs under the deck plate

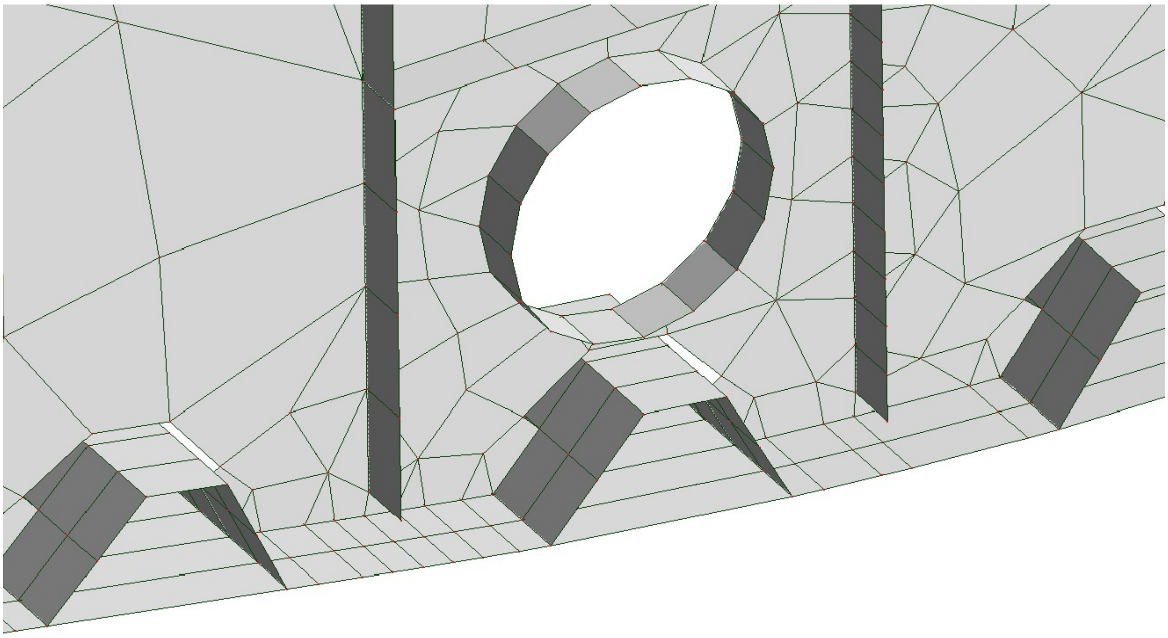

Figure 9-26 Plot of the mesh at openings and the bottom plate troughs

The following three ULS load cases have been implemented to the FE-model for the roadway girder:

1. Maximum My in the centre of the span
2. Maximum Vz in the centre of the span
3. Maximum Ms in the diaphragm

The traffic load has been fixated in the global IBDAS model, for maximising the My and Vz sectional forces in the centre of the span. The load acting within the FE-Local model has been applied according to the influence line plots from the global IBDAS model.

For the third load case (Ms+) the live load has been applied only directly on the FE-Local model to get the maximum sagging moment for the diaphragm. Further more the heaviest loaded lane in most of the fixations is the position furthest from centre of the bridge and to get a higher verity in the verification this load case has been added to the verification of the FE-Local model. The boundary conditions for the model in this load case are therefore the reactions from the model calibrated so the actions have the same numerically value as the reactions. The stresses from the applied traffic load are therefore not superimposed with the global section stresses. The three implemented load cases are specified in Table 9-10 to Table 9-12 with load factors.

*Table 9-10 Loads and load factors applied to the local FE-model for maximum My in centre of span (*load factors are included in IBDAS results)*

Load Cases	**Load Type**	**Description**	**Load factors**
PP	Automatically calculated by ROBOT	Self-weight	1.35
PN UDL on deck plate	Uniformly distributed line load	Parapets, lighting masts, traffic gantries, windscreens applied as a line load on the edge of the deck plate in respectively positions.	1.50
PN Interior	Point loads	Cables, internal deck, access walkways, interior and drainage system applied on diaphragms in respectively positions.	1.50
PN Service lane	Point loads	Point load applied on cantilevered beams for service lane.	1.50

Boundary conditions	Section forces received from global IBDAS model for max. My in centre span (LC6561).	Sectional forces applied on the centre of gravity at the end of the bridge deck cross-section.	1.0*
High way Axle load	Uniformly distributed loads. Size and position comply with global IBDAS model.	Live load according to load model 1.	1.35
High way UDL	Uniformly distributed loads. Size and position comply with global IBDAS model.	Live load according to load model 1.	1.35

Table 9-11 Loads and load factors applied to the local FE-model for maximum Vz in centre of span

Load Cases	**Load Type**	**Description**	**Load factors**
PP	Automatically calculated by ROBOT	Self-weight	1.35
PN UDL on deck plate	Uniformly distributed line load	Parapets, lighting masts, traffic gantries, windscreens applied as a line load on the edge of the deck plate in respectively positions.	1.50
PN Interior	Point loads	Cables, internal deck, access walkways, interior and drainage system applied on diaphragms in respectively positions.	1.50
PN Service lane	Point loads	Point load applied on cantilevered beams for service lane.	1.50
Boundary conditions	Section forces received from global IBDAS model for max. My in centre span (LC6567).	Sectional forces applied on the centre of gravity at the end of the bridge deck cross-section.	1.0
High way Axle load	Uniformly distributed loads. Size and position comply with global IBDAS model.	Live load according to load model 1.	1.35
High way UDL	Uniformly distributed loads. Size and position comply with global IBDAS model.	Live load according to load model 1.	1.35

Table 9-12 Loads and load factors applied to the local FE-model for maximum Mz in the diaphragm

Load Cases	**Load Type**	**Description**	**Load factors**
PP	Automatically calculated by ROBOT	Self-weight	1.35
PN UDL on deck plate	Uniformly distributed line load	Parapets, lighting masts, traffic gantries, windscreens applied as a line load on the edge of the deck plate in respectively positions.	1.50
PN Interior	Point loads	Cables, internal deck, access walkways, interior and drainage system applied on diaphragms in respectively positions.	1.50
PN Service lane	Point loads	Point load applied on cantilevered beams for service lane.	1.50
Boundary conditions	Section forces applied so the reaction and action is in equilibrium.	Sectional forces applied on the centre of gravity at the end of the bridge deck cross-section.	1.0
Highway Axle load	Uniformly distributed loads. Size and position comply with global IBDAS model.	Live load according to load model 1.	1.35
Highway UDL	Uniformly distributed loads. Size and position comply with global IBDAS model.	Live load according to load model 1.	1.35

Figure 9-27 to Figure 9-30 is showing how the PN dead load from the global IBDAS model is applied to the model.

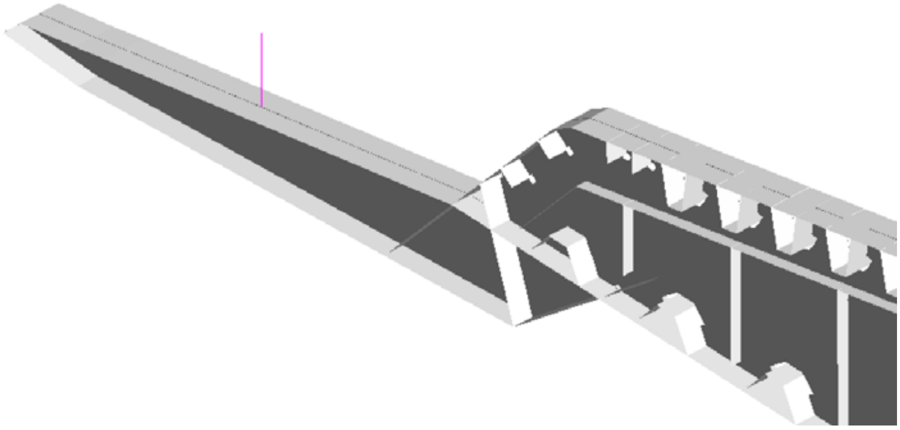

Figure 9-27 Plot of cantilevered beam with service lane PN load

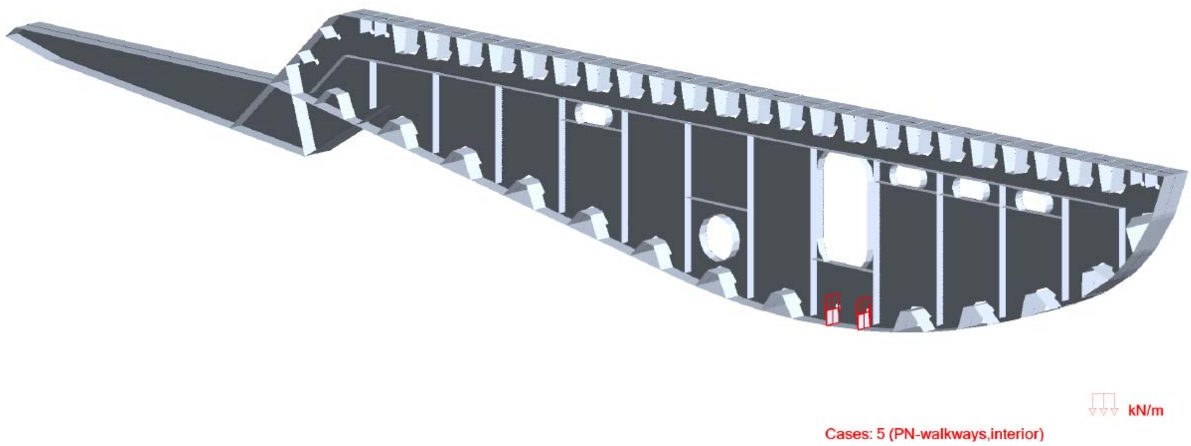

Figure 9-28 Plot of model with walkways PN load

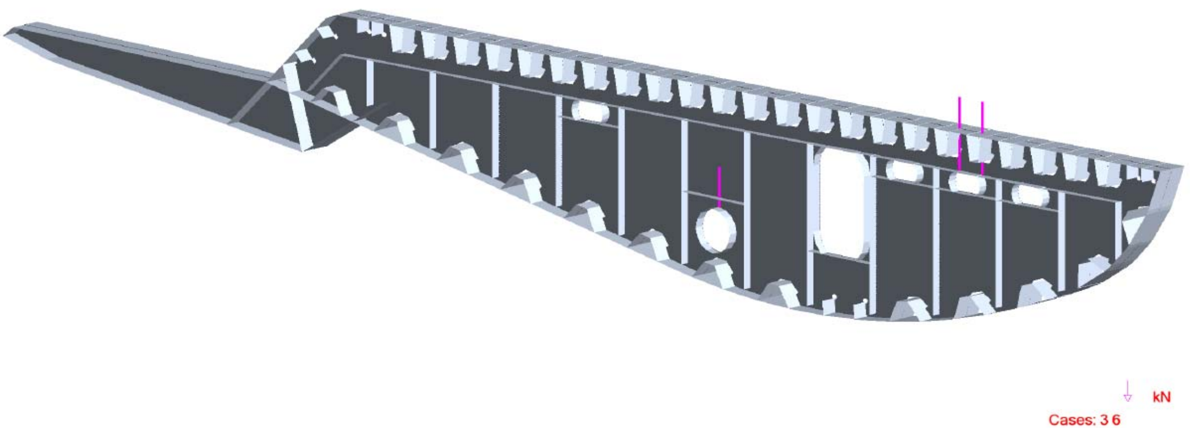

Figure 9-29 Plot of model with drainage and cables PN load

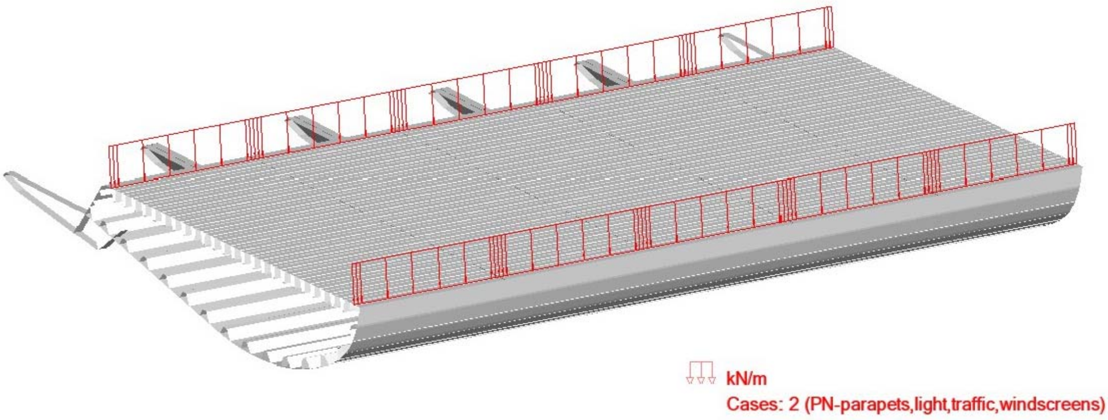

Figure 9-30 Plot of model with parapets, lighting masts, traffic gantries and windscreens

The pavement is applied as an UDL PN load with an equivalent area of 20.7x11.95 m.

An example of the applied traffic load is given in Figure 9-31 for maximum sagging moment in the centre of the span with the loads applied according to IBDAS model for load model 1.

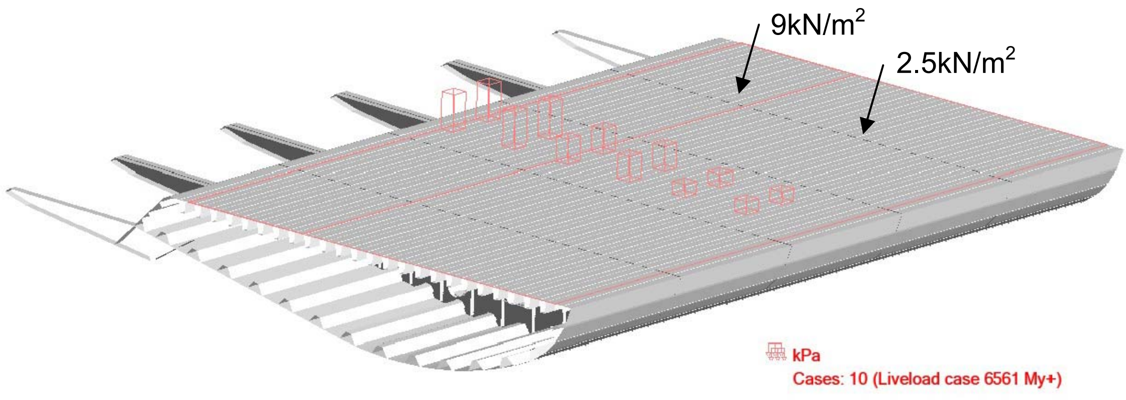

Figure 9-31 Plot of model with applied load for load case with maximum sagging moment at centre span

The patch loads shown in Figure 9-31 are equivalent to an axel load of relatively 300 kN, 200 kN and 100 kN which are distributed over 400x400 mm.

In "Design Report - Roadway, Railway and Cross Girders" plots are shown for the applied load combinations and a full documentation of the von Mises stresses is given.

9.5 Railway Girder

9.5.1 Geometry

The models consist of shell elements (FE-panels) with thicknesses consistent in values and names to the ones stated in the design drawings mentioned in Table 9-13.

Table 9-13 Drawings used as geometrical basis of the model

CG1000	P	WX	D	P	SV	I3	CF	00	00	00	01
CG1000	P	AX	D	P	SV	I3	CS	00	D0	00	01
CG1000	P	BX	D	P	SS	P2	FE	00	00	00	03

Figure 9-32 shows a plot of the model with beam elements in each end connected to the plates with rigid links and supported with a fixed support in the right end of the model. The notation at the left end of the model indicates the rigid link between the beam element and the shell model.

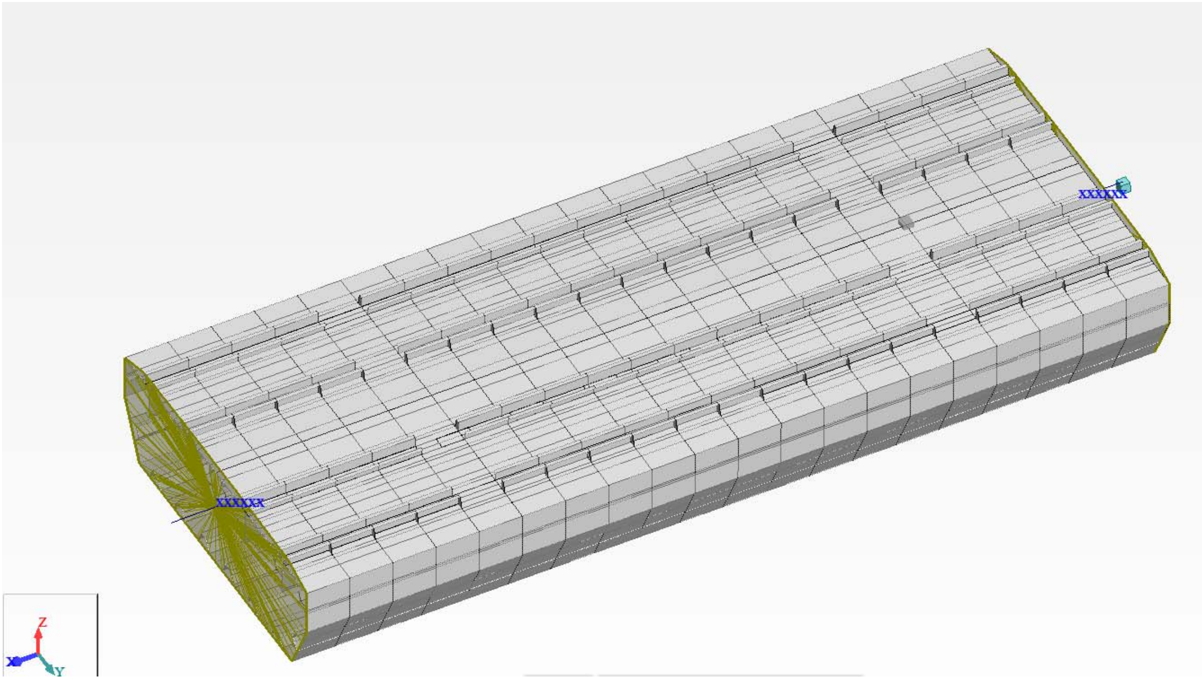

Figure 9-32 Plot of FE-model showing beam elements, rigid links and fixed support

In Figure 9-33 a plot of the FE-model of the outer longitudinal steel in the railway girder is shown. Figure 9-34 shows a plot of the longitudinal internal plates and Figure 9-35 shows the diaphragm modelled fairly detailed with plate stiffeners and stiffening of holes for drainage and cable trays. The change in thickness of the plates is marked with colours in all plots.

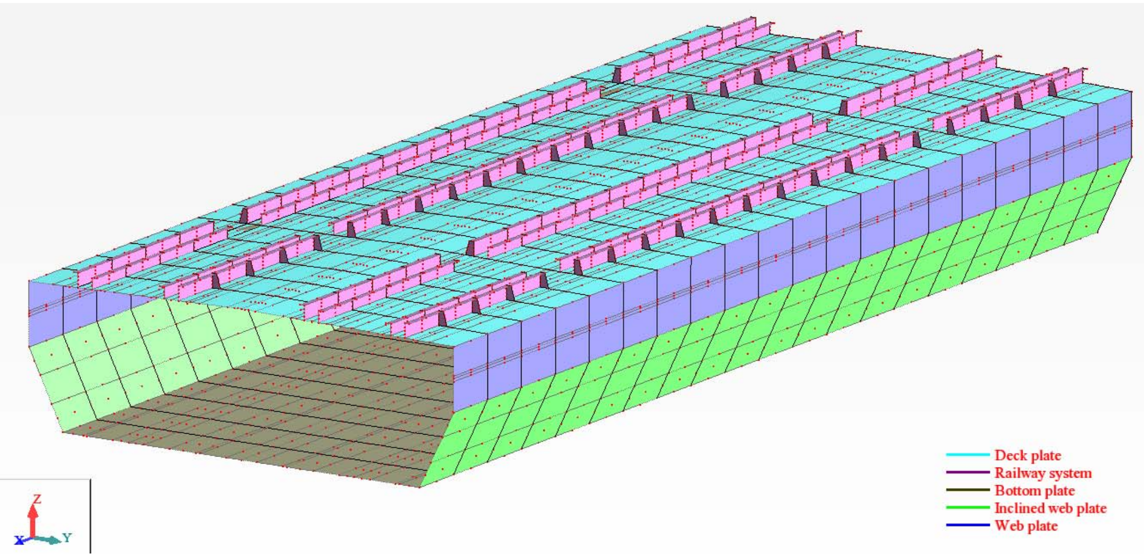

Figure 9-33 Plot of the FE-model of the outer longitudinal steel in the railway girder with the change of plate thicknesses marked with colours

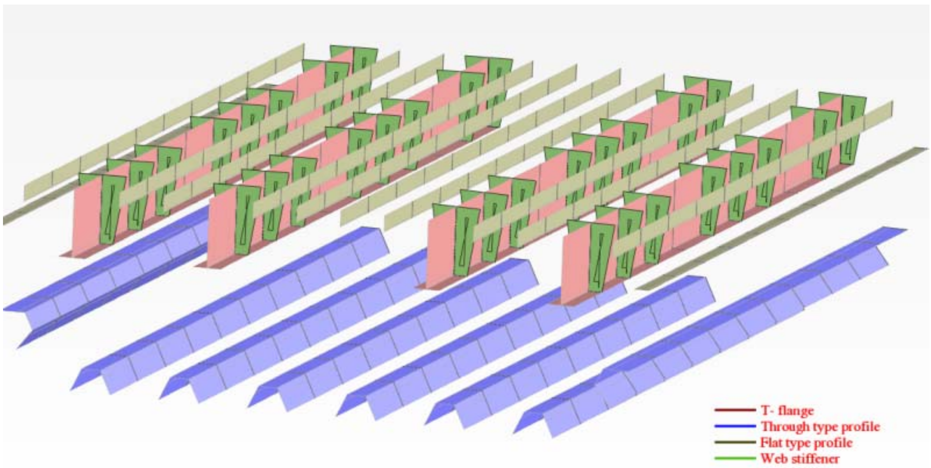

Figure 9-34 Plot of the FE-model of the internal longitudinal steel in the railway girder with the change of plate thicknesses marked with colours

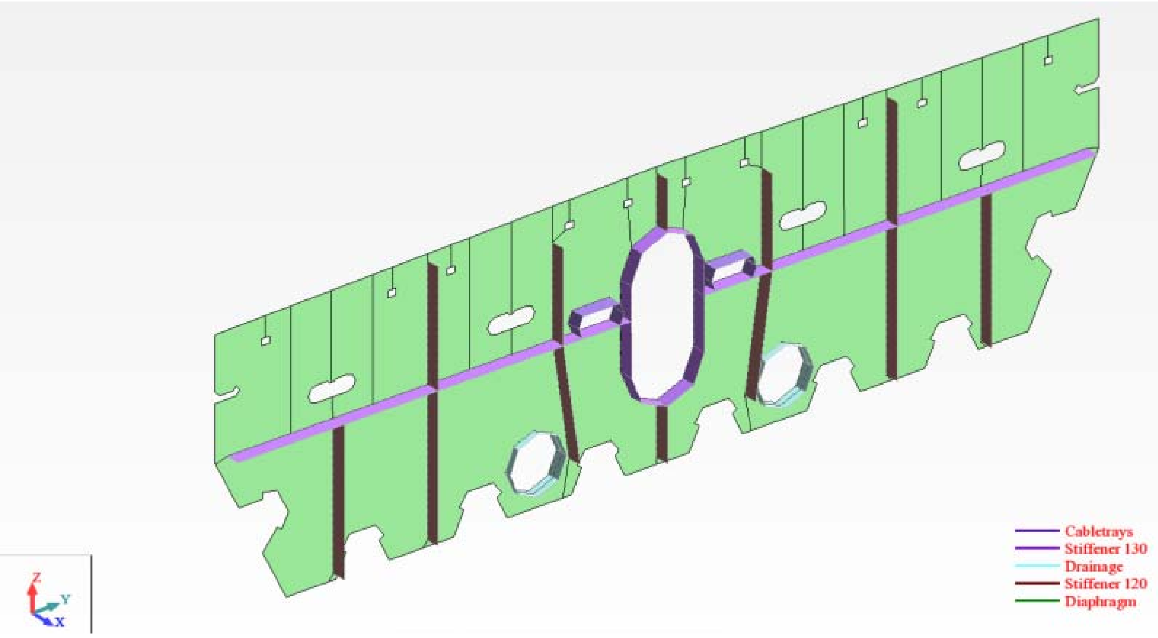

Figure 9-35 Plot of the diaphragm with stiffeners. Plate thicknesses are marked with colours

In the following, Table 9-14 gives a list of the elements and plate thicknesses included in the model.

Table 9-14 List of elements and plate thicknesses included in the model

Included in FE-model	**Plate thickness [mm]**
Deck plate	15
Bottom plate	10
Web plate	10
Inclined web plate	10
T-beam, flange	22
T-beam, web	14
Flat stiffener on deck plate	18
Flat stiffener on web plate	16
Trough	6
Diaphragm type 1*	8/10/15

Diaphragm type 2	12
Stiffening of cable trays, width = 110 mm	8
Stiffening of holes for drainage, w = 110 mm	8
Diaphragm stiffeners (vertical) w = 120 mm	10
Diaphragm stiffeners (horizon.) w = 130 mm	10
Stiffening of manhole, w = 130 mm	10
Angle profiles for railway system	16

*For specification of diaphragm thicknesses see CG.10.00-P-AX-D-P-DV-I3-CF-00-D0-00-01

9.5.2 Mesh

The dimension of the elements is 47 cm in length corresponding to the modules of 3.75 m between diaphragms being split in 8 parts. The width of the elements is approximately 6 to 50 cm. The diaphragms have triangular mesh shape with maximum size of 100 cm but relatively fine mesh at corners and openings. The generated mesh comprises of 13319 nodes and is shown in Figure 9-36 for the outer plates and in Figure 9-37 for the diaphragm.

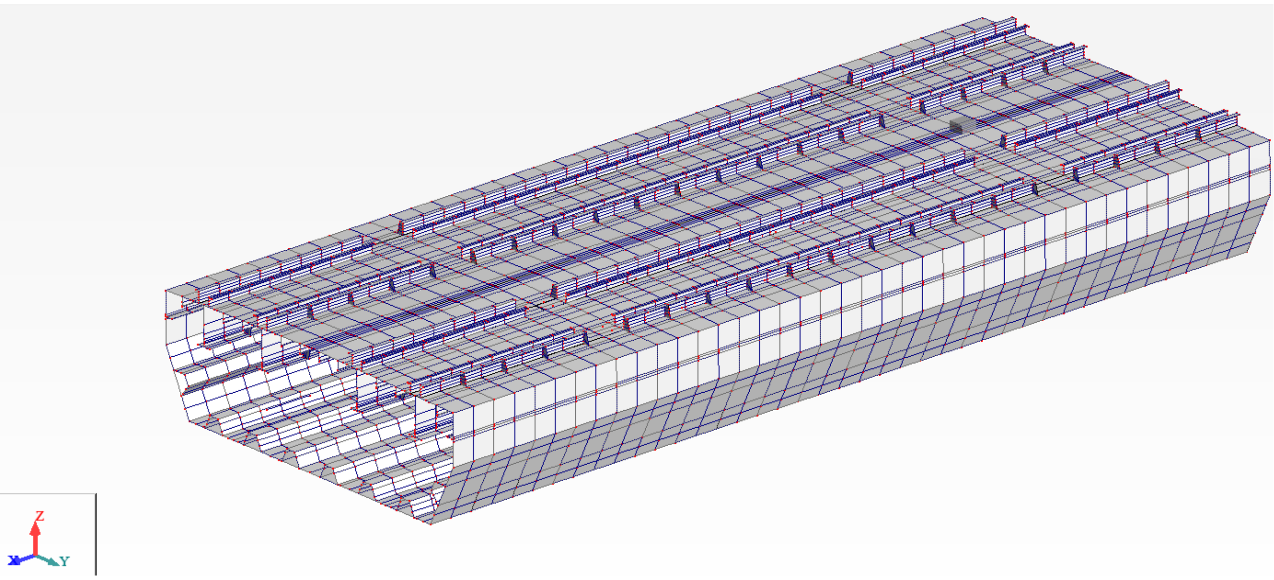

Figure 9-36 Mesh shown for the outer plates

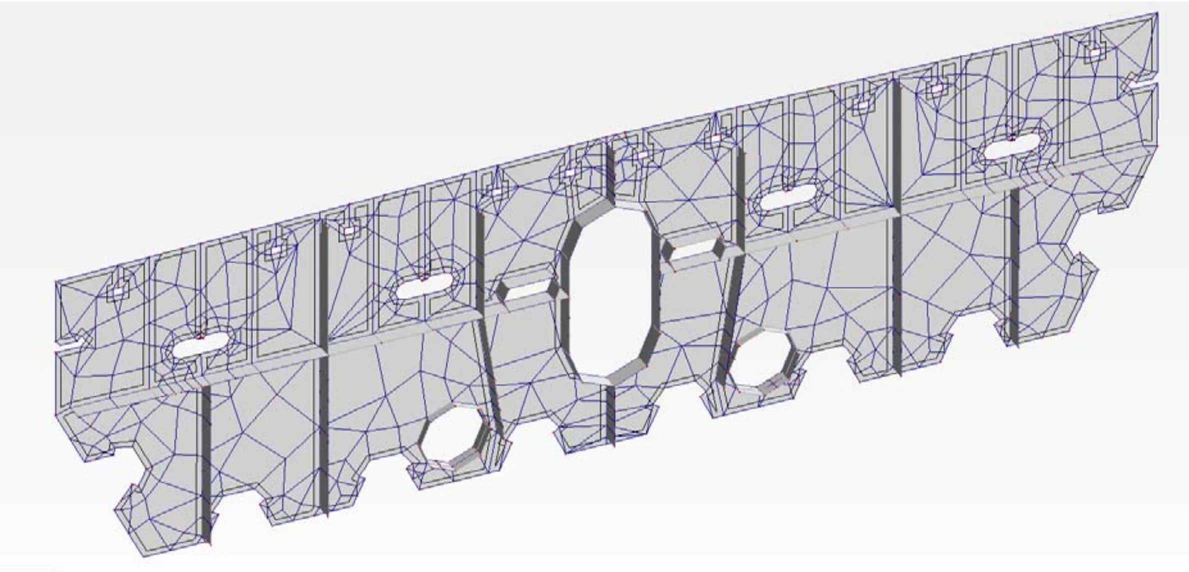

Figure 9-37 Mesh shown for the outer longitudinal steel and diaphragm

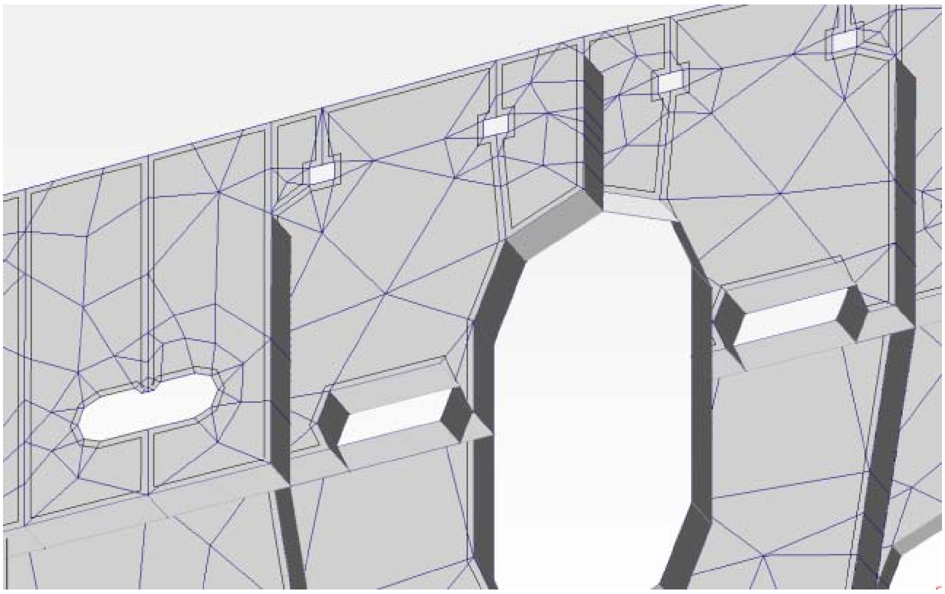

Figure 9-38 Plot of the mesh in the diaphragm at openings and the troughs at the deck plate

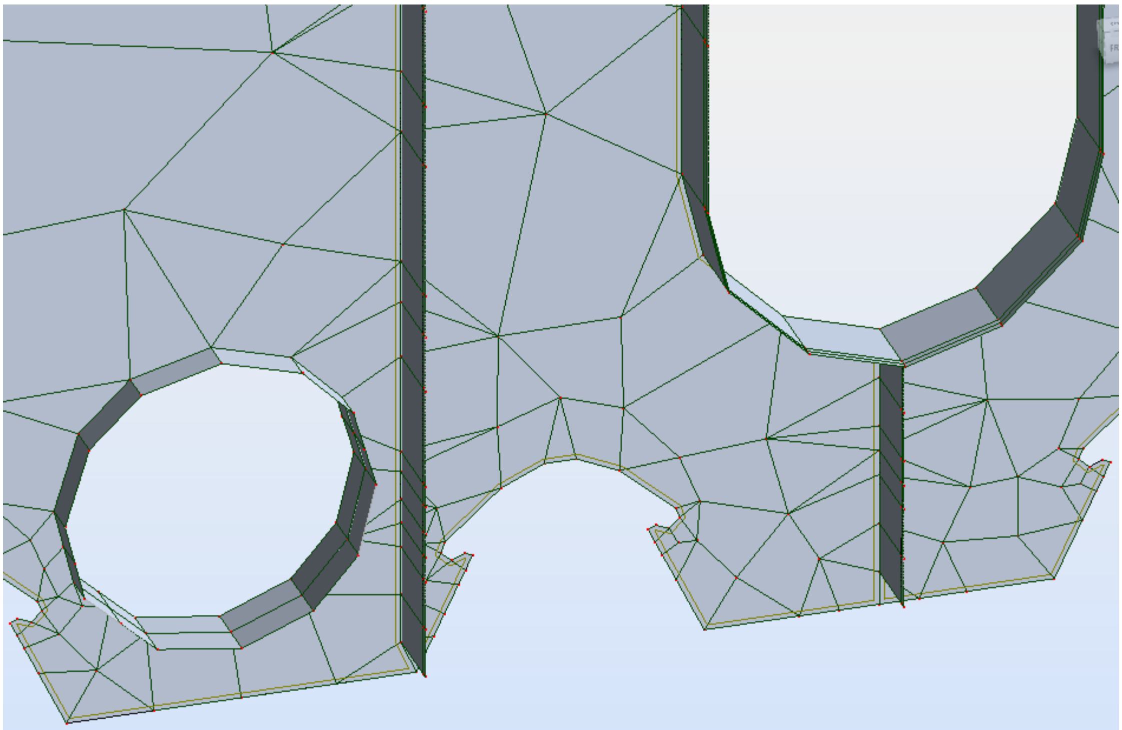

Figure 9-39 Plot of mesh in the diaphragm at openings and troughs at the bottom plate

9.5.3 Loads and Load Combinations

The loads applied are dead loads, superimposed dead loads and live loads. Generally the loads are specifically applied to the elements from where they are supposed to load. Superimposed dead load is applied as a uniform distributed load over the whole length of the model. This is due to the total size of the load of 22 kN/m and the assumption that a relatively more accurate application of superimposed loads from e.g. cables, catenary masts, drainage system will not reflect a real issue considering stress distribution.

The following two load cases have been implemented to the FE-model for the railway girder:

1. Maximum My in the centre of the span
2. Maximum Mt in the centre of the span

The rail load has been fixated for maximising the sectional forces from maximum bending moment, My, and torsional moment, Mt, in the centre of the span and the load has been applied to the model according to IBDAS influence line plots of the governing load case of rail load. The three implemented load cases are specified in Table 9-15 and Table 9-16, where loads and load factors are according to Design Basis and description of application.

*Table 9-15 Loads and load factors applied to the local FE-model for maximum bending moment My in centre of span (*load factors are included in IBDAS results)*

Load Cases	**Load Type**	**Description**	**Load factors**
PP	Automatically calculated by ROBOT	Self-weight	1.35
PN	Line load	Superimposed dead load Applied as line load at centre of deck plate in whole length of the model	1.50
Boundary conditions	Section forces received from global IBDAS model for max. My in centre span (case 6571).	Six sectional forces applied at one end of the beam element.	1.0*
Rail load SW/2	Uniformly distributed load. Size and position comply with global IBDAS model.	Live load according to load model SW/2 applied at location of each rail in track 1	1.45
Rail load LM71	Uniformly distributed loads. Size and position comply with global IBDAS model.	Live load according to load model LM71 applied at location of each rail in track 2.	1.45
Braking forces	Uniformly distributed loads. Size and position comply with global IBDAS model.	Live load according to load model SW/2 applied on track 1 and load model LM71 applied on track 2.	1.45
Nosing forces	Uniformly distributed loads. Size and position comply with global IBDAS model.	Live load according to load model SW/2 applied on track 1 and load model LM71 applied on track 2. Applied to railway system over an area of 150x200 mm.	0.73

Table 9-16 Loads and load factors applied to the local FE-model for maximum torsional moment, Mt, in centre of span

Load Cases	**Load Type**	**Description**	**Load factors**
PP	Automatically calculated by ROBOT	Self-weight	1.35
PN	Uniformly distributed load	Superimposed dead load. Applied as line load at centre of deck plate in whole length of the model.	1.50
Boundary conditions	Section forces received from global IBDAS model for max. Mt in centre span (case 6575).	Six sectional forces applied at one end of the beam element.	1.0
Rail load LM71 (y-)	Uniformly distributed loads. Size and position comply with global IBDAS model.	Live load according to load model LM71 applied at location of each rail in track 1.	1.16
Rail load LM71 (y+)	Uniformly distributed loads. Size and position comply with global IBDAS model.	Live load according to load model LM71 applied at location of each rail in track 2.	1.16
Braking forces	Uniformly distributed loads. Size and position comply with global IBDAS model.	Live load according to load model LM71 applied on track 1 and 2.	0.58
Nosing forces	Uniformly distributed loads. Size and position comply with global IBDAS model.	Live load according to load model LM71 applied on track 1 and 2. Applied to railway system over an area of 150x200 mm.	1.16

An example of the applied load is given in Figure 9-40 and Figure 9-41 for maximum My with train type SW2 applied in track 1 (y- according to coordinates in the global IBDAS model) and LM71 applied in track 2 (y+ according to coordinates in the global IBDAS model). Figure 9-40 shows the vertical loads and Figure 9-41 shows the horizontal loads in the load combination. In "Design Report - Roadway, Railway and Cross Girders" plots are shown for the applied load in all load combinations and a full documentation of the von Mises stresses are given.

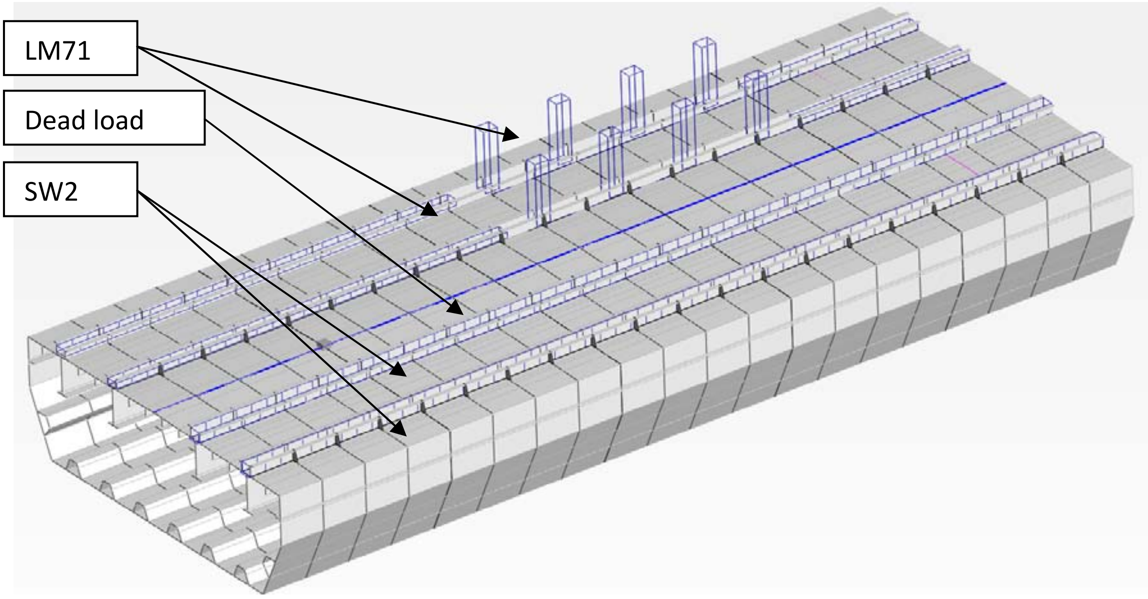

Figure 9-40 Plot of model with applied vertical loads for load case with maximum bending moment, My+, at centre span

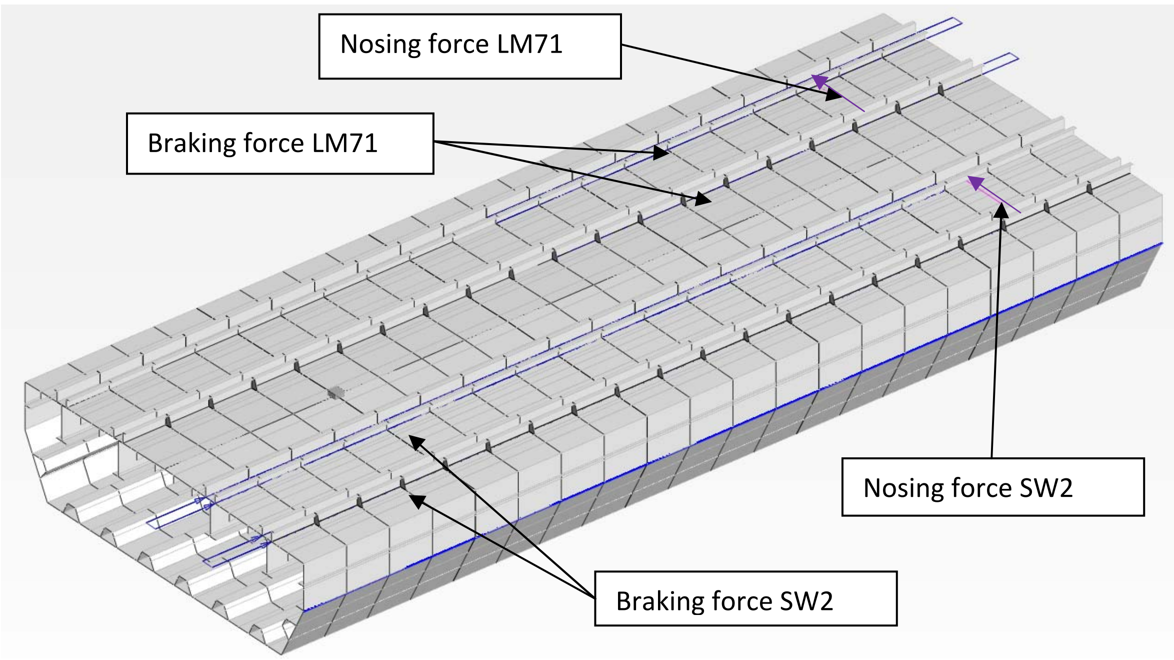

Figure 9-41 Plot of model with applied horizontal loads for load case with maximum bending moment, My+, at centre span

9.6 Hanger Anchorage

Four local shell FE-models of the hanger anchorages are created for verification of the local stress distribution from the hanger anchorage and into the cross girder and roadway girder. The overall length of the model is 30m between mid-spans of the longitudinal roadway girder and a width of 26m for half a cross girder. The relatively long span of the model ensuring correct boundary condition and hereby stress flow and distribution for the plates related to the hanger anchorage.

Following hanger anchorages have been modelled:

- AP1 with spherical bearings and highest rotations,
- AP1 with spherical bearings,
- AP2
- AP3

These four models represent the hanger anchorages from cross girder number 9 to 111.

The models consist of shell elements with thicknesses consistent to the ones stated in the design drawings mentioned in Table 9-17.

Table 9-17 Drawings used as geometrical basis of the model

CG1000	P	AX	D	P	SV	I3	TP	00	00	00	03
CG1000	P	WX	D	P	SV	I3	CS	00	00	00	01
CG1000	P	WX	D	P	SV	I3	TP	00	00	00	01

The interface geometry of the adjacent girders for the boundary conditions is taken as T1 cross girder and CS1 roadway girder for all four models.

The overall geometry of the FE-Local model of the hanger anchorages is presented in Figure 9-42 showing the shell elements for the cross girder, roadway, hanger anchorage and the supports.

The model is supported in each end of the 30 meter roadway in the longitudinal direction and the cross girder is supported in the centreline of the bridge in transverse direction and in two points in three directions direction as shown in Figure 9-42.

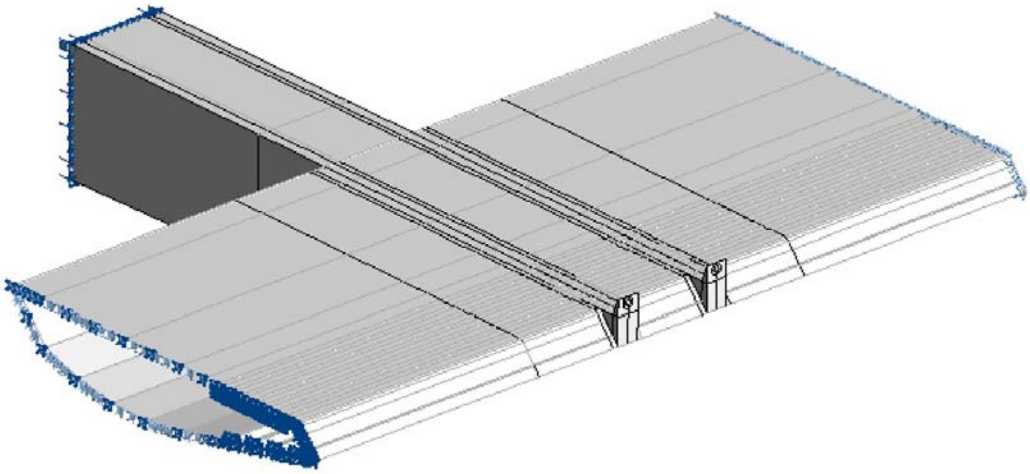

Figure 9-42 Plot of the overall geometry and supports.

To comply for the vertical shear distribution in the longitudinal direction, an external force has been applied. This force is determined according to the shear distribution in the global IBDAS model which shows that 75% of the reaction is distributed to the cross girder and 25% to the road way girders in total. These external calibration forces are applied on the model as shown in Figure 9-43.

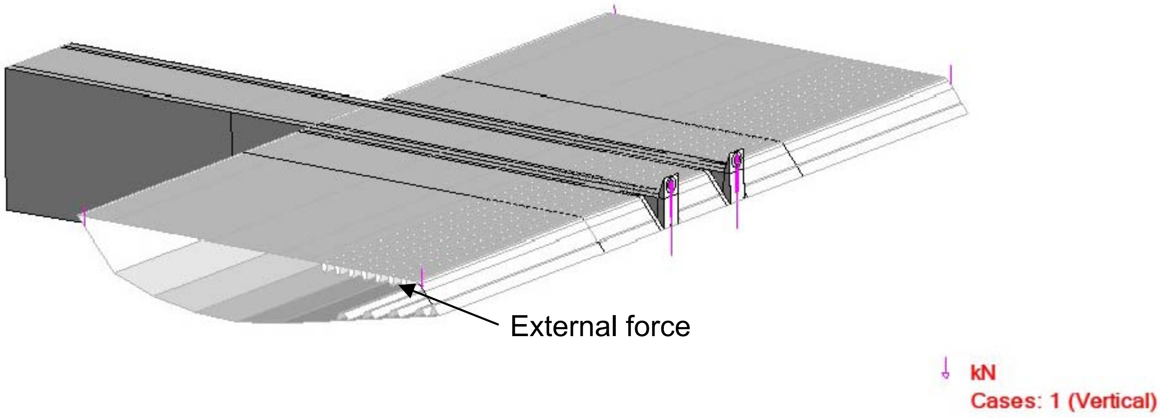

Figure 9-43 External force to comply of the vertical shear distribution to the roadway girders

The plate thicknesses for AP1 hanger anchorage with highest rotations is shown in Figure 9-44 and Figure 9-45.

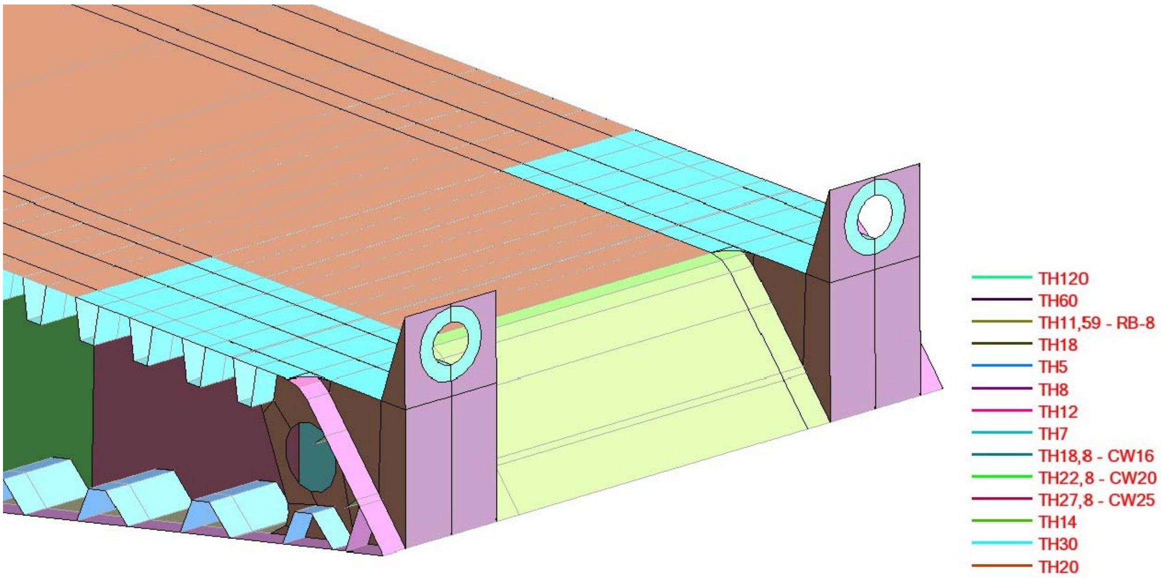

Figure 9-44 Plot of the hanger anchorage with the different plate thicknesses marked with colours

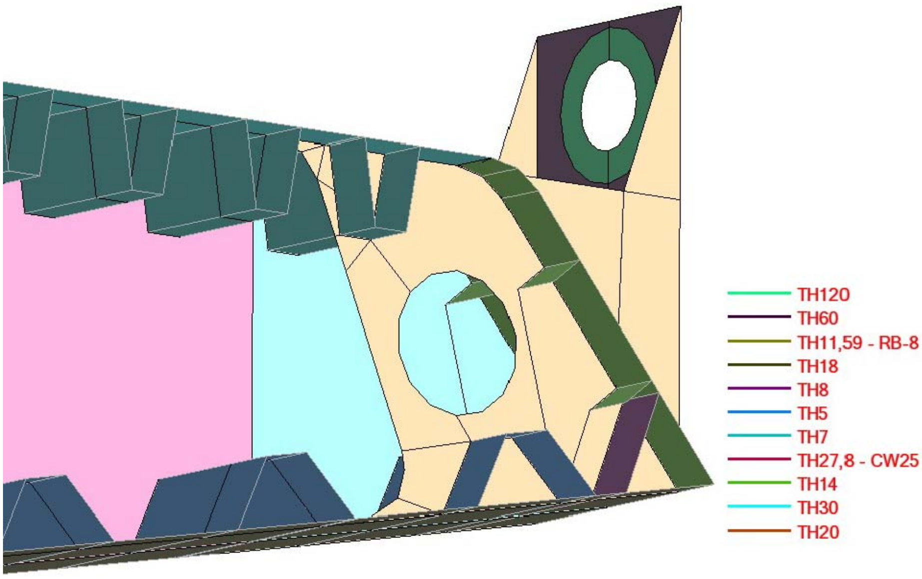

Figure 9-45 Plot of the hanger anchorage with the different plate thicknesses marked with colours

Due to the fairly constant geometry in the longitudinal direction, the generation of the longitudinal shell elements have been done by extrusion of the given cross section. The mesh is automatic generated and comprises of 9654 nodes and is shown in Figure 9-46 and Figure 9-47 for the external and internal mesh.

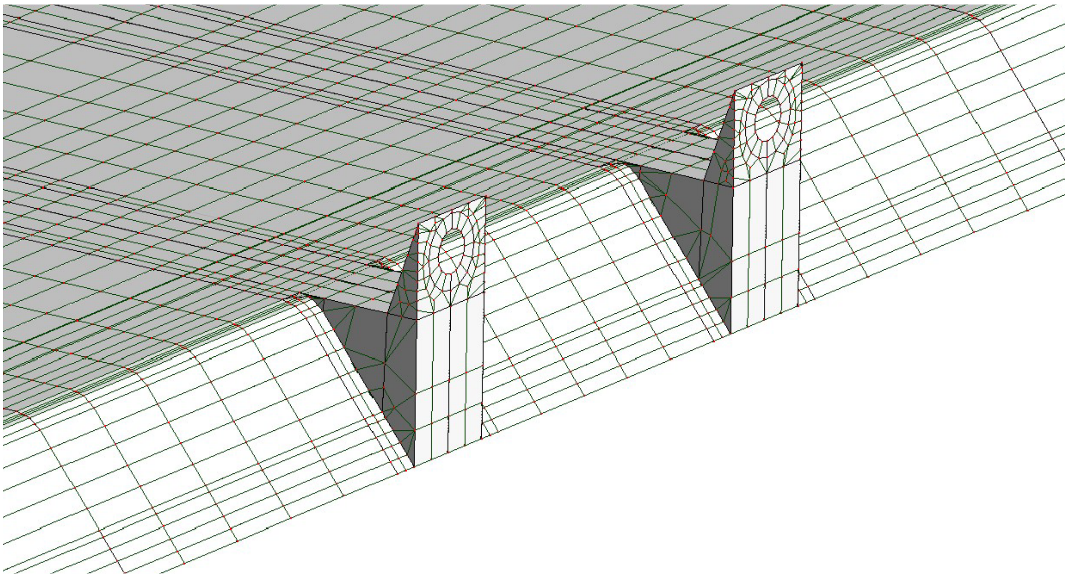

Figure 9-46 Plot of the external mesh

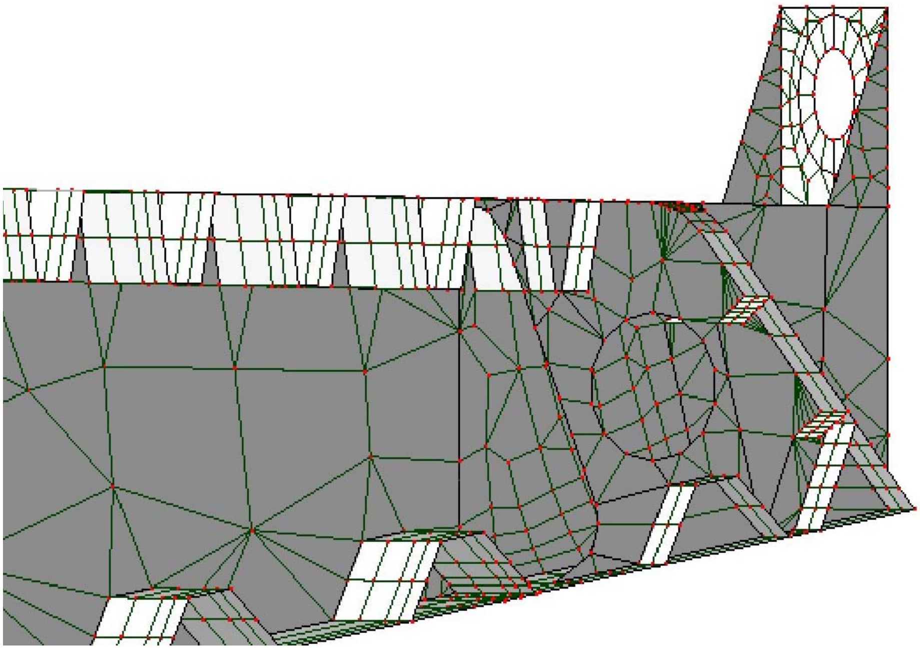

Figure 9-47 Plot of the internal mesh

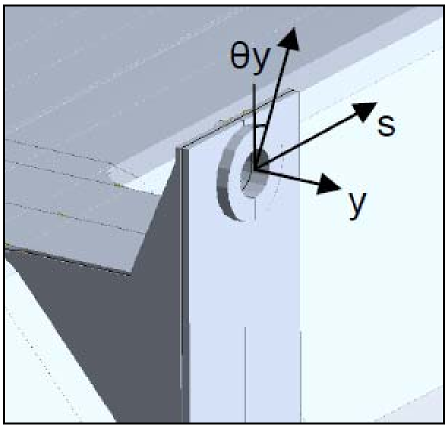

Figure 9-48 Sign convention for hanger forces in the global IBDAS model

The global ULS hanger force and ULS hanger rotations are applied according to the results from the global IBDAS model. The global hanger force from IBDAS is applied in centre the pinhole and is applied as an approximation of hertz stress distribution as shown in Figure 9-49.

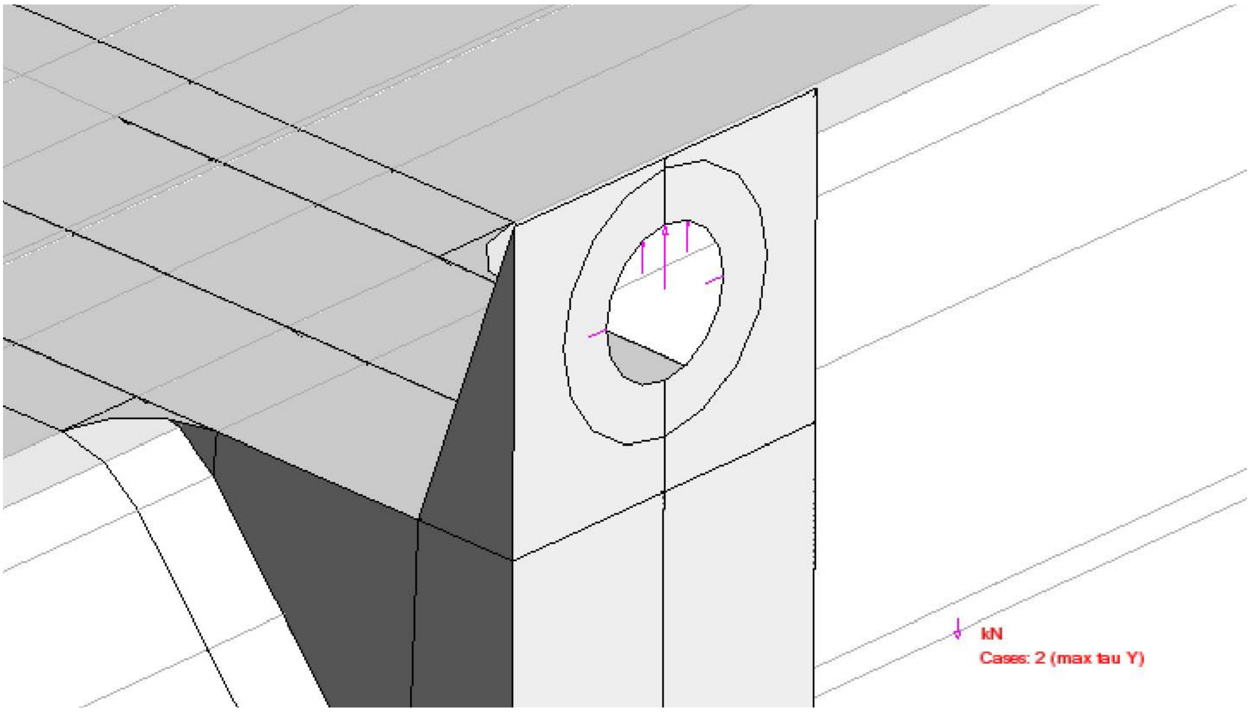

Figure 9-49 Applied ULS hanger load under maximum Y-rotation

The hanger force is applied under an ULS rotation of maximum 13.9 degrees for the y-axis rotation and 7.4 degrees for the ULS s-axis rotation. The sign convention for the rotations is shown in

Figure 9-48. The maximum y-rotations are both represented in cross girder 60 which is exactly in the centre of main span.

The results in "Design Report - Roadway, Railway and Cross Girders" reflect that the hanger anchorages on cross girder number 52 to 68 have been reinforced with an extra stiffener due to the relatively short hangers and hereby large hanger rotation in this area.

In "Design Report - Roadway, Railway and Cross Girders" plots are shown for the applied load in all load combinations and a full documentation of the von Mises stresses is given. Furthermore the position of the traffic load in the three load cases is presented.

The AP2 model is furthermore used for fatigue check which is done by applying the fatigue hanger force for the unlimited load case situation with a train EN5 and a roadway vehicle LM2(3) passing. The stress plots for this load case is then subject for further fatigue investigations, see section 11.11.5.

10 Fatigue Assessments

10.1 Introduction

According to the Design Basis, the railway fatigue load has been based on the standard traffic mix whose composition may be found in EN 1991-2 Table D.1; it includes 67 train transits expected per day per track with a traffic volume of 24.95 million tonnes per year. The roadway fatigue load comprises of 2 million transits per year of heavy roadway vehicles for each direction fulfilling the traffic category 1 defined in EN 1991-2 4.6.1. During the 200 years design life of the bridge the total number of transits for the railway girder hence becomes 4.89 million for each track and 400 million for the roadway girder in each direction (slow lane).

The "unlimited life method" and the damage accumulation method (Palmgren-Miners summation of damage) have both been used for the fatigue assessment of the main structural components subjected to direct man generated loads. The two methods are described in the following section 11.5 and 11.6. In addition the wind induced fatigue degradation has been accounted for in the damage accumulation method by a damage of 0.05; this implies the verification to be fulfilled only when the damage from traffic loads is lower then 0.95. The contributions to fatigue for the non man generated loads refer to section 11.3.

10.2 Application of loads

When considering the roadway girder for fatigue verification, all the vehicles have been considered driving in the slow lane. The roadway girders are loaded with one vehicle at a time for the fatigue verification. The investigation includes 8 different fatigue trains indicated in Annex D of Eurocode 1991-2:2003.

When a train passes the bridge, this is always in the track towards the loaded roadway girder. For the fatigue loads the following assumptions have been made:

- Railway traffic: 67 trains per day giving a total of 4.89 million in 200 years per track
- Roadway traffic: 2 million heavy vehicles per year, i.e. 400 million in the 200 year design life
- Speed of trains: maximum speed of trains
- Dynamic factors have been calculated in accordance with Eurocode EN 1991-2 Annex D “Basis for the fatigue assessment of railway structures”
- The likelihood of two train meets at any given point on the bridge during passing is 12%

According to the "Safe Life" assessment method in EN1993-1-9 3 and the recommendation included in the RFI44/F the following partial factors have been used: γ_m =1.15 has been applied to local details of the orthotropic roadway deck, while a safety factor of γ_m =1.35 has been applied to all other details.

10.3 Non man generated loads

The non man generated loads accounted for are temperature, seismic and wind loads. The following have been considered:

- Wind during the design life of 200 years.
- +/- 10˚C uniform variation daily during the design life of 200 years.
- SLS1 earthquake 4 times, 5 minutes per event (i.e. total of 20 minutes)

The effect of temperature and seismic loads have been considered isolated and their effects have none or a minor contribution to the fatigue damages, and hence according to the basis of design needs not to be considered for fatigue assessments in combination with man generated loads.

WIND

Wind load due to natural turbulent wind can be considered as the sum of a static mean wind and a stochastic fluctuating wind load known as buffeting. The response of the bridge structure can thus be divided into response to mean wind (static contribution) and response due to buffeting (dynamic response).

During meteorological storm events the maximum mean wind speed encountered during the storm is registered (10 min average / hourly average). This value is applied for extreme wind statistics – as also carried out for the Messina Strait project. As only one maximum value is used the extreme wind statistics is well suited as a basis for assessing the contribution to the fatigue damage during the entire life of the structures from the mean wind component.

Due to a fairly low number of cycles (storm return periods) the contribution from mean wind to the fatigue damage is very limited and can be disregarded in the fatigue calculations. However the dynamic wind response (buffeting) produce a large number of stress cycles of the bridge and will contribute to the fatigue damage in a notable scale.

The accumulated damage is calculated for the following combinations in order to estimate the effect of wind buffeting on the total damage:

Roadway girder:

- LM3 vehicle (global and local load effects) + 1 train (EN5) without train meetings
- LM3 vehicle (global and local load effects) + 1 train (EN5) without train meetings + wind

Railway girder:

- 1 train (EN5) on both tracks (global and local loads, without train meetings)
- 1 train (EN5) on both tracks (global and local loads, without train meetings) + wind

In order to assess the effects of wind, time series of wind fluctuations at a mean wind speed of 35 m/s perpendicular to the bridge alignment are used. The wind time series are scaled to a series of different mean wind speeds considered in the analyses (5, 10, 15, 20, 25, 30, 35 and 39 m/s) by a power law. However the damage obtained for each of the considered interval of wind speed is weighted by the occurrence and distribution of wind speed components perpendicular to the bridge girder to obtain the accumulated damage from the combination of man-generated loads and wind.

The following points are considered in the roadway and railway girders respectively:

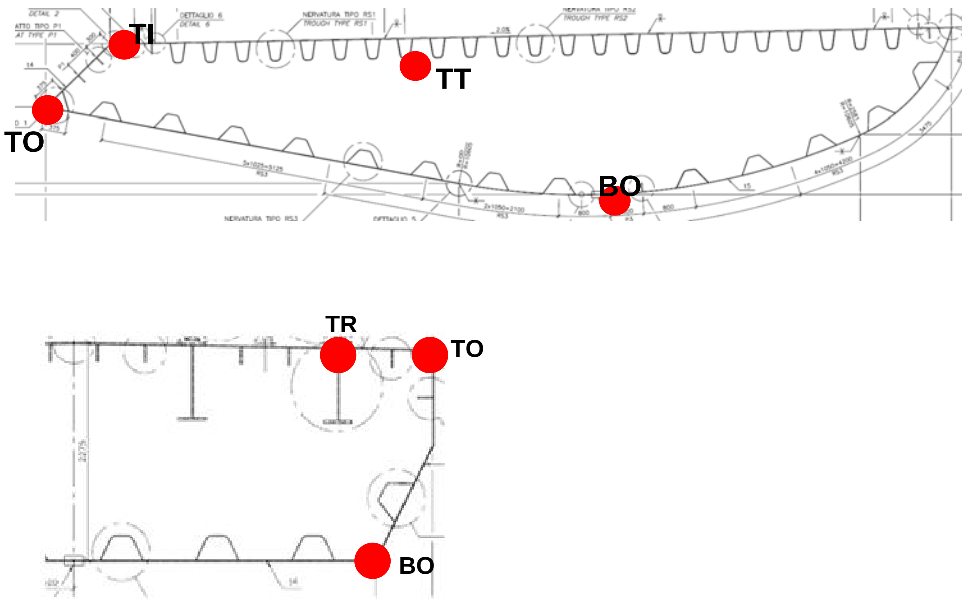

Figure 11-1 Considered points in roadway and railway girder for evaluation of wind load effects on fatigue damage

The calculated accumulative damages are summarised in Table 11-1 and Table 11-2 below for the roadway and railway girders respectively. A more detailed description of the calculations can be found in "Design Report - Fatigue Calc. of Suspended Deck".

Table 11-1 Comparison of accumulated damage of points in roadway girder

Structural detail	Stationing	Train alone EN5	Train + Wind fluctuations	Percentage increase
BO	885	0.019524	0.019759	+1.21%
TO	885	NA	4.61E-5	NA
TI	885	NA	5.57E-5	NA
TT	885	0.45682	0.45763	+0.18%
BO	1005	0.024185	0.024804	+2.56%
TT	1005	0.468657	0.471574	+0.62%

Where "NA" is shown in the table is due to the stress ranges obtained from traffic loading alone is below the cut-off limit and no direct comparison is possible. The small effect from traffic is mainly due to the location close to the neutral axis.

Table 11-2 Comparison of accumulated damage of points in railway girder

Structural detail	Stationing	Train alone EN5	Train + Wind fluctuations	Percentage increase
TO	1425	0.062759	0. 062809	+0.1%
TR	1425	0.083127	0.084488	+1.6%
BO	1425	0.015851	0.016540	+4.4%
TO	1650	0.024211	0.024505	+1.2%
TR	1650	0.122338	0. 122507	-0.7%
BO	1650	0.024211	0.024345	+0.6%

The results given in the preceding tables all indicate a modest increase in fatigue damage when wind is combined with man generated loads. The percentage increase is for all selected points below 5 %. It is hence suggested simply to subtract 5% from the allowable damage in the verification inequality and then limit the verification to the fatigue damage from trains and road traffic.

The assessment of damage is consequently performed following the formula of Palmgren-Miner, checking that the following result is obtained

$$D=\sum_i \frac{n_i(rail+road)}{N_i} \leq 1.0-0.05=0.95$$

10.4 Constant Amplitude Fatigue Limit

When all loading events result in stress ranges that are all below the constant amplitude fatigue limit, $\Delta\sigma_D$, the detail will still remain undamaged, and hence the detail will have an unlimited life. The stress ranges may vary significantly, but as long as the maximum stress ranges are kept below the constant amplitude fatigue limit $\Delta\sigma_D$ no further fatigue verification is needed. This can be illustrated by a limitation in stresses as the red curve in the S-N diagram in Figure 11-2.

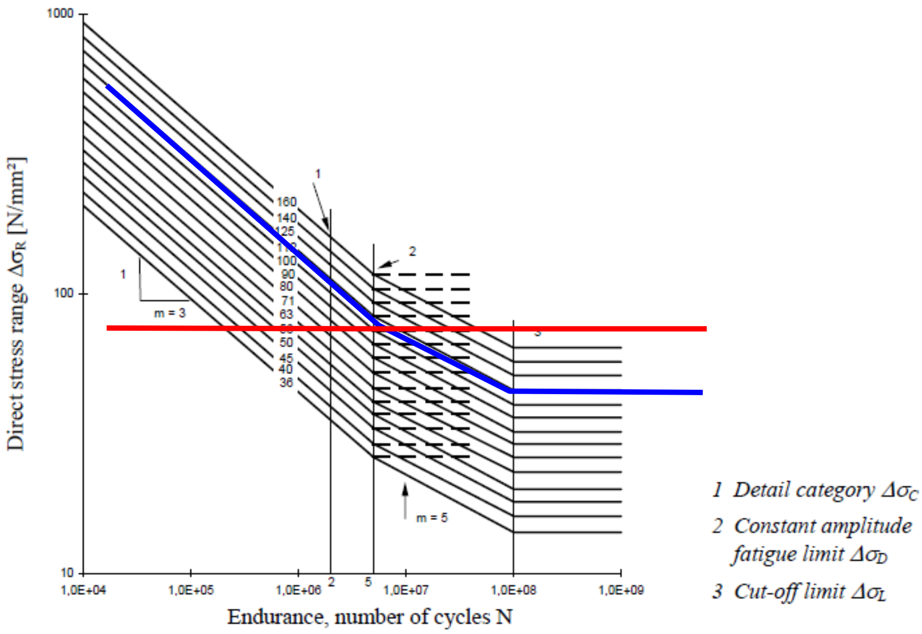

Figure 11-2 Red curve: S-N diagram for unlimited life verification constant amplitude fatigue loading, detail category 100 indicated by the constant amplitude fatigue limit $\Delta\sigma_D$ Blue curve: S-N diagram for variable amplitude fatigue loading detail category 100 indicated. Horizontal line shown at the constant amplitude fatigue limit $\Delta\sigma_D$

This is utilised in codes to define an *unlimited life method* for fatigue verification, which is a simple verification of all stress ranges being below the c*onstant amplitude fatigue limit* $\Delta\sigma_D$. The assessment of unlimited life for structural components can be expressed in the equation $\Delta\sigma_{\max,d} = \gamma_m \cdot \Delta\sigma_{\max} \leq \Delta\sigma_D$, where $\Delta\sigma_{\max,d}$ is the design values of the maximum normal stress range induced in the detail considered by the roadway and railway fatigue loading, and $\Delta\sigma_D$ is the constant amplitude fatigue limits.

10.5 Variable Amplitude Stress Variation

When stress ranges exceed the constant amplitude fatigue limit $\Delta\sigma_D$ these stress ranges contribute to the cumulative fatigue damage in the detail and furthermore the stress ranges below this level, but above the cut-off level $\Delta\sigma_L$, will contribute to the cumulative damage accumulation, i.e. the blue curve indicated in Figure 11-2 for detail category 100 shall be used.

For stress ranges below the constant amplitude fatigue limit $\Delta\sigma_D$, but above the cut-off limit $\Delta\sigma_L$, the number of stress cycles to failure for use in a cumulative damage summation is obtained from the equation:

$$\Delta\sigma_R^5 N_R = \Delta\sigma_D^5 \cdot 5 \cdot 10^6 \; for \; N < 1 \cdot 10^8$$

The damage accumulation shall include all the fatigue stress ranges within the lifetime of the bridge in a cumulative damage summation $D = \sum_i^k \frac{n_i}{N_i}$. Stress ranges less than the cut off limit ΔσL gives no contribution to the accumulated fatigue damage. The design requirement is that the accumulated damage D from man generated loading must be less than 0.95 hereby also accounting for the effect of wind. The damage accumulation method is often referred to as the Palmgren-Miner summation or briefly the Miner sum, D.

10.6 Particulars of a Suspension Bridge Deck

The suspended deck will experience stress ranges due to different effects during a loading event (passage of a fatigue train/vehicle) - typically three types of load effects are relevant:

- Global load effects are related to the presence of the entire train. The global load effect is a result of the elastic support of the suspended deck by the hangers and the main suspension system. Global load effects will appear for all points in the suspended deck, but the associated stress range will be very dependent upon the location of the considered detail. As the global load effects are associated with the train passage the related no of stress range variations will be small (a few times the number of train passages)

- Semi-local load effects related to the characteristics of the individual train wagons / trucks. The magnitude of the associated stress ranges will be very dependent upon the location in the structure of the considered detail. A particular point in the structure will experience a number of semi-local stress ranges guided by the no of trucks or wagons in a train.

- Local load effects related to the passage of the individual wagon or truck wheels. The associated stress ranges will mainly depend upon the detailing of the structure locally. The number of stress ranges associated with local load effects will be guided by the number of wheels passing the detail and hence be high e.g. related to the passage of wheel loads on the orthotropic roadway deck spanning 3.75 m between diaphragms.

The Table 11-3 below gives an indication of the number of the stress ranges for the different types of load effects.

Table 11-3 Number of stress ranges for different load effects

	No. of stress ranges
Global load effects	Small
Semi-local load effects	Medium
Local load effects	High

Figure 11-3 shows an example of the axial stress variation in the bottom plate of the railway girder for a train passing the bridge at the location indicated by an arrow. The magnitude of the axial stress is shown at the location on the bridge where the front of the train is located (running from left to right)

The considered point will experience a few peaks leading to a few occurrences of large stress ranges combined with much larger number of stress ranges at a significantly lower level.

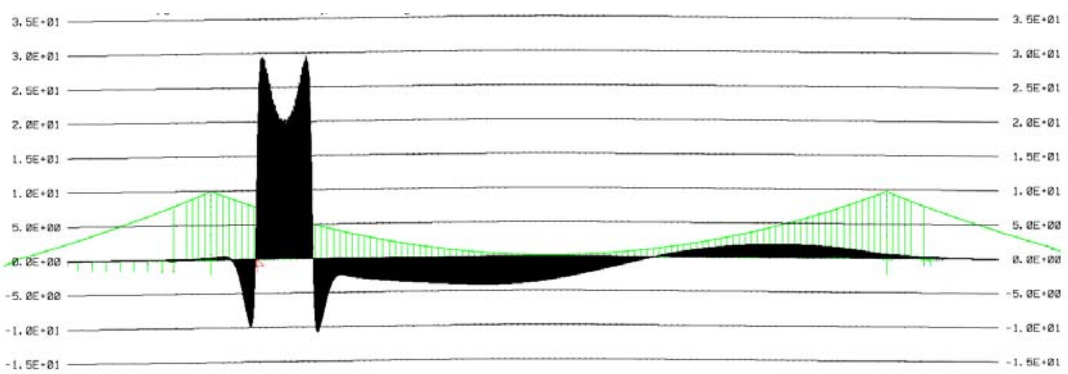

Figure 11-3 Example of axial stress variation in the bottom of the railway girder at the arrow for a train passing the bridge

The maximum stress ranges for the suspended deck are in general high and in many cases when two heavy freight trains meet each other at an arbitrary location on the bridge significantly above the constant amplitude fatigue limit. In such cases it is not possible to obtain unlimited life. For structural details where the stress ranges are dominated by global and semi-local effects the number of stress cycles will be moderate and the typical approach is then in accordance with Italian NTC08 and RFI 44 F and Eurocodes to carry out the fatigue verification using Miner's summation and verify that the fatigue life is minimum 200 years.

For structural details where the stress ranges are dominated by local load effects and hence high in numbers it enforced keeping the stress ranges below the endurance limit in order to achieve the required fatigue resistance. In practise this will entail application of the unlimited life method for fatigue verification.

For suspension bridge deck design it is observed that the unlimited life method is appropriate when all loading events result in a high numbers of stress cycles but with small variations in stress range, while Miner's summation is more appropriate when large variations in stress range appear.

According to the Design Basis all the elements shall be capable of fulfilling unlimited life method based on one freight train and the roadway LM2 as well as damage accumulation method. Exception is provided for the verification of point F of the roadway deck plate at the location of the web of cross girder for which unlimited life method has been verified including two EN5 meeting on the bridge alongside with roadway load LM2. By this approach the unlimited life has been verified for the maximum stress range and therefore the damage accumulation is not relevant.

10.7 Unlimited Life Method

In the unlimited life method the number of occurrences is of no importance as it is only the maximum fatigue stress range, which is important for the fatigue assessment. Therefore all stress ranges shall be below the constant amplitude stress range.

10.7.1 Design principles

When the "unlimited life method" has been applied, the fatigue contribution is based on the most onerous fatigue train in one track in combination with fatigue Load Model 2 (LM2) being applied on the roadway girder closest to the train. No other fatigue loading is considered for the unlimited life method.

10.7.2 Roadway Fatigue Loading

Fatigue load model 2 (LM2) is utilised as fatigue vehicles passing the bridge on the roadway girder for analyses of local effects of the orthotropic steel deck as well as the entire roadway girder, the cross girder and the railway girder. The dynamic effects are included in the load model. The different vehicles are passing the bridge and the worst load effects are selected. The different vehicles of load model 2 (LM2) is shown in Figure 11-4.

1 LORRY SILHOUETTE	2 Axle spacing (m)	3 Frequent axle loads (kN)	4 Wheel type (see Table 4.8)
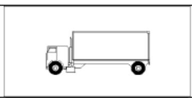	4,5	90 190	A B
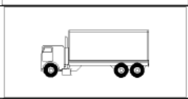	4,20 1,30	80 140 140	A B B
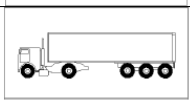	3,20 5,20 1,30 1,30	90 180 120 120 120	A B C C C
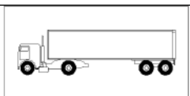	3,40 6,00 1,80	90 190 140 140	A B B B
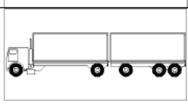	4,80 3,60 4,40 1,30	90 180 120 110 110	A B C C C

Figure 11-4 Load model 2 (LM) vehicles

Typical stress ranges for a LM2 vehicle passing the bridge is shown for the roadway girder in Figure 11-5, for the cross girder in Figure 11-6 and for the railway girder in Figure 11-7.

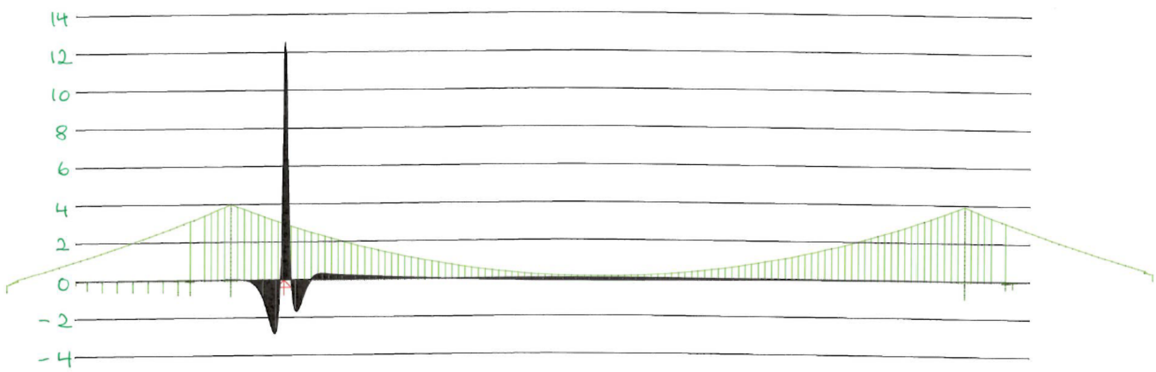

Figure 11-5 Unlimited life method - stress ranges in bottom plate of roadway girder for vehicle LM2 passing the bridge

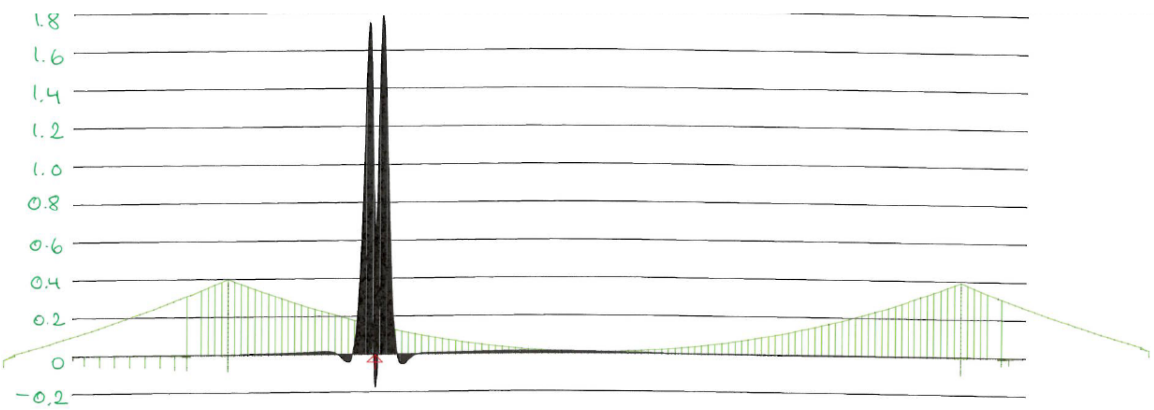

Figure 11-6 Unlimited life method - stress ranges in bottom plate of cross girder for vehicle LM2 passing the bridge

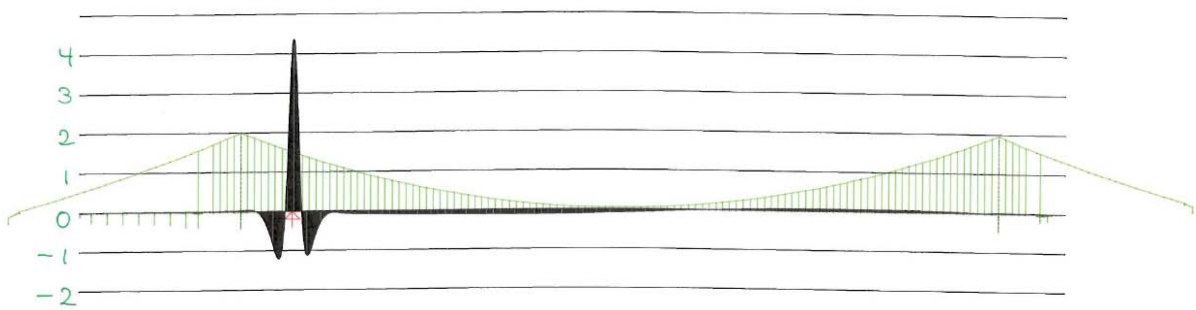

Figure 11-7 Unlimited life method - stress ranges in bottom plate of railway girder for vehicle LM2 passing the bridge

From the figures are seen that vehicles passing on the roadway girder also give stresses in the cross girder and railway girder as well which are to be taken into account in the fatigue assessment.

10.7.3 Railway Fatigue Loading

The railway fatigue stress range shall be selected as the most onerous stress range from the eight fatigue trains indicated in the standard train mix of Annex D of Eurocode 1991-2:2003. A heavy fatigue train EN5 with characteristics as seen in Figure 11-8 is considered.

$\Sigma Q = 21600kN \quad V = 80km/h \quad L = 270,30m \quad q = 80,0kN/m'$

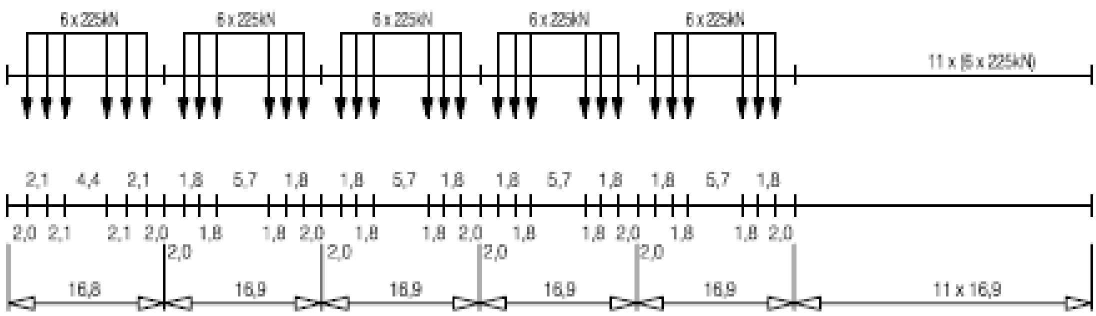

Figure 11-8 Characteristics for a heavy fatigue train EN5

Fatigue stress ranges for EN5 train passing the bridge is shown for the railway girder in Figure 11-9, for the cross girder in Figure 11-10 and for the roadway girder in Figure 11-11.

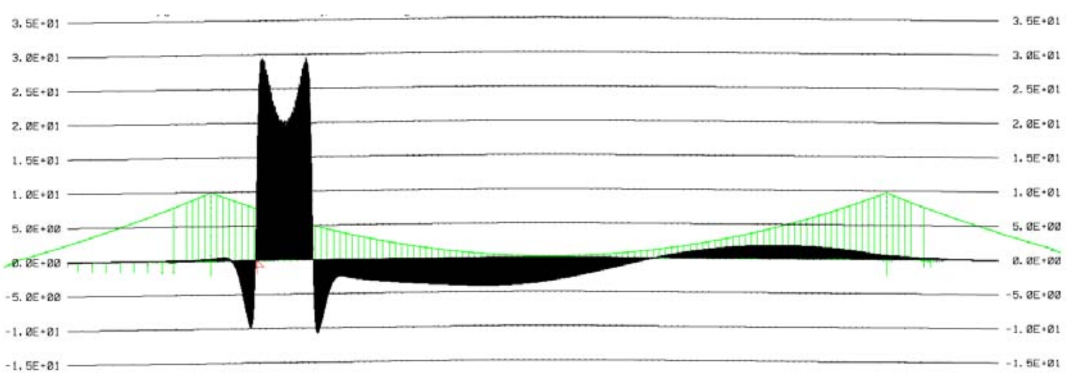

Figure 11-9 Unlimited life method - stress ranges in bottom plate of railway girder for EN5 train passing the bridge

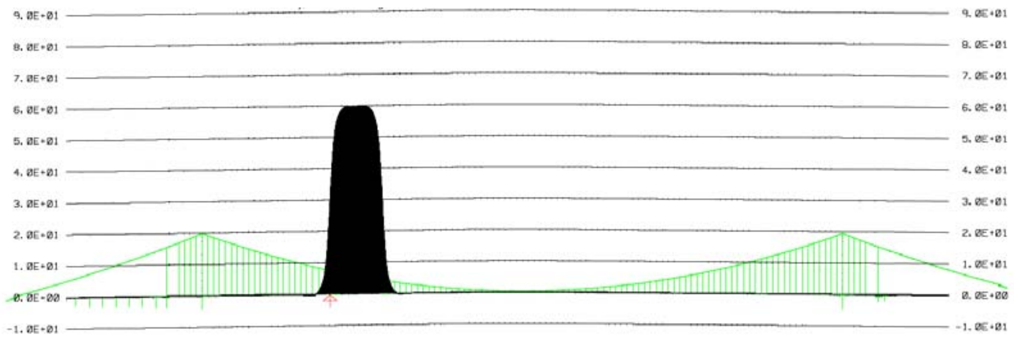

Figure 11-10 Unlimited life method - stress ranges in bottom plate of cross girder for EN5 train passing the bridge

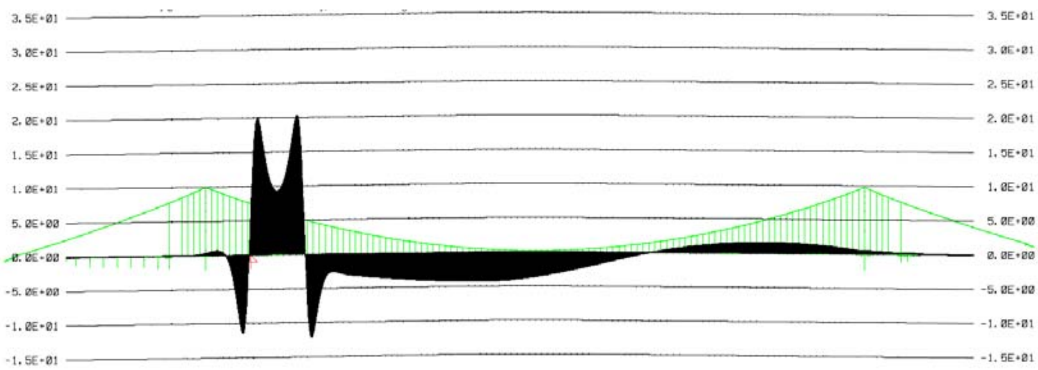

Figure 11-11 Unlimited life method - stress ranges in bottom plate of roadway girder for EN5 train passing the bridge

10.7.4 Effect of Roadway and Railway Fatigue Loading

For the unlimited life method the following equation has been used:

$$\Delta\sigma_{rail+road}=(\Delta\sigma_{LM2}+\Delta\sigma_{EN5}{}^{*}\ \varphi_{real,1})^{*}\gamma < \Delta\sigma_{D}, \text{ where:}$$

- $\Delta\sigma_{LM2}$ is the maximum stress range given by the algebraic difference between the two extremes of the stress history plot of the fatigue load model 2 for the given detail
- $\Delta\sigma_{EN5}$ is the maximum stress range given by the algebraic difference between the two extremes of the stress history plot of train type 5 running in one track for the given detail

- $\gamma_{MF} = \gamma_f * \gamma_m$ is the partial factor for fatigue strength (fatigue partial factor * resistance partial factor) equal to 1.15 for local details of the roadway orthotropic deck plate and 1.35 for all the others components
- $\varphi_{real,i}$ is the dynamic factor where the index i refers to the loaded track. Depending to the detail to be verified and to the determinant length L_Φ it is necessary to distinguish in local and global dynamic factors: dynamic factors for local effects have been accounted for by assuming L_Φ=3 times the span of deck element and for global effects by assuming L_Φ=1,5 times the span of the main girder spanning between cross girders. Considering the maximum design speed the real dynamic factors are summarised in Table 11-4.

Table 11-4 Real dynamic factors

		speed	local effects	global effects
Fatigue trains EN 1991-2: 2003	EN 1	200	1.300	1.165
	EN 2	160	1.230	1.125
	EN 3	250	1.400	1.224
	EN 4	250	1.400	1.224
	EN 5	80	1.181	1.056
	EN 6	100	1.190	1.071
	EN 7	120	1.200	1.088
	EN 8	100	1.190	1.071

Structural details have been distinguished between bottom plate elements for which local effects have not been accounted for and deck plate elements which include local loading effects. Based on said division different damage contributions apply as shown in the following.

Bottom Plate details of roadway, railway and cross girder:

- $\Delta\sigma = (\Delta\sigma_{LM2,\ glob} + \Delta\sigma_{EN5,glob} * \varphi_{glob}) * \gamma_{MF} < \Delta\sigma_D$

Deck plate details of railway girder:

- $\Delta\sigma = (\Delta\sigma_{LM2\ ,glob} + \Delta\sigma_{EN5,glob} * \varphi_{glob} + \Delta\sigma_{EN5,loc} * \varphi_{loc}) * \gamma_{MF} < \Delta\sigma_D$

Deck plate details of roadway girder:

- $\Delta\sigma = (\Delta\sigma_{LM2\,,glob} + \Delta\sigma_{LM2\,,loc} + \Delta\sigma_{EN5,glob} * \varphi_{glob,1}) * \gamma_{MF} < \Delta\sigma_D$

10.8 Damage Accumulation Method

In the damage accumulation method (Miners summation) the number of occurrences is important when calculating the Miners sum. All stress ranges above the cut off value contributes to the accumulated fatigue damage.

10.8.1 Design principles

For the "damage accumulation method" (Palmgren-Miners summation of damage) the fatigue contribution is based on the passing of all 8 fatigue trains in combination with roadway fatigue Load Model 3 (LM3) being applied on the roadway girder closest to the train. Fatigue loading from mean wind as well as buffeting have been also included in the damage evaluation by a damage factor of 0.05 which lower the damage limit due to traffic load only to 0.95. When considering combinations of roadway fatigue loading and railway fatigue loading the following statements applies:

- No trains + 1 roadway vehicle + wind
- 1 train + 1 roadway vehicle + wind
- 2 trains + 1 roadway vehicle + wind

10.8.2 Roadway Fatigue Loading

Fatigue load model 3 (LM3) is utilised as fatigue vehicles passing on the bridge on the roadway girder for the analyses of the global and the local effects of the orthotropic steel deck as well as the whole roadway girder, the railway girder and the cross girders. The dynamic effects are included in the load model. The load model 3 vehicle (LM3) is shown in Figure 11-12.

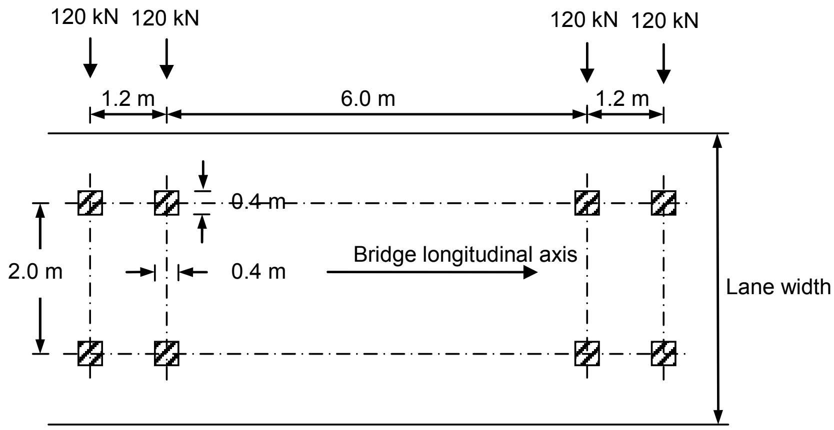

Figure 11-12 Load model (LM3) vehicle

This model consists of four axles, each of them having two identical wheels. The geometry is shown in the above figure. The weight of each axle is equal to 120 kN, and the contact surface of each wheel is a square of 0.40x0.40 m.

Typical stress ranges for the LM3 vehicle passing the bridge is shown for the roadway girder in Figure 11-13, for the cross girder in Figure 11-14 and for the railway girder in Figure 11-15.

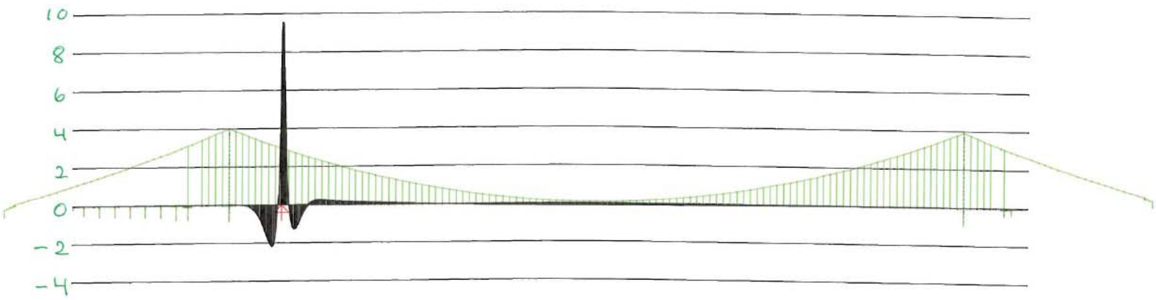

Figure 11-13 Damage accumulation method - stress ranges in bottom plate of roadway girder for vehicle LM3 passing the bridge

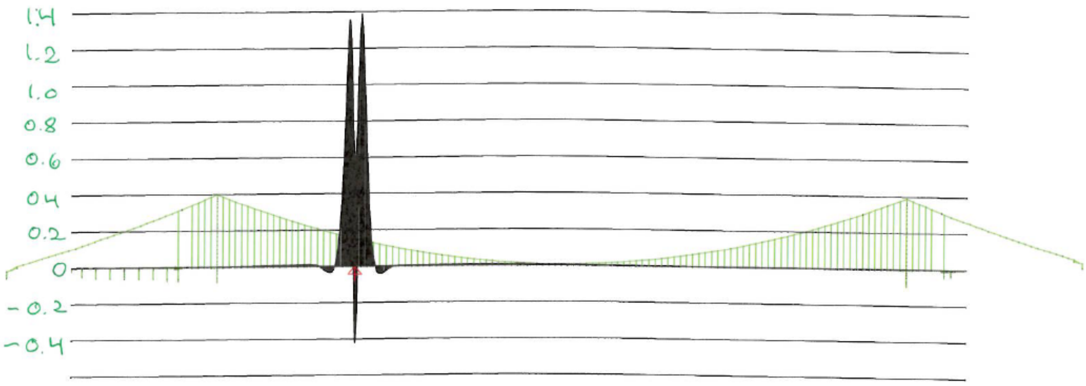

Figure 11-14 Damage accumulation method - stress ranges in bottom plate of cross girder for vehicle LM3 passing the bridge

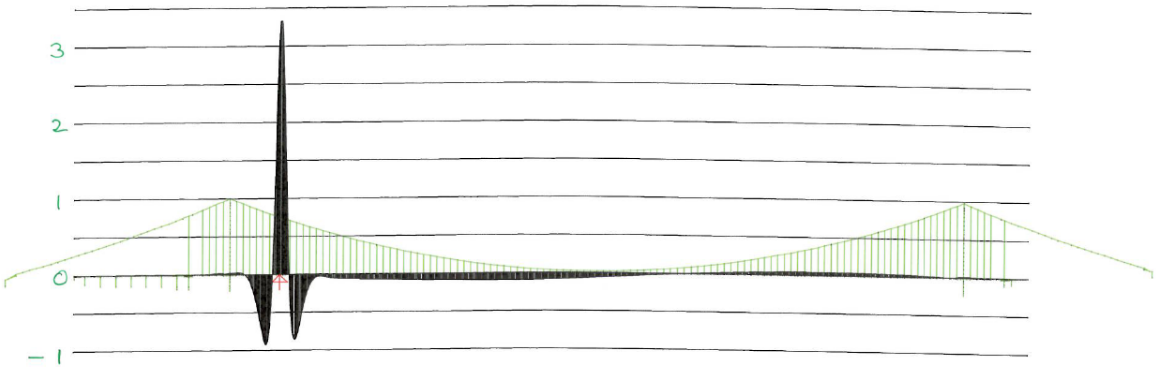

Figure 11-15 Damage accumulation method - stress ranges in bottom plate of railway girder for vehicle LM3 passing the bridge

From the figures are seen that vehicles passing on the roadway girder also gives stresses in the cross girder and railway girder, which also shall be taken into account in the fatigue assessment.

Considering the LM3 for fatigue assessment the number of passing becomes 4.0×10^8 within the 200 year lifetime, which requires that the maximum stress range shall be below the cut off value $\Delta\sigma_L$.

10.8.3 Railway Fatigue Loading

The railway trains are the eight fatigue trains indicated in Annex D of Eurocode 1991-2:2003. The daily number of trains is 67 per track with a traffic mix defined in the Design Basis and shown in Table 11-5.

Table 11-5 Total number of trains in 200 years per track

		Trains/day	1 year	200 years	Ni for train meeting (12%)	Ni for train alone (88%)
fatigue trains - EN 1991-2: 2003	EN 1	12	4380	876000	105120	770880
	EN 2	12	4380	876000	105120	770880
	EN 3	5	1825	365000	43800	321200
	EN 4	5	1825	365000	43800	321200
	EN 5	7	2555	511000	61320	449680
	EN 6	12	4380	876000	105120	770880
	EN 7	8	2920	584000	70080	513920
	EN 8	6	2190	438000	52560	385440

The number of events for each of the 8 x 8 different combinations is summarised in Table 11-6.

Table 11-6 Number of train intersections in 200 years

	EN 1	EN 2	EN 3	EN 4	EN 5	EN 6	EN 7	EN 8
EN 1	18827	18827	7845	7845	10983	18827	12552	9414
EN 2	18827	18827	7845	7845	10983	18827	12552	9414
EN 3	7845	7845	3269	3269	4576	7845	5230	3922
EN 4	7845	7845	3269	3269	4576	7845	5230	3922
EN 5	10983	10983	4576	4576	6407	10983	7322	5491
EN 6	18827	18827	7845	7845	10983	18827	12552	9414
EN 7	12552	12552	5230	5230	7322	12552	8368	6276
EN 8	9414	9414	3922	3922	5491	9414	6276	4707

The principles for the train fatigue stress ranges for the damage accumulation method are similar the ones for the unlimited life method. For the railway girder reference is made to Figure 11-9, for the cross girder to Figure 11-10 and for the roadway girder to Figure 11-11.

10.8.4 Effect of Roadway and Railway Fatigue Loading

When the combination of roadway and railway loads has been considered for the fatigue assessment, in general terms the following equation has been used:

$\Delta\sigma_{rail+road} = ((\Delta\sigma_1 * \varphi_{real,1}) + (\Delta\sigma_2 * \varphi_{real,2}) + \Delta\sigma_{LM3}) * \gamma_{MF}$, where:

- $\Delta\sigma_1$ is the maximum stress range given by the algebraic difference between the two extremes (max, min) of a particular stress cycle derived from a stress history diagram by one of the 8 trains on track 1. $\Delta\sigma_1$ is zero if no trains are present
- $\Delta\sigma_2$ is the maximum stress range given by the algebraic difference between the two extremes (max, min) of a particular stress cycle derived from a stress history diagram by one of the 8 trains on track 2. $\Delta\sigma_2$ is zero if only one train is present
- $\Delta\sigma_{LM3}$ is the maximum stress range given by the algebraic difference between the two extremes of a particular stress cycle derived from a stress history diagram using load model 3 (LM3)
- $\gamma_{MF} = \gamma_f * \gamma_m$ (fatigue partial factor * resistance partial factor) equal to 1.15 for local details of the orthotropic roadway deck and 1.35 for all the others components
- $\varphi_{real,i}$ is the dynamic factor. Due to the determinant length it is necessary to distinguish in local and global dynamic factors. Considering the maximum of real train speed the real dynamic factors are summarised in Table 11-4.
- For the damage accumulation calculations the damage sum has to be below 0.95 to take account of the wind contribution to fatigue (refer to Section 11.3), hence:
- $\Sigma\, n_i / N_i <= 0.95$, where
- N_i is the endurance (in cycles) obtained from the $\Delta\sigma_C$ - N_R curve for a stress range of $\Delta\sigma_{i,d}$, n_i is the number of cycles associated with the stress range $\Delta\sigma_{i,d}$ for band *i* in the factored spectrum. This number for the railway loads has been carried out on the basis of the traffic mix defined in the Design Basis described in .

When considering roadway loads the Fatigue Load Model 3 has been used.

Structural details have been distinguished between bottom plate elements for which local effects have not been accounted for and deck plate elements which include local loading effects. Based on said division different damage contributions apply as shown in the following.

Bottom Plate details of roadway, railway and cross girder:

- train on track 1 + LM3
- train on track 2 + LM3
- train on track 1 + train on track 2 + LM3

Deck plate details of railway girder:

- train on track 1 + LM3 + local of train on track 1
- train on track 2 + LM3
- train on track 1 + train on track 2 + local of train on track 1 + LM3
- LM3 only

Deck plate details of roadway girder:

- train on track 1 + LM3 + local LM3
- train on track 2 + LM3 + local LM3
- train on track 1 + train on track 2 + LM3
- LM3 + local LM3

It must be noted that when the roadway girder deck plate is under investigation, since the life time of the bridge is 200 years, it is affected by 4.0×10^8 global load cycles and even more local load cycles. Thus the maximum stress amplitude given by a single event multiplied by γ_{MF} must be less than $\Delta\sigma_L$ to prevent damage. This is valid when looking at both the bottom flange (i.e. without local effects) and at the trough (i.e. including local effects). For the latter element it has been verified that the stiffener is capable to limit the stress due to the application of the local load, below the cut off limit for the detail category 71 representative of the trough splice at the structural joint. This has induced a local thickening of the trough in correspondence and next to the trough splice in correspondence of the structural joints.

It must be noted that in the stress-history plots any stress range below the cut off limit $\Delta\sigma_L$ has been neglected.

10.9 Fatigue Details

All fatigue categories have been taken from the EN 1993-1-9:2005 table 8.1 to table 8.10, EN 1993-2:2006.

10.9.1 Roadway bottom plate details

The fatigue analysis of the most critical locations in the roadway girder is solved using the sectional forces of the global IBDAS model.

The fatigue assessment concerns the following construction details:

- Full penetration butt weld between top plate of the girder and top plate of the cross girder. The weld corresponds to detail category 80, see EN1993-1-9 Table 8.3, detail no.11.
- Full penetration weld between bottom plate of the girder and web of the crossbeam. The weld corresponds to detail category 80, see EN1993-1-9 Table 8.5, detail no.1.
- Full penetration longitudinal butt weld between plates of top and bottom plates of the girder at mid and at end span. The weld corresponds to detail category 90, see EN1993-1-9 Table 8.2, detail no.10.
- Fillet weld between the web and the top and bottom plate at mid and at end span. The weld corresponds to detail category 100, see EN1993-1-9 Table 8.2, detail no.6.
- Welded connection of the girder diaphragm to the plate or the web. The weld corresponds to detail category 80, see EN1993-1-9 Table 8.4, detail no.8.
- Transverse full penetration welds between the plates crossed by continuous longitudinal weld of stiffener. The weld corresponds to detail category 80, see EN1993-1-9 Table 8.3, detail no.9.

- Transverse joint in troughs with full penetration butt weld with steel backing plate. The bottom plate trough splices occurs at both the erection joint and the shop joint. The weld corresponds to detail category 71, see EN1993-1-9 Table 8.8, detail no.4.

In the calculations only the most onerous details for the fatigue verification have been considered, namely:

1. The connection of the diaphragm to bottom plate. The weld corresponds to detail category 80 (EN1993-1-9 Table 8.4, detail no.8)

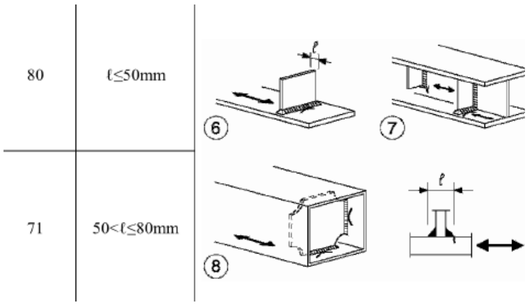

2. The bottom plate trough splices in correspondence of the erection joint and the shop joint (EN1993-1-9 Table 8.8, detail no.4).

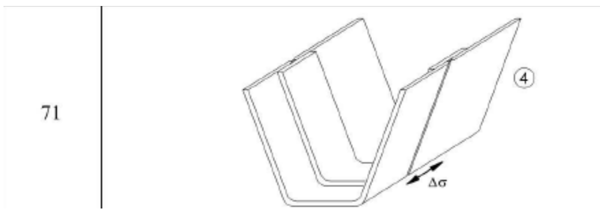

All other details are of same or higher category or capable of improvement up to a higher class and thus indirectly covered in the calculation.

10.9.2 Hanger anchorage

Three fatigue checks of stress ranges are carried out for the anchor plate in correspondence with the bearing connection to the hanger, and in one position of the side plate, as shown in *Figure* 11-16.

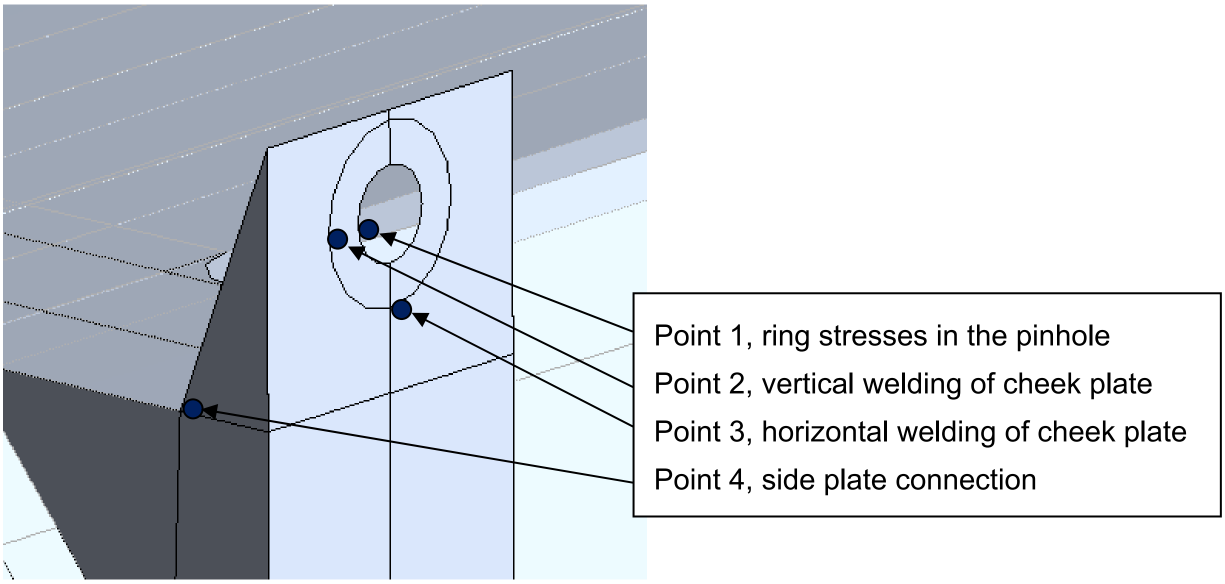

Figure 11-16   Positions of stress points for fatigue evaluation

The fatigue categories for the four points are:

- Point 1 is 160 see EN1993-1-9 Table 8.1, detail no.1
- Point 2 is 80 see EN1993-1-9 Table 8.5, detail no.8
- Point 3 is 40 see EN1993-1-9 Table 8.5, detail no.6
- Point 4 is 56 see EN1993-1-9 Table 8.5, detail no.1.

The stress range values are compared with the stress ranges in the local FE-Model of the hanger anchorage, see section 11.11.5.

10.9.3 Roadway deck details

The fatigue analyses of the local actions in points A, B, C, D, E, F has been performed using a local IBDAS model of the orthotropic steel deck, refer to General Design Principles for Suspended Deck section 10.9.2 for more information.

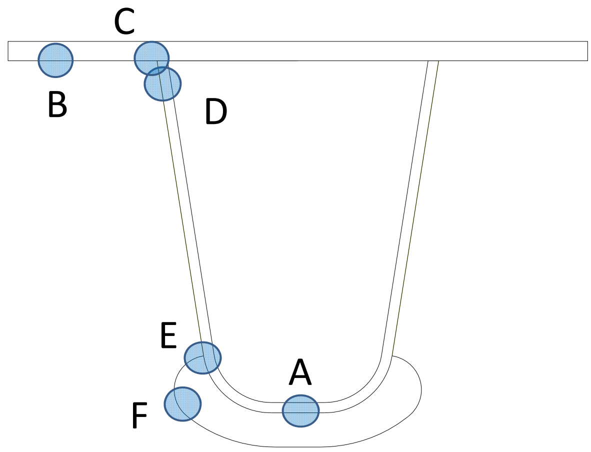

Figure 11-17   Roadway orthotropic deck details

The fatigue assessment concerns the following details:

1. Point A represents the full penetration butt weld in trough with steel backing plate. The weld corresponds to detail category 71, see EN1993-1-9 Table 8.8, detail no.4.

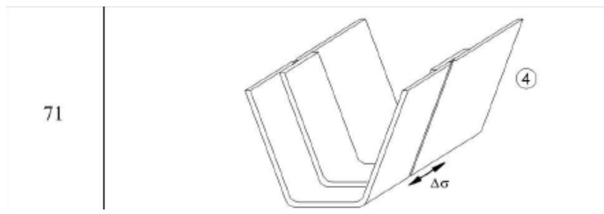

2. Point B represents the deck connected to the diaphragm. The weld corresponds to detail category 80, see EN1993-1-9 Table 8.4, detail no.8.

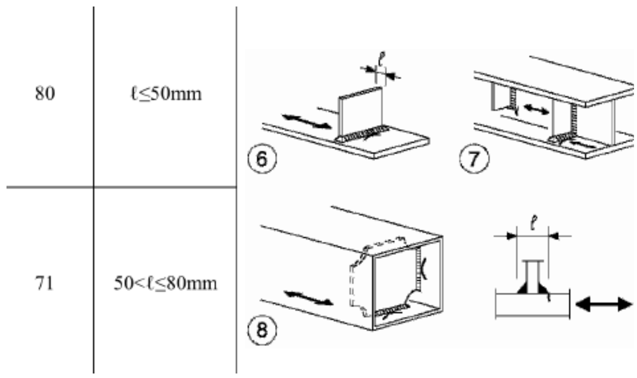

3. Point C represents the continuation in the plate of the limitation due to the trough splice; this is thus taking place only at the structural joints (erection and shop). The detail category must then fulfil the same limitation as for point A. External to the structural joints it represents also the sections where the longitudinal fillet weld of the trough intersects a transverse full penetration butt weld splice of the deck plate and a fatigue detail 80 is prescribed, see EN1993-1-9 Table 8.3, detail no.9. In the latest configuration being a shop weld the category might be increased to 112 MPa thus becoming less critical then detail B and therefore it has never been considered.

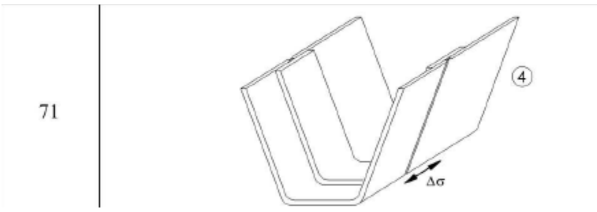

4. Point D represents the weld connecting deck plate to trough web. Being a partial penetration weld, an additional parasite bending moment becomes present due to the compression in the web of the trough and the eccentricity of the weld. This detail is only subjected to local effects. The weld corresponds to a detail category 71, see EN1993-1-9 Table 8.8, detail no.7.

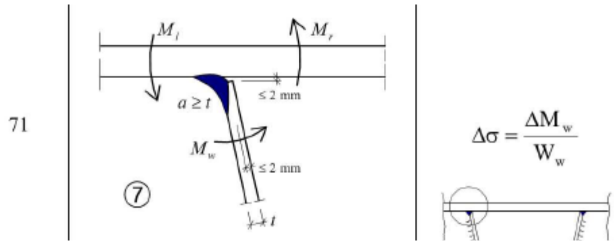

5. Point E represents the connection between the trough and the cut out in the diaphragm. As the diaphragm thickness is 15mm the weld corresponds to detail category 71, see EN1993-1-9 Table 8.8, detail no.1.

80	t≤12mm
71	t>12mm

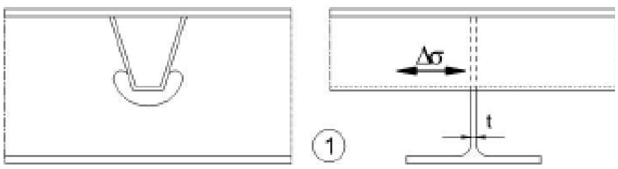

Point F represents one end of the critical section in the diaphragm due to cut outs. The tooth plate at the diaphragm is only subject to stresses due to local roadway loads and being not affected by other global effects such as the railway girder load. Thus it is only verified according to the unlimited life method. The same detail has been also verified at the cross girder web and the verification has also included the combined effects of the local wheel load and the global railway load.

71

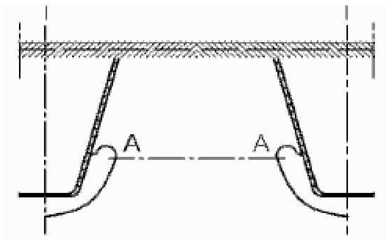

6

Points A and D have been checked at specific points between two diaphragms as the results at point A have been used to optimise the trough splice location whereas point D must be fulfilled at any location between diaphragms; for more information see the local roadway FE-model in the document General Design Principles for Suspended Deck, section 10.9.2. Points B, E and F have been checked only at the location of the diaphragms.

10.9.4 Railway bottom plate details

The fatigue analysis of the most critical locations in the railway girder is solved using stress history plots determined from the global IBDAS model of the bridge. The fatigue assessment concerns the following construction details:

- Full penetration butt weld between top plate of the girder and top plate of the cross girder. The weld corresponds to detail category 80, see EN1993-1-9 Table 8.3, detail no.11.
- Full penetration weld between bottom plate of the girder and web of the cross girder. The weld corresponds to detail category 80, see EN1993-1-9 Table 8.5, detail no.1.
- Full penetration longitudinal butt weld between top and bottom plates of the girder at mid and at end span. The weld corresponds to detail category 90, see EN1993-1-9 Table 8.2, detail no.10.
- Automatic fillet weld carried out from both sides between the web and the top plate at mid and at end span. The weld corresponds to detail category 100, see EN1993-1-9 Table 8.2, detail no.5.

- Welded connection of the girder diaphragm to the deck plate, bottom plate or the web. The weld corresponds to detail category 80, see EN1993-1-9 Table 8.4, detail no.8.
- Transverse full penetration weld between the plates crossed by continuous longitudinal weld of stiffener. The weld corresponds to a detail category 80, see EN1993-1-9 Table 8.3, detail no.9.

In the calculations only the most onerous for the fatigue verification have been considered, namely:

1. The connection of the diaphragm to bottom plate (EN1993-1-9 Table 8.4, detail no.8)

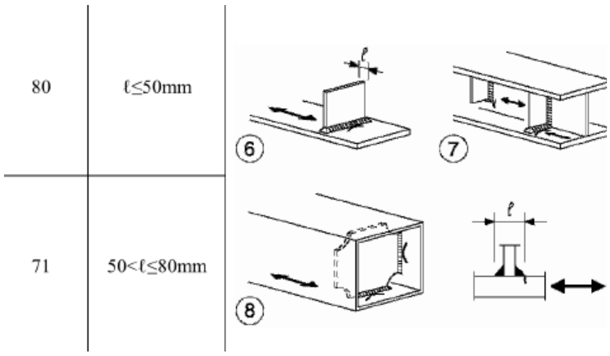

2. The bottom plate trough splices in correspondence of the erection joint and the shop joint (EN1993-1-9 Table 8.8, detail no.4).

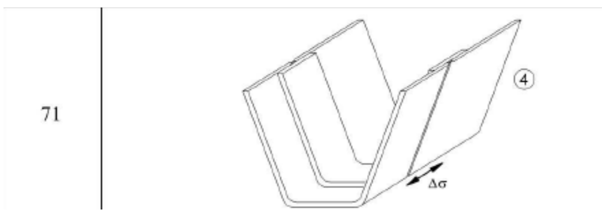

All other details are of same or higher category or capable of improvement up to a higher class and thus indirectly covered in the calculation.

10.9.5 Railway deck details

The fatigue analyses of the local actions of points WA and WB has been performed using a local IBDAS model of the T stiffener including the effective top plate, refer to General Design Principles for Suspended Deck 10.9.4.

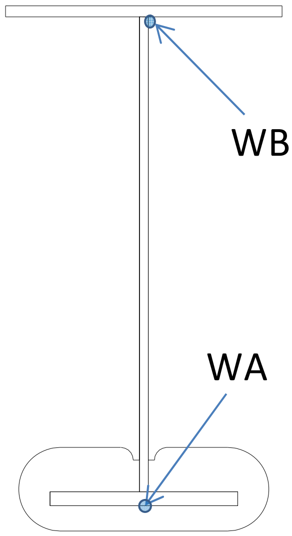

Figure 11-18 Railway orthotropic deck details

The fatigue assessment concerns the following details in proximity of the structural joints:

1. Point WA represents the longitudinal fillet weld with a cope hole height not grater than 60 mm. The weld corresponds to detail category 71, see EN1993-1-9 Table 8.2, detail no.9.

71	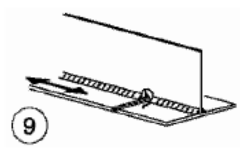

2. Point WB represents the top of the stiffener web connected to the either the main diaphragms or the intermediate diaphragms. Detail category 80, see EN1993-1-9 Table 8.4, detail no.8.

80	ℓ≤50mm	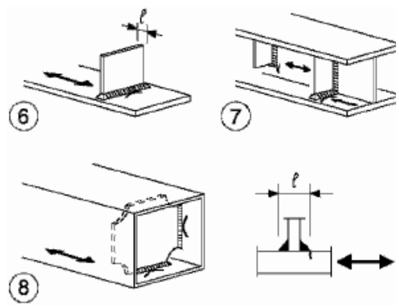
71	50<ℓ≤80mm	

10.9.6 Cross girder details

The fatigue analysis of the most critical locations in the cross girder is solved using the sectional forces of the global IBDAS model. For the top and bottom plate fatigue details have been checked at plate connections.

The fatigue assessment concerns the following construction details:

- Full penetration butt weld between top plate and bottom plate. The weld corresponds to detail category 112, see EN1993-1-9 Table 8.3, detail no.1.
- Fillet weld between the web and the top and bottom plate at mid span. The weld corresponds to detail category 100, see EN1993-1-9 Table 8.2, detail no.6.
- Transverse full penetration weld between the plates crossed by continuous longitudinal weld of stiffener. The weld corresponds to detail category 112, see EN1993-1-9 Table 8.3, detail no.2.
- Welded connection of the girder diaphragm to the top plate, bottom plate or the web. The weld corresponds to detail category 80, see EN1993-1-9 Table 8.4, detail no.8.

In the following calculations only the most onerous for the fatigue verification have been considered, namely:

1. Welded connection of the girder diaphragm to the top plate, bottom plate or the web. The weld corresponds to detail category 80, see EN1993-1-9 Table 8.4, detail no.8 .

10.9.7 Improvements of Fatigue Detail Categories

At present fatigue detail categories of 80 have been selected in general. Some of the detail categories can however be improved by weld treatment.

One detail category is governing for major parts of the suspended deck elements, which is the connection of the skin plates to the diaphragms. This detail is categorised class 80 as shown in Figure 11-19.

80	ℓ≤50mm	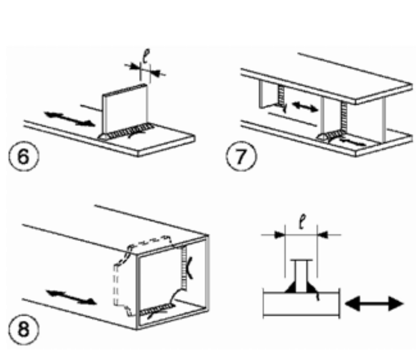	Transverse attachments: 6) Welded to plate. 7) Vertical stiffeners welded to a beam or plate girder. 8) Diaphragm of box girders welded to the flange or the web. May not be possible for small hollow sections. The values are also valid for ring stiffeners.	Details 6) and 7): Ends of welds to be carefully ground to remove any undercut that may be present. 7) $\Delta\sigma$ to be calculated using principal stresses if the stiffener terminates in the web, see left side.
71	50<ℓ≤80mm			

Figure 11-19 Connection of skin plates and diaphragm - detail category 80

With reference to the "International Institute of Welding (IIW) recommendations for fatigue design of welded joints and components" an enhanced class of 100 MPa has been used for the detail as shown in Figure 11-20.

IIW Fatigue Recommendations XIII-2151-07/XV-1254-07 May 2007

No.	Structural Detail	Description (St.= steel; Al.= aluminium)	FAT St.	FAT Al.	Requirements and Remarks
500	Non-load-carrying attachments				
511	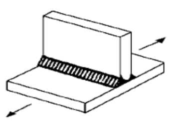	Transverse non-load-carrying attachment, not thicker than main plate K-butt weld, toe ground Two sided fillets, toe ground Fillet weld(s), as welded thicker than main plate	 100 100- 80 71	 36 36 28 25	Grinding parallel to stress An angular misalignment corresponding to $k_m = 1.2$ is already covered
831	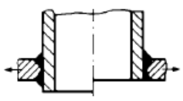	Tubular branch or pipe penetrating a plate, K-butt welds.	80	28	If diameter > 50 mm, stress concentration of cutout has to be considered Assessment by structural hot spot is recommended.

Figure 11-20 Structural details according to IIW recommendations

10.10 Models for Verification of Fatigue

The fatigue verification is carried out using the 5 models described below.

10.10.1 Global IBDAS Model

The 8 railway fatigue train load models, the LM2 and the LM3 roadway fatigue load models have been implemented to the global IBDAS model. The analysis type for calculating the stress history is a 1st order p-delta analysis with the reference condition as p-delta effects. This means that the results from our traffic loads are very close to the results coming from a 2nd order analysis because the dead load is dominating.

The stress history has been calculated for each of the load events (8 trains + LM3 load) in the mid and in the end of the 30 m spans in different locations of the bridge. The worst 30 m span has been found to be between the IBDAS s-coordinate -1440 and -1410 m measured from centre of the bridge (the 7th 30m span from the Sicilia tower). In this span the stress history has been fully developed.

When the "damage accumulation method" (Palmgren-Miners summation of damage) has been applied only one cycle per train has been taken into consideration as the second relevant cycle has always been found to be lower than the cut-off limit of the actual detail.

Conservatively, when the combination of road and rail loads has been done, the maximum value of $\Delta\sigma$ for both of them has been considered simultaneously.

10.10.2 Local IBDAS Model of Orthotropic Deck

A detailed local shell FE-model has been developed in IBDAS for the assessment of fatigue loads on the orthotropic roadway steel deck. The scope of this model is to obtain a detailed understanding of the local stress state induced by the fatigue load models LM2 and LM3 specified in EN 1991-2:2003 (E). Hence the benefits in a global FE-model are out of scope in this regard, and instead a small section of the steel deck including stiffeners and diaphragms has been modelled in much greater detail than possible in the global FE-model due to computational time.

10.10.2.1 Geometry

While the full width of the roadway steel deck supported by troughs constitutes roughly 12 m, the local FE-model is made up of a cross section comprising seven troughs. Likewise only eight diaphragms are included in the longitudinal direction. The key dimensions of the local FE-model read:

Table 11-7 Local FE-model geometrical dimensions

Outer dimensions	Width	0.51 m x 7 = 3.57 m
	Length	3.75 m x 7 = 26.25 m
Other dimensions	Deck thickness	0.017 m
	Trough thickness	0.009 m
	Trough height (bottom steel deck to bottom trough)	0.309 m
	Trough width at steel deck (centre-centre)	0.239 m
	Trough width at bottom (centre-centre)	0.139 m
	Roadway surfacing thickness	0.012 m
	Diaphragm thickness	0.015 m

The roadway surfacing has not been modelled directly in the FE-model as the purpose is to calculate traffic induced stresses, i.e. with no contribution from dead load. Instead a diffusion of the wheel foot prints is taken into account by assuming a load dispersion of 45° through the surfacing. The diaphragms have been modelled directly in the FE-model with a fully detailed inclusion of the cut-outs around the lower part of the troughs. The diaphragms are modelled to 1 m beneath the steel deck in order not to introduce boundary effects in the vicinity of the regions of interest. Figure 11-21 shows the geometry of the IBDAS model.

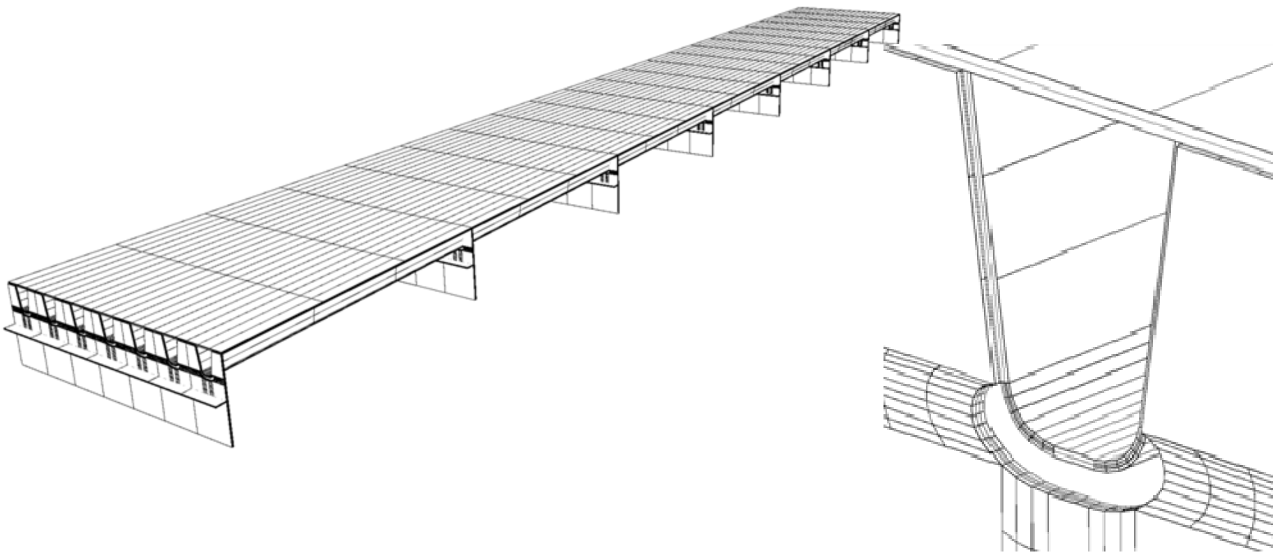

Figure 11-21 Geometry of the local IBDAS model of the orthotropic roadway steel deck and diaphragm

10.10.2.2 FE-Model

The finite element model is made as a full shell model where the curved geometry in the troughs and cut-outs in the diaphragm is reflected in the FE-model as shown below. In order to ensure converged stress results in the diaphragm around the cut-outs where high stress gradients can be expected a very dense mesh has been applied in this region.

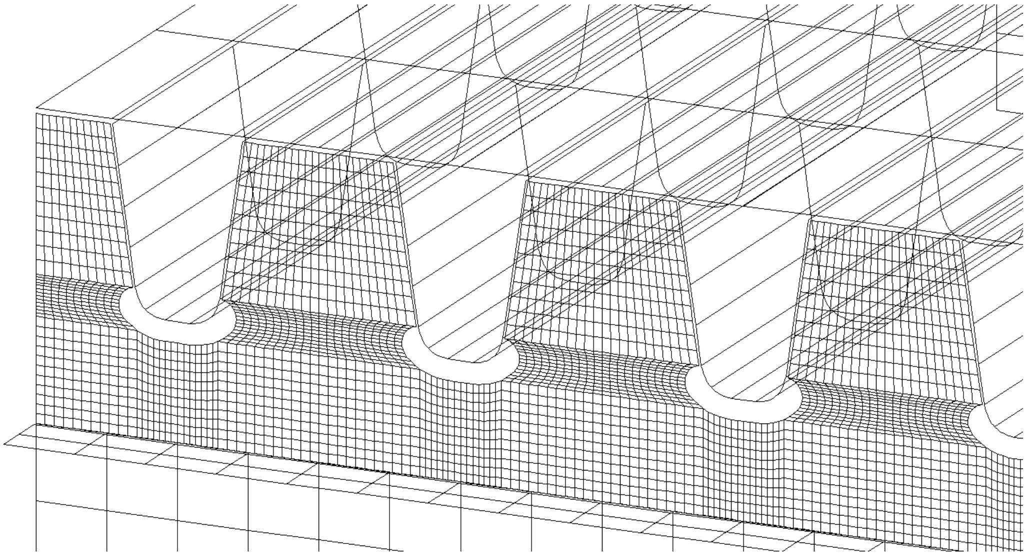

Figure 11-22 Part of the FE-model shell mesh

The nodes at the sides and the bottom of the diaphragms have been supported in the vertical and the transverse direction by means of springs. The influence of the spring stiffness on the stress results has proved marginal. At one of the end boundaries of the model, the longitudinal translational degrees of freedom have been supported as well. The figure below shows an exaggerated deformation shape of the model loaded by dead load only. The boundaries at the sides of the model are not supported apart from the outermost nodes at the diaphragms.

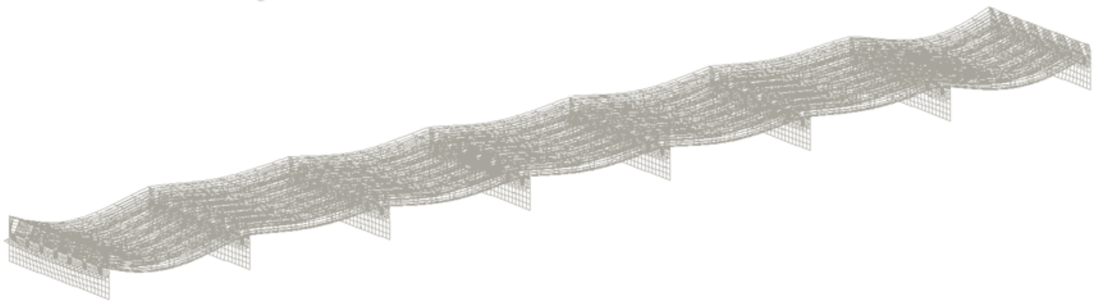

Figure 11-23 Deformed shape of local FE-model when exposed to dead load (scale 8000)

As appears from the above certain artificial boundary conditions have been introduced in order to establish a local model which still retains integrity as a stand-alone structure. This means that analysis results can only be used with confidence when the structural element in question as well as the applied loads is placed well away from these boundaries. Hence all stresses are calculated for the middle trough in the middle section of the model as shown below.

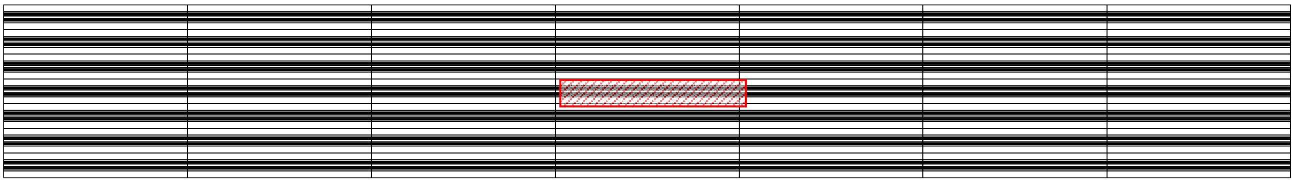

Figure 11-24 Analysis section of local FE-model

10.10.2.3 Fatigue Loads

For the assessment of fatigue loading two different load models have been applied to the local IBDAS model: The LM2 (EN 1991-2:2003 (E) section 4.6.3) and the LM3 (EN 1991-2:2003 (E) section 4.6.4) respectively.

LM2 consists of five individual vehicles which share the same three geometrical wheel foot prints as shown below.

WHEEL/ AXLE TYPE	GEOMETRICAL DEFINITION
A	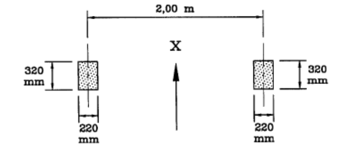
B	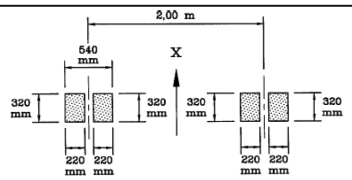
C	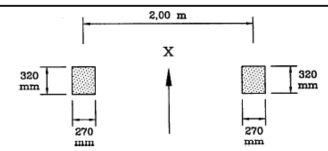

Figure 11-25 Geometrical definition of wheel foot prints in LM2

The five vehicles are defined on the below figure which refers to the three wheel definitions.

1 **LORRY SILHOUETTE**	2 **Axle spacing** (m)	3 **Frequent axle loads** (kN)	4 **Wheel type** (see Table 4.8)
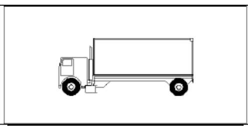	4,5	90 190	A B
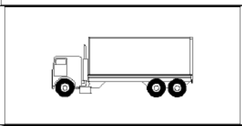	4,20 1,30	80 140 140	A B B
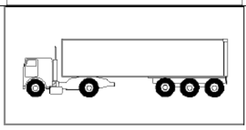	3,20 5,20 1,30 1,30	90 180 120 120 120	A B C C C
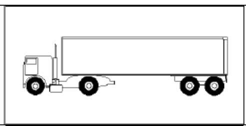	3,40 6,00 1,80	90 190 140 140	A B B B
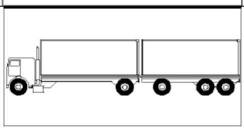	4,80 3,60 4,40 1,30	90 180 120 110 110	A B C C C

Figure 11-26   The five "frequent" vehicles in LM2

LM3 consists of a single vehicle with the below shown geometrical composition, see Figure 11-27. All wheel loads are 120 kN.

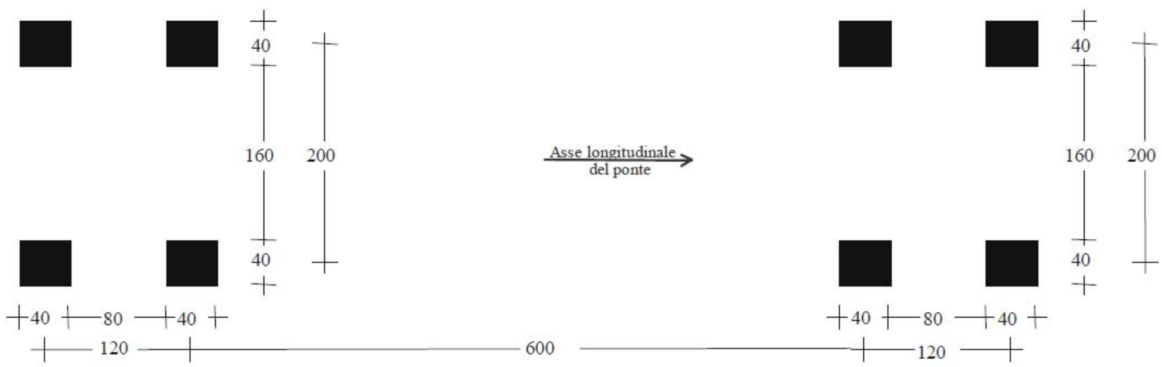

Figure 11-27   LM3 vehicle geometry

In the IBDAS model only one side of the vehicles has been applied. This is due to the fact that the model would have to be considerably wider in order to provide space enough for a full vehicle to be placed well away from the boundaries. Instead it is estimated that the most adverse load case for a trough will be with one side of the axle placed in the vicinity of the trough and hence the influence of the far axle side can be neglected.

The vehicle loads are automatically placed in the most adverse position by utilisation of influence surfaces. In the longitudinal direction IBDAS can move the vehicles completely continuous for determination of worst case loads whereas the transversal position is investigated in seven intervals of 10 cm starting from a placement symmetrically above the middle trough. The Figure 11-28 shows an example of truck nr. 3 in LM2 placed most adverse for determination of extreme tension forces in the trough flange. The small arrow points out the actual stress point whereas the red bars represent relative magnitude in wheel loads.

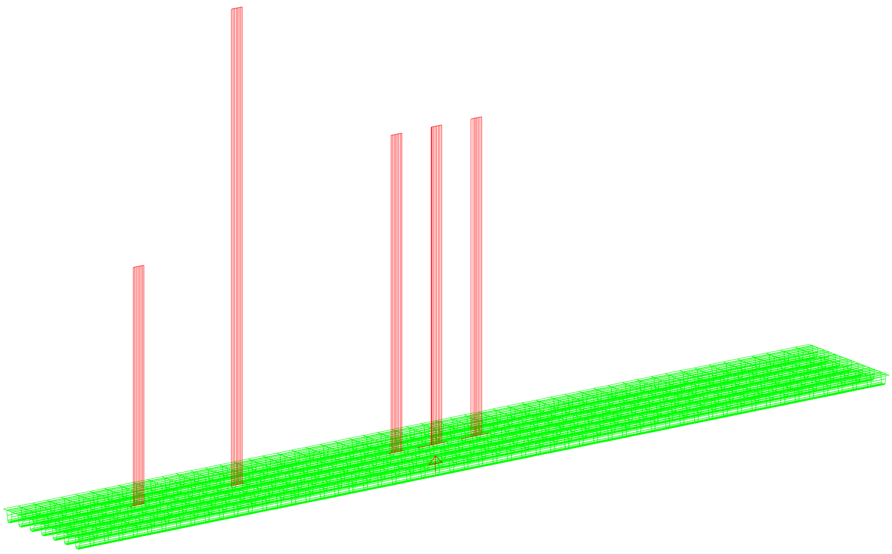

Figure 11-28 Example of the automatic position of vehicle loads in IBDAS

The IBDAS model can provide both envelopes of stresses as well as fixed load cases with coincident sectional forces.

10.10.3 Local Roadway FE-Model

The roadway FE-local model, see section 9.4, has been used to check the point H, see section 11.10.3, applying the patch loads equivalent to the position of the wheels that maximise the vertical stress in the trough web.

10.10.4 Local Railway FE-Model

A local IBDAS model has been developed to analyse the local effects of the eight Eurocode fatigue trains on the T-stiffener of the railway girder. The model is a continuous beam of 21 spans supported every 3.75 m by diaphragms used to determine the bending moment variation and consequently the stress ranges in various location of the central span due to the full transit of the trains, see Figure 11-29.

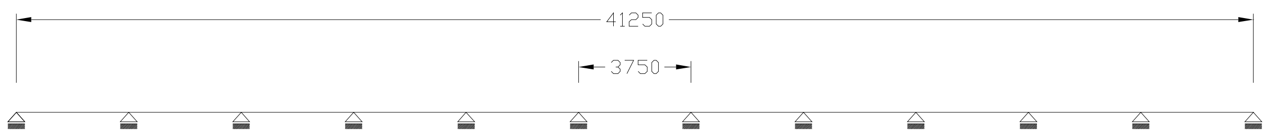

Figure 11-29 Continuous beam model of the T-stiffener

The central span has been chosen in order to assume negligible the side effects. To carry out the fatigue verification of the T-stiffener six locations have been investigated in correspondence of the support, at 200, 400, 600, 1250 and 1875 mm from the diaphragm, see Figure 11-30

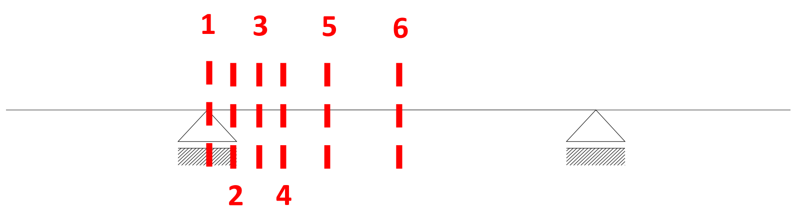

Figure 11-30 Locations where the bending moment influence line has been calculated

From those location has been possible to verify the most favourable location to place the stiffener splices as well as to verify the weld of the T-stiffener to both the main diaphragm and the intermediate diaphragm.

Based on the bending moment influence lines the stress-history plots have been generated, an example can be seen in Figure 11-31. Stress range spectrums have then been calculated and all the relevant secondary cycles (for which the stress range is higher than the cut-off limit) have been accounted for.

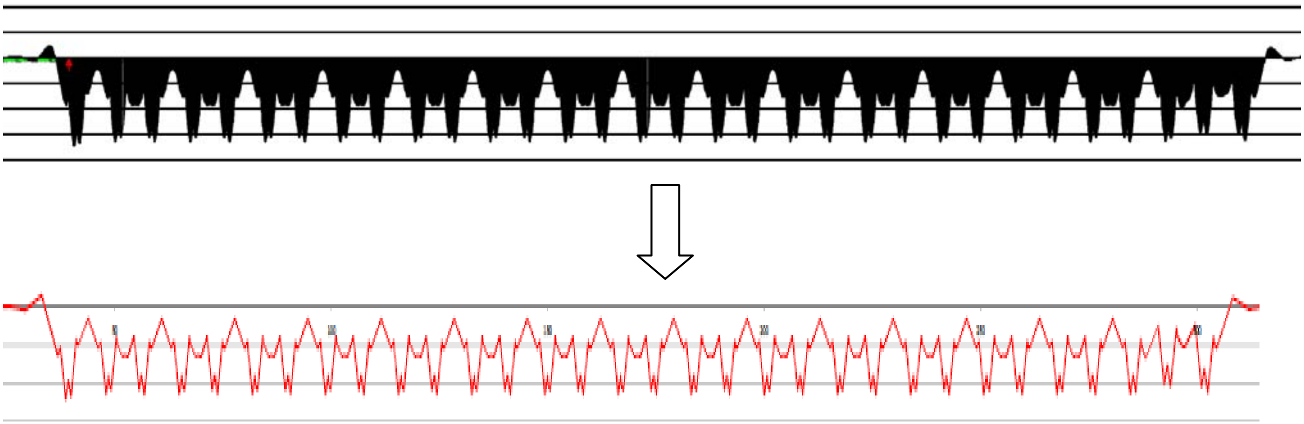

Figure 11-31 Bending moment influence line on top and stress-history for a given location in the bottom

10.10.5 Local Hanger Anchorage FE model

The local FE-model of the hanger anchorage has been used for the fatigue assessment of the hanger anchorage. For more information regarding this model see section 9.6. The most representative hanger anchorage for fatigue throughout the length of the bridge is hanger anchorage type AP2 (84 out of 476 throughout the length of the bridge). The maximum hanger reaction at type AP2 is hanger no. 40. The load considered in this investigation is a passage of one EN5 train in the track closest to the considered hanger anchorage. Load and rotations applied to the hanger anchorage are obtained from the global IBDAS beam model. Variation in rotation angle around the S-axis is taken in the end node at cross girder beam element for a passage of a EN5 train.

In the global IBDAS beam model the hangers are modelled as one hanger at each end of the cross girder. Due to the higher rigidity from two hangers relatively to one, this support will have a higher force than the half of the IBDAS result. This extra contribution is taken into account by increasing the hanger force range with 10%.

Relatively to the local FE-model of the hanger anchorage used for the ULS verification, the mesh has been refined for the fatigue limit state, as shown in Figure 1-1.

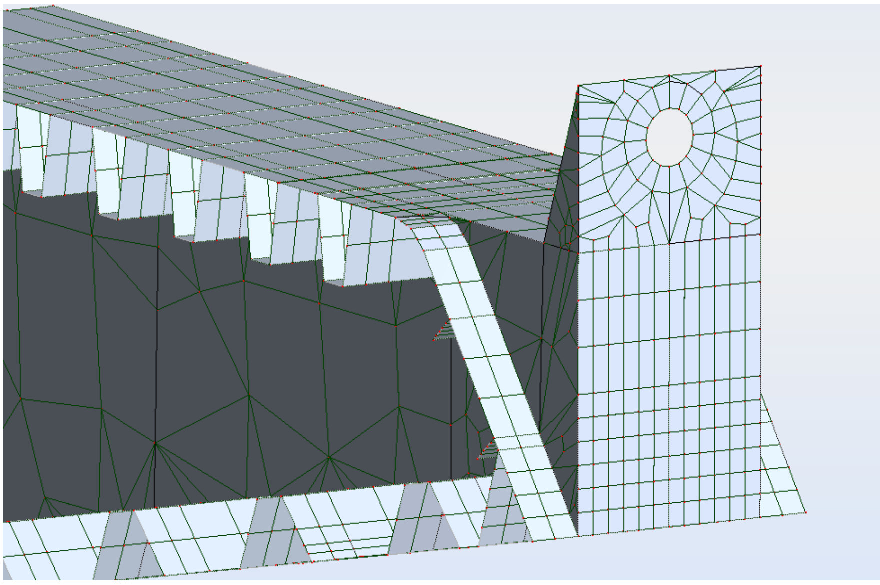

Figure 1-1 Mesh in local FE-model of hanger anchorage

The hanger reaction is applied to the local FE-model as described in section 9.6.

11 Support Structures

11.1 Introduction

This section describes the different support structures applicable for the suspended deck. The structures are designed primary by hand calculations based on reactions from the global IBDAS FE-model. The calculations can be found in "Design Report - Support Structures".

11.2 Hanger Anchorages

The hanger anchorages are primary verified by a local FE-model. In total 4 different types are modelled - see section 9.6. The global ULS hanger force and rotations are applied according to the results from the global IBDAS model. Additional calculations are carried out and can be found in "Design Report - Support Structures".

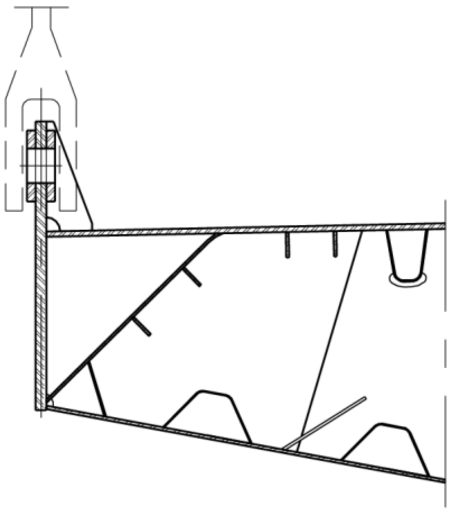

Figure 14-1 Hanger Anchorage - type AP1 shown

11.3 Buffers, Lateral Restraint and Bearings at Towers

11.3.1 Introduction

Movements of the suspended deck are reduced by introducing a system of longitudinal and lateral restraints of the bridge deck at the towers.

The suspended deck is in longitudinal direction connected to the towers by hydraulic buffers, which under "normal" working conditions remain closed and thus act as rigid connections. In the event of high temperature or an earthquake, the buffers will allow movement of the deck while hydraulically limiting the force transferred between the towers and the suspended deck and also reducing the movements of the girder.

In order to reduce the load on the abutments the roadway decks are discontinued at the towers and only the railway deck is continuous. The adjacent cross beams are linked by means of two "triangles" of struts connected at the centre, thus forming an elastic hinge.

The concept of the system is shown in Figure 14-2, where the longitudinal buffers are marked by D2. The seismic isolator in the lateral connection to the tower is marked by D1.

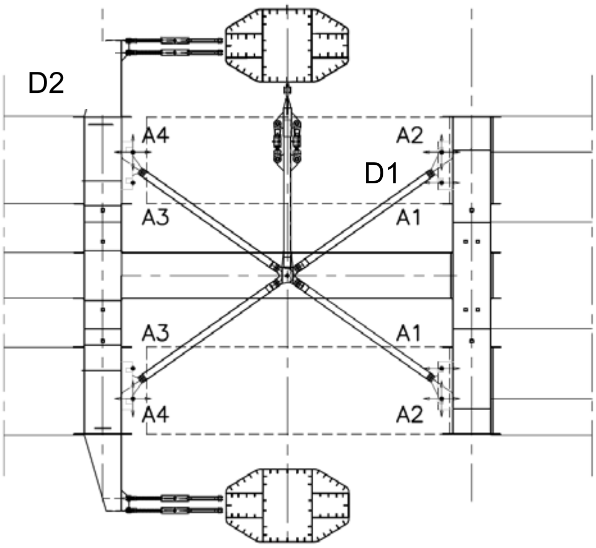

Figure 14-2 Restraint of deck at towers - bearing supports are named A1-A4

For the suspended deck the following structures will be verified in "Design Report - Support Structures".

11.3.2 Cross Girder Extensions

The cross girders at the towers (T4a and T4b) are extended in transverse direction to support the buffer arrangements (D1). The global ULS hanger force and buffer rotations are applied according to the results from the global IBDAS model. Hand calculations are carried out and can be found in "Design Report - Support Structures".

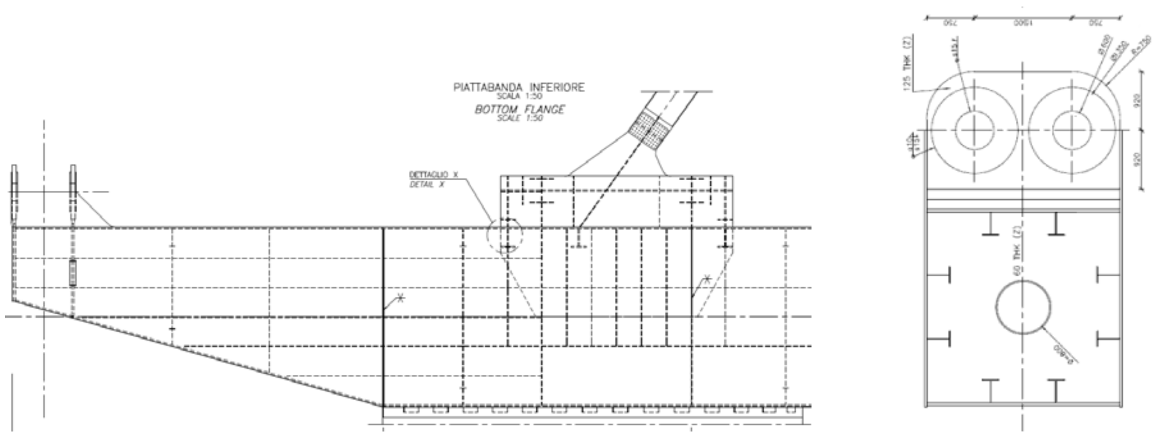

Figure 14-3 Cross girder extension - plan and section at buffer anchorage

11.3.3 Corbels for Support of Drop in Span

The two cross girders at each tower (T4a and T4b) form the support for the 60 m roadway drop in span. The global ULS bearing reactions and movements are applied according to the results from the global IBDAS model. Hand calculations are carried out and can be found in "Design Report - Support Structures".

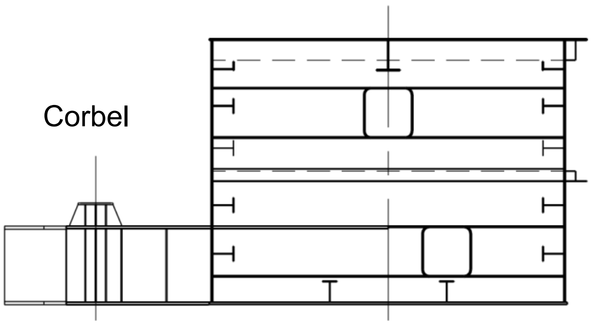

Figure 14-4 Corbel for support of drop in span

11.3.4 Support arrangement and cut out for expansion joint

The end of the roadway drop in span is designed to accommodate the bearing reactions (A1 to A4) and geometrical requirements of the expansion joint. The global ULS bearing reactions and movements are applied according to the results from the global IBDAS model. Hand calculations are carried out and can be found in "Design Report - Support Structures".

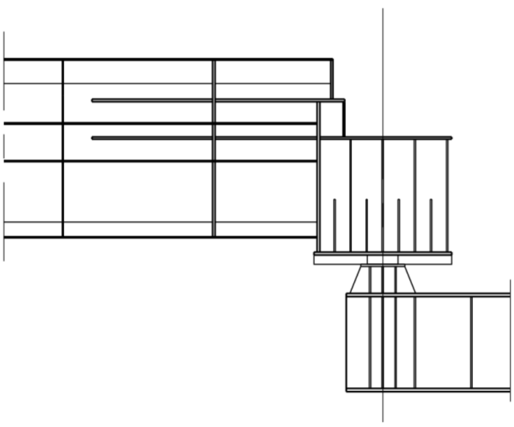

Figure 14-5 Support arrangement at drop in span

11.3.5 Vertical Support of Triangular Strut Structure

At the centre of the 60 m railway span, a vertical support is located for the triangular strut structure (D2). The global ULS bearing reactions and rotations are applied according to the results from the global IBDAS model. Hand calculations are carried out and can be found in "Design Report - Support Structures".

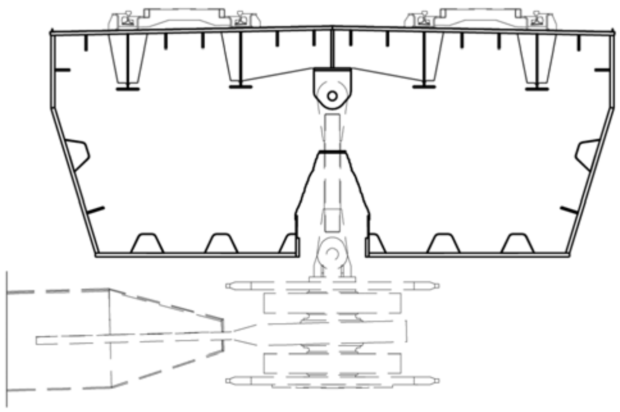

Figure 14-6 Vertical support of triangular strut structure

11.4 Bearings and Expansion Joints at Terminal Structures

11.4.1 Introduction

The suspended deck structure is supported on the terminal superstructures at the bearings A5, A8, A9, A10 and A11, see Figure 14-7.

Three bearings (2xA5 and A8) are located at the entry of the terminal structure underneath the last cross girder, where the roadway girders end. The railway girder is however protruding longer into the terminal structure and bearings for vertical loads are located at two locations - bearings 2xA9 and A10/A11 at the end of the railway girder.

In the transverse direction the railway and road girder is guided by bearings A11 and A8. The two bearings A5 and A9 are furthermore experiencing high uplift forces.

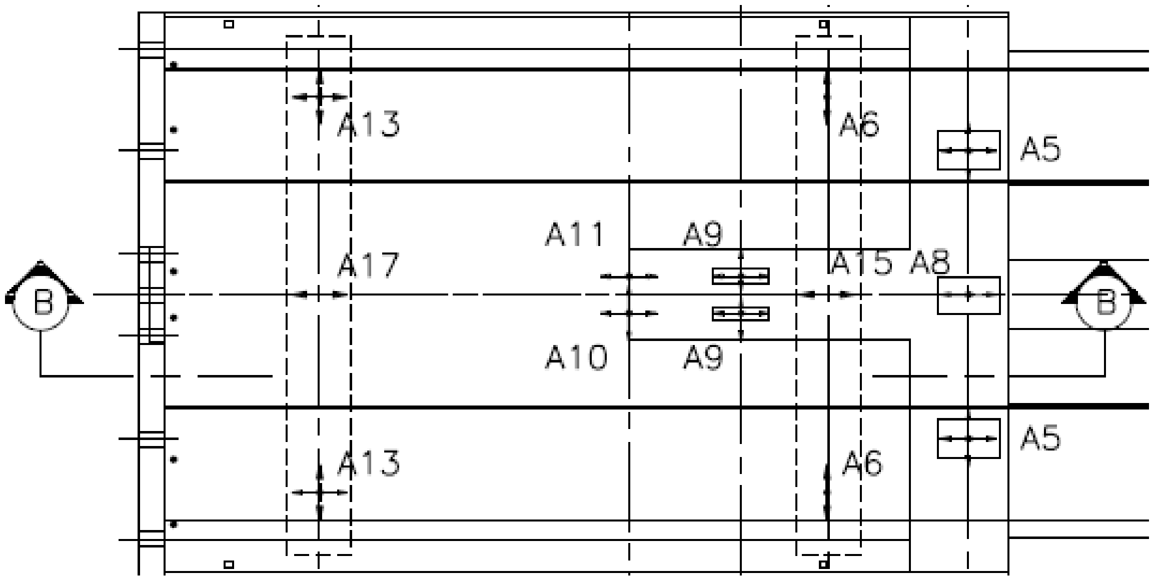

Figure 14-7 Bearing layout at terminal structure on Sicilia side

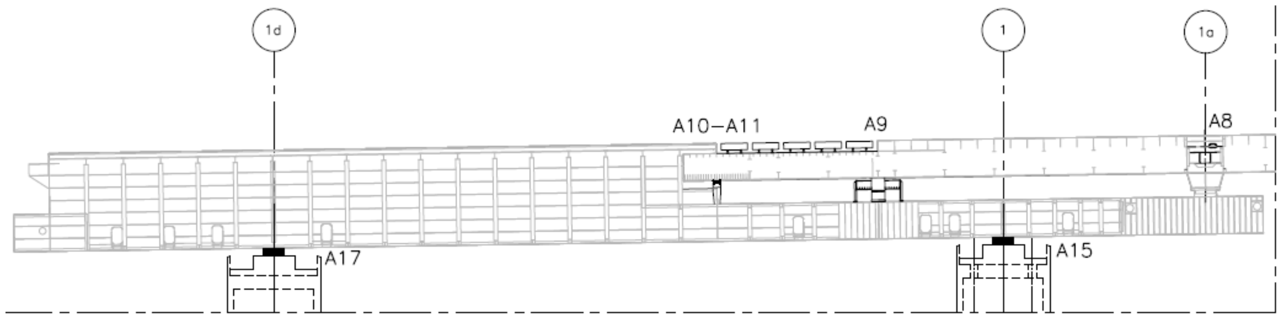

Figure 14-8 Bearing layout at terminal structure on Sicilia side - side view (section B-B in Figure 14-7)

11.4.2 Bearings at Entry of Terminal Structure

The bearings at the entry of the terminal structure are located underneath the last cross girder. They are designed to accommodate the bearing reactions including lifting forces and geometrical requirements of the expansion joint. The global ULS bearing reactions and movements are applied according to the results from the global IBDAS model. Calculations are carried out and can be found in "Design Report - Support Structures".

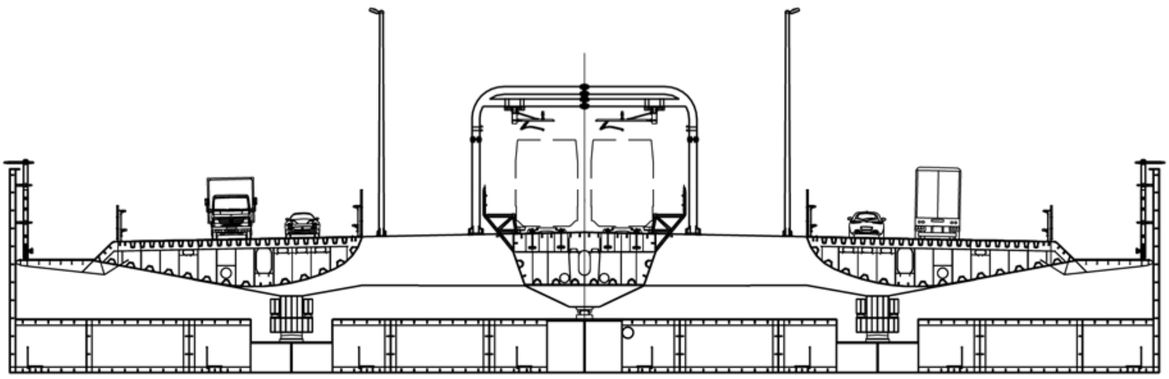

Figure 14-9 Support Arrangements at entry of terminal (last cross girder)

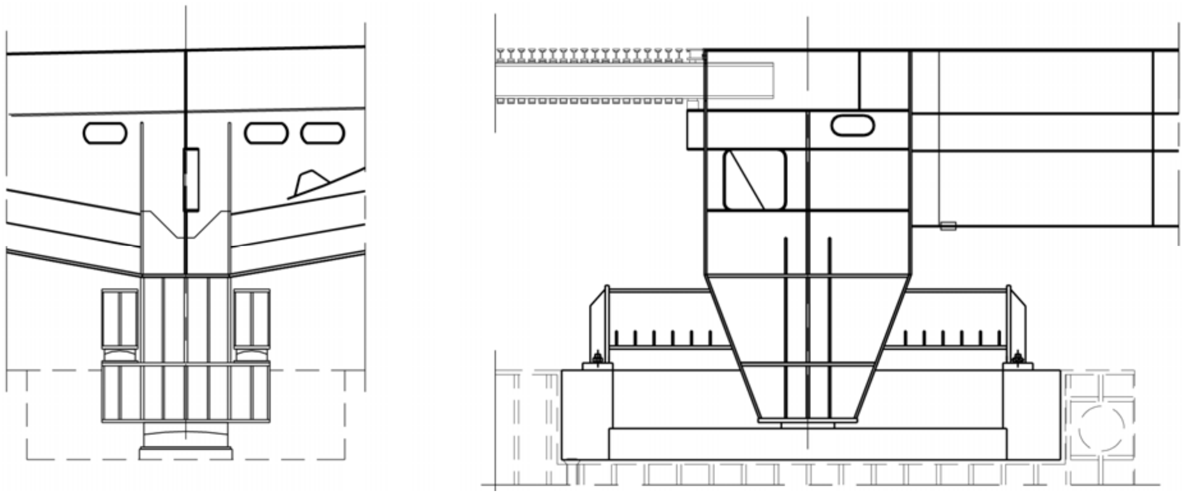

Figure 14-10 Bearing A6 at Terminal Structure with anti lifting device

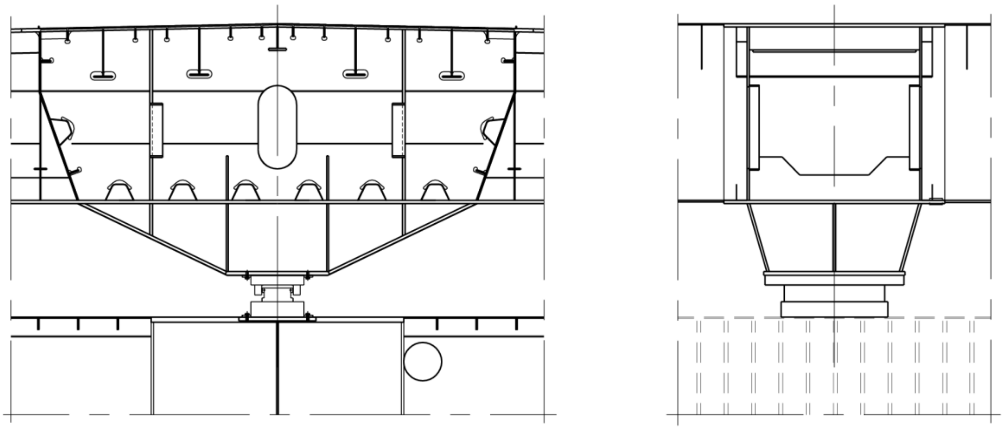

Figure 14-11 Bearing A8 at Terminal Structure - only for lateral support

11.4.3 Bearings at Railway Extension

The bearings at the railway girder extension are located in two lines due to comfort requirements of the railway track line. The bearings are designed to accommodate the reactions including lifting forces and geometrical requirements according to the results from the global IBDAS model. Hand calculations are carried out and can be found in "Design Report - Support Structures".

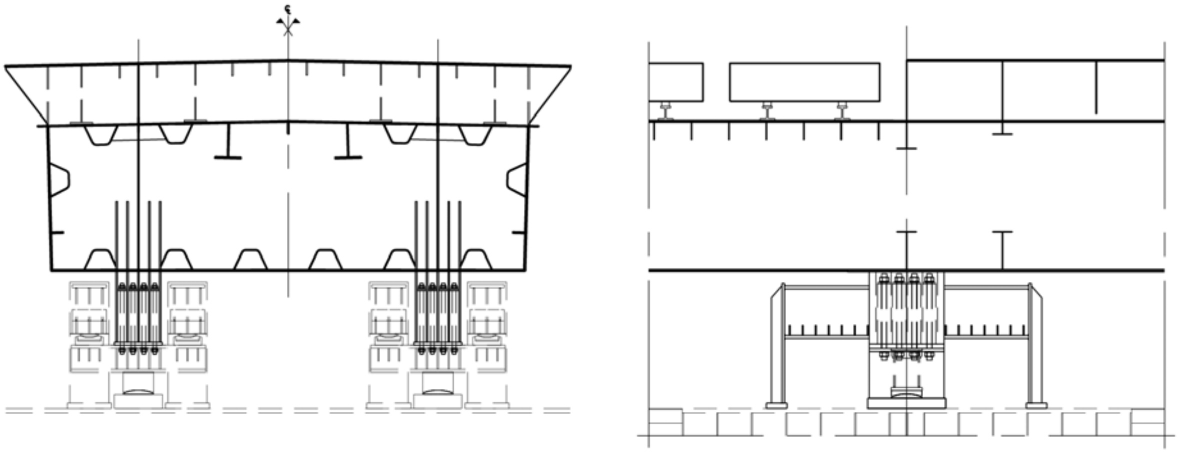

Figure 14-12 Bearing 2 x A9 at railway extension with anti lifting device

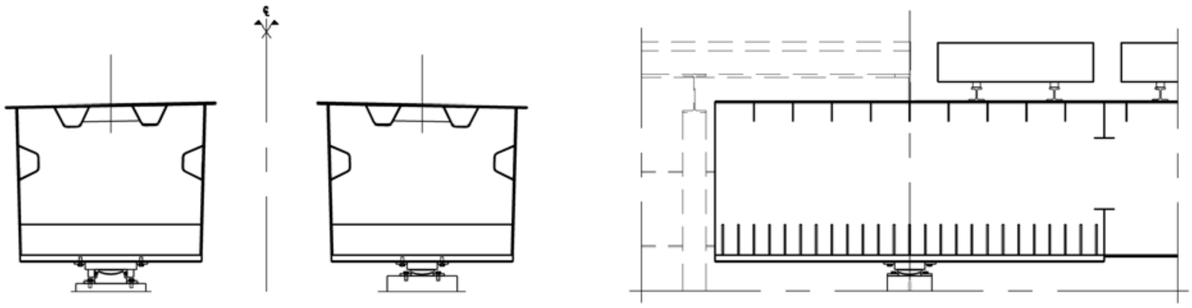

Figure 14-13 Bearing A10 and A11 at end of railway extension

11.4.4 Roadway Expansion Joint

The roadway expansion joints are of the modular type with two movable sides. At present the design requirements are only geometrical so that the joint can be constructed and that it can accommodate the ULS movement.

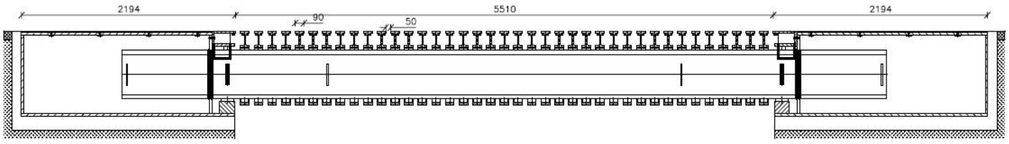

Figure 14-14 Elevation of roadway expansion joint

11.4.5 Railway Expansion Joints

The railway expansion joints are longitudinally moveable stock rails type which can facilitate large longitudinal and rotational movements. The support for the railway expansion joints are designed to accommodate the reactions geometrical requirements of the expansion joint. Hand calculations are carried out and can be found in "Design Report - Support Structures".

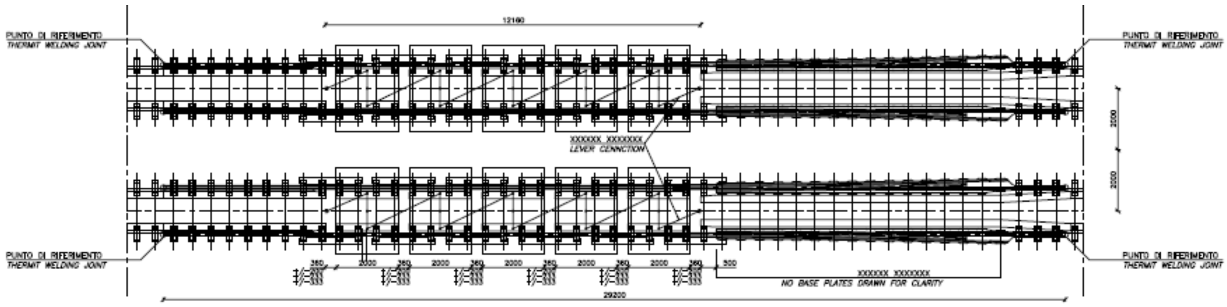

Figure 14-15 Plan of railway expansion joint

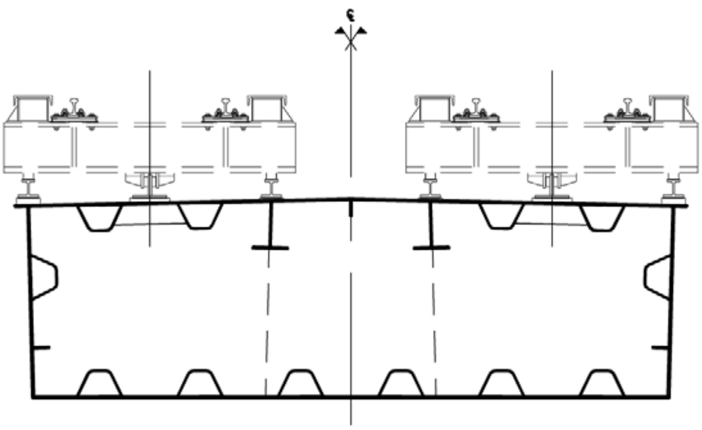

Figure 14-16 Section in railway expansion joint

11.5 Extension of Roadway Deck at Cross Overs/Service Areas

The extension of the roadway deck is designed to accommodate the traffic loading on the cross overs and service areas. Hand calculations are carried out for the extension and the consoles and can be found in "Design Report - Support Structures".

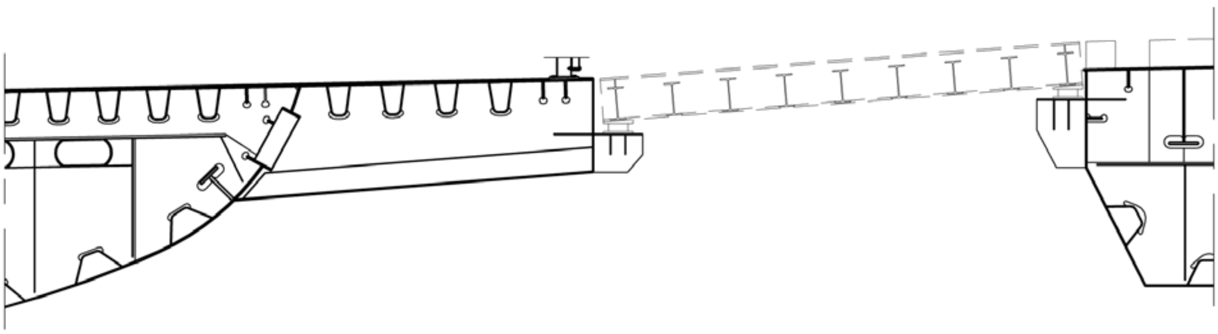

Figure 14-17 Layout of extended roadway deck at crossover

11.6 Back-up for Secondary Structures

Back-up for the most common secondary structures can also be found in the "Design Report - Support Structures":

- Service lane
- Crash barriers
- Portal for road signs
- Light masts
- Catenary masts
- Walkway along railway including railway crash barriers

12 Special Design Investigations

As special design investigations the following load situations have been considered at the ultimate limit state (ULS).

- Hanger replacement
- Hanger rupture (ALS)

12.1 Hanger Replacement

Regarding the replacement of hangers the effect of removing the hangers while the bridge is under operation has been calculated in IBDAS and the effect on the suspended deck has been verified in ADVERS using the sectional forces calculated in the global model.

For the verification of the suspended deck structure during the hanger replacement a few different locations has been selected in the side span and in the main span. For the side span hangers 3 and 5 have been considered. Hanger 3 is located in the centre of the side span and hanger 5 is located in one end of the 60m drop-in span. Hanger 1 is acting as a tie-down, and will need temporary hangers during the replacement, and hence is not investigated. For the main span hangers 45 and 60 has been considered, see Figure 15-1. The result of the analysis can be seen in the "Design Report - Special Design Investigations" for the suspended deck structural elements

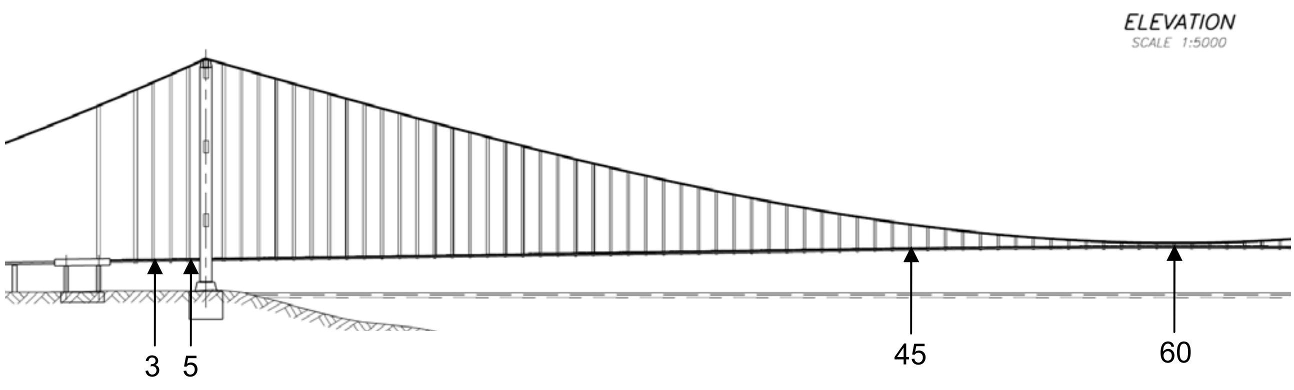

Figure 15-1 Location of selected hangers considered for replacement

A replacement operation of hangers without using temporary hangers is only possible at locations in the main span without affecting the deck structure and cause structural failure. Since also such a replacement strategy will cause an adverse loading effect in the adjacent hangers a replacement strategy using temporary hangers have been found more feasible and is adopted for the Messina bridge, refer "Design Report - Cable System_ANX".

12.2 Hanger Rupture

The analysis in IBDAS has been done in the dynamic region assuming instant rupture of both hangers simultaneously. The effect of this on the suspended deck has been verified using ADVERS using the sectional forces calculated in the global model.

For the verification of the suspended deck structure during the hanger rupture a few different locations has been selected in the side span and around towers, see Figure 15-2. This location has been chosen due to the largest dynamic effects will occur at this location. Most critical is the tie-down hanger and the hangers around the 60m drop-in span, since the girder span will increase significantly after rupture.

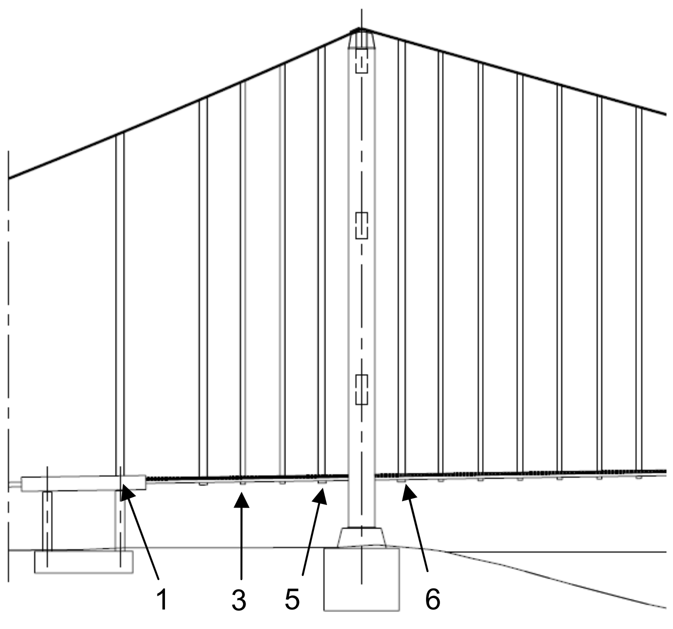

Figure 15-2 Location of hangers considered for rupture

In accordance with the project specific Design Basis the accidental load situation such as hanger rupture have been considered using the partial safety factor on the γ_M=1.0. The result of the analysis can be seen in the "Design Report - Special Design Investigations" for the suspended deck structural elements.